indicate total subsidence at the end of the simulation period (2055) averages about 2 to 4 feet in the Diamond Valley agricultural area; however, for a localized area in south-central Diamond Valley, the projected subsidence is 8 to 10 feet, assuming that pumping rates continue into the future at current rates and that the observed rate of subsidence remains similar to historic rates. This equates to a maximum subsidence rate of approximately 0.2 feet per year and an average of 0.04 to 0.09 feet per year. The maximum subsidence rate is comparable to the maximum subsidence of 1.2 feet in 8 years of study (0.15 ft/yr) interpreted from the InSAR data (**Appendix N**). The average rate of land subsidence over the area of agricultural pumping is approximately one-half to one-quarter the maxiumum rate. Subsidence is non-uniform in Diamond Valley, reflecting the distribution of inelastic storage and drawdown projected under the No Action Scenario.

In Kobeh Valley, simulations of future subsidence for the Proposed Action Altenative result in a broad area of projected subsidence ranging from approximately 0.5 to 3.0 feet at the end of mine life (Year 2055), distributed over the northern and central portions of the proposed wellfield (**Figure 4.6-6**). Land deformation due to the Proposed Action pumping is projected to be greatest in the northern portion of the wellfield in the vicinity of wells 222P, PoO-1, 228P, and 229P. Subsidence for the southern portion of the proposed wellfield is projected to be less than 0.5 feet. Projected subsidence in Kobeh Valley is based on the base case wellfield pumping distribution as described in **Section 4.4.1.4**.

The maximum localized subsidence for Kobeh Valley may be similar to that observed in Diamond Valley, being 2 to 4 times greater than the average predicted subsidence, assuming similar levels of heterogeneity in shallow valley fill materials.

The Proposed Action subsidence results were determined using the same process as was used to determine the Proposed Action water table drawdown (**Section 4.4**), i.e. the No Action Alternative subsidence results were subtracted from the Cumulative Action

Scenario results, and the Proposed Action subsidence results were presented relative to current (2009) conditions.

The Cumulative Action Scenario integrates pumping from the proposed mining project and the simulated continued agricultural pumping in Diamond Valley and southwestern Kobeh Valley (**Sections 4.4.1.1 and 4.4.1.2**). The predicted land subsidence in the Cumulative Action Scenario is computed relative to pre-development (1955) conditions. **Figure 4.6-7** presents the Cumulative Action Scenario subsidence prediction for year 2055.

CHAPTER 5 – REFERENCES

Anderson, R.E., 2000, **Fault number 1160b, Pinon Range fault zone, southern section**, in *"Quaternary fault and fold database of the United States"*, U.S. Geological Survey website: http://earthquakes.usgs.gov/regional/qfaults, 04/08/2008, 04:27 PM.

Anderson, M.P., and W. W. Woessner, 1992, **Applied groundwater modeling: Simulation of flow and advective transport**, Academic Press, San Diego, California, 381 p.

Arteaga, F.E., J.L. Smith, and J.R. Harrill, 1995, **Irrigated croplands, estimated pumpage, and water-level changes in Diamond Valley, Eureka and Elko Counties, Nevada, through 1990**, U.S. Geological Survey Open-File Report 95-107, 68 p.

ASTM, 1993, **Standard guide for application of a ground-water flow model to a site-specific problem, Standard D5447-93**, American Society for Testing and Materials, Philadelphia, Pennsylvania, 15 p.

Avon, L., and T. Durbin, 1994, **Evaluation of the Maxey-Eakin method for estimating recharge to ground-water basins in Nevada**, American Water Resources Association, Water Resources Bulletin, vol. 30, no. 1, pp. 99-111.

Bates, R.L., and J.A. Jackson, editors, 1984, **Dictionary of geological terms, Third Edition**, Prepared under the direction of the American Geological Institute, Anchor Books, published by Doubleday, New York.

Bedinger, M.S., J.R. Harrill, W.H. Langer, J.M. Thomas, and D.A. Mulvihill, 1984, **Maps showing ground-water levels, springs, and depth to water, Basin and Range Province, Nevada**, Water-Resources Investigations Report, 83-4119-B, 11 p. with plates.

Belcher, W.R., P.E. Elliott, and A.L. Geldon, 2001, **Hydraulic-property estimates for use with a transient ground-water flow model of the Death Valley Regional Ground-Water Flow System, Nevada and California**, U.S. Geological Survey Water-Resources Investigations Report 01-4120, 27 p. with 1 plate.

Belcher, W.R., D.S. Sweetkind, and P.E. Elliott, 2002, **Probability distributions of hydraulic conductivity for the hydrogeologic units of the Death Valley Regional Ground-Water Flow System, Nevada and California**, U.S. Geological Survey Water-Resources Investigations Report 02-4212, 17 p.

Belcher, W.R., 2004, **Death Valley Regional Ground-Water Flow System, Nevada and California – Hydrogeologic framework and transient ground-water flow model**, U.S. Geological Survey, Scientific Investigation Report 2004-5205.

Bell, J.W., 2008, **Evaluation of potential for groundwater subsidence in Kobeh Valley**, prepared for General Moly, Inc., Nevada Bureau of Mines and Geology, University of Nevada, Reno, 9 p.

Bell, J.W., F. Amelung, A. Ferretti, M. Bianchi, and F. Novali, 2008, **Permanent scatterer InSAR reveals seasonal and long-term aquifer-system response to groundwater pumping and artificial recharge**, Water Resources Research, vol. 44, W02407, 18 p.

Bell, J.W., and R. Arai, 2009, **InSAR studies in the Diamond-Kobeh Valley area, final technical report to General Moly, Inc.**, Nevada Bureau of Mines and Geology, 11 p.

Berger, D.L., 2000a, **Water budgets for Pine Valley, Carico Lake Valley, and Upper Reese River Valley hydrographic areas, Middle Humboldt River basin, North-central Nevada—Methods for estimation and results**, U.S. Geological Survey Water-Resources Investigations Report 99-4272, 38 p.

_____, D.L., 2000b, **Water-budget estimates for the 14 hydrographic areas in the Middle Humboldt River basin, North-central Nevada**, U.S. Geological Survey Water-Resources Investigations Report 00-4168, 55 p.

Berger, D.L., D.K. Maurer, T.J. Lopes, and K.J. Halford, 2004, **Estimates of natural ground-water discharge and characterization of water quality in Dry Valley, Washoe County, West-central Nevada, 2002-2003**, U.S. Geological Survey Scientific Investigations Report 2004-5155, 39 p.

Blaney, H.F., C.A. Taylor, and A.A. Young, 1930, **Rainfall penetration and consumptive use of water in Santa Ana River Valley and coastal plain**, California Department of Public Works, Water Resources Division Bulletin 33, 162 p.

Blaney, H.F., P.A. Ewing, O.W. Israelson, C. Rohwer, and F.C. Scobey, 1938, **Regional planning, Part IV, the Rio Grande Joint Investigation in the upper Rio Grande Basin in Colorado, New Mexico, and Texas, 1936-1937, Part III, Water resource utilization**, United States Bureau of Agricultural Engineering Report, Natural Resources Committee, vol. 1, pp. 293-427.

Blaney, H.F., and W.D. Criddle, 1962, **Determining consumptive use and irrigation water requirements**, Technical Bulletin 1275, USDA, Agricultural Research Service, Washington, DC.

Brew, D.A., M.J. Gordon, 1971, **Mississippian stratigraphy of the Diamond Peak area, Eureka County, Nevada**, *with a section on* the biostratigraphy and age of the Carboniferous formations by Mackenzie Gordon, Jr., U.S. Geological Survey Professional Paper 661, 84 p., scale 1:24,000.

Bunch, R.L., and J.R. Harrill, 1984, **Compilation of selected hydrologic data from the MX Missile-siting Investigation, East-central Nevada and western Utah**, U.S. Geological Survey Open File Report 84-702, 199 p.

Buqo, T.S., 2008, **Mount Hope Project, water supply exploration, testing and evaluation**, February 2008 draft submitted to BLM, 18 p. plus figures and appendices.

Bureau of Land Management (BLM), 1997, **Nevada Perennial Streams Spatial Dataset**, accessed via USGS website: http://sagemap.wr.usgs.gov/ftp/nevada/BLM/pernstream.htm#t1.

_____, 1999, **Spring dataset for Nevada**, accessed via EPA website: www.epa.gov/esd//land-sci/nvgeospatial/pages/nvgeogis10springsmd.htm#1.

_____, 1985, **Archaeological data recovery associated with the Mount Hope Project, Eureka County, Nevada**, Cultural Resource Series Monograph No. 8, Nevada State Office of the Bureau of Land Management, Reno, Nevada.

_____, 2005, **Supplemental Environmental Impact Statement (SEIS) to analyze the potential environmental effects of the Ruby Hill Mine Expansion – East Archimedes Project**, Bureau of Land Management-Battle Mountain District, 3 numbered sections and appendices.

Businger, J.A., M. Miyake, A.J. Dyer, and E.F. Bradley, 1967, **On the direct determination of the turbulent heat flux near the ground**, Journal of Applied Meteorology.

Call and Nicholas, Inc., 2007, **Unpublished memorandum to Idaho General Mines, Inc.**

Childress, J.M., and G.C. Ferdock, 2008, **Geologic Map of the Roberts Mountains and Mount Hope Area, Eureka County, Nevada**, prepared for General Moly, Inc., 1 plate, scale 1:50,000.

Cook, H.E., and J.J. Corboy, 2004, **Great Basin Paleozoic carbonate platform: facies, facies transitions, depositional models, platform architecture, sequence stratigraphy and predictive mineral host models — Field trip guidebook: Metallogeny of the Great Basin Project**, August 17-22, 2003, U.S. Geological Survey Open-File Report 2004-1078, 129 p.

Cooper, H.H., Jr., and Jacob C.E., 1946, **A generalized graphical method for evaluating formation constants and summarizing well-field history:** American Geophysical Union, Transactions, vol. 27, pp. 526-534.

Council, G.W., 1999, **A lake package for MODFLOW (LAK2), documentation and user's manual, Version 2.2**: HSI GEOTRANS, a Tetra Tech Company.

Craig, H., 1961, **Isotopic variations in meteoric waters**, Science, vol. 133, pp.1702-1703.

Daley, C., R.P. Neilson, and D.L. Phillips, 1994, **A statistical-topographic model for mapping climatological precipitation over mountainous terrain**, Journal of Applied Meteorology 33: 140-158.

Dettinger, M.D., 1989, **Reconnaissance estimates of natural recharge to desert basins in Nevada, USA, by using chloride-balance calculations**, Journal of Hydrology, vol. 106, pp. 55-78.

Dettinger, M.D., J.R. Harrill, D.L. Schmidt, and J.W. Hess, 1995, **Distribution of carbonate-rock aquifers and the potential for their development, southern Nevada and adjacent parts of California, Arizona, and Utah**, U.S. Geological Survey Water-Resources Investigations Report 91-4146, 100 p.

Doherty, J., 2005, **PEST Version 9 user's guide**, Brisbane, Queensland, Australia: Watermark Numerical Computing.

Dohrenwend, J.C., M.A. McKittrick, and B.C. Moring, 1991, **Reconnaissance photogeologic map of the young faults in the Lovelock 1° by 2° Quadrangle, Nevada and California**: U.S. Geological Survey Miscellaneous Field Studies Map MF-2178, scale 1:250,000.

Dohrenwend, J.C., B.A. Schell, and B.C. Moring, 1992, **Reconnaissance photogeologic map of young faults in the Millett 1 degree by 2 degrees Quadrangle, Nevada**, U.S. Geological Survey Miscellaneous Map Series 92-2176.

Dohrenwend, J.C., R.C. Jachens, B.C. Moring, and P.C. Schruben, 1996, **Indicators of subsurface basin geometry in Nevada**, Chapter 8 in *"An Analysis of Nevada's metal-bearing mineral resources"*: Nevada Bureau of Mines and Geology Open-File Report 96-2, ed. D. A. Singer, 8 p.

Driscoll, F.G., 1986, **Groundwater and wells**, Second Edition, Johnson Division, St. Paul, Minnesota, 1,089 p.

Duell, L.F.W., 1990, **Estimates of evapotranspiration in alkaline scrub and meadow communities of Owens Valley, California, using the Bowen-Ratio, Eddy-Correlation, and Penman-Combination Methods**, U.S. Geological Survey Water-Supply Paper 2307-E, pp. 39.

Eakin, T.E., G.B. Maxey, T.W. Robinson, J.C. Fredericks, and O.J. Loeltz, 1951, **Contributions to the hydrology of eastern Nevada**, Nevada Department of Conservation and Natural Resources, Water Resources Bulletin 12.

Eakin, T.E., 1961, **Ground-water appraisal of Pine Valley, Eureka, and Elko Counties, Nevada**, U.S. Geological Survey Ground-Water Resources Reconnaissance Series Report 2, 39 p.

_____, 1962, **Ground-water appraisal of Diamond Valley, Eureka, and Elko Counties, Nevada**, U.S. Geological Survey Ground-Water Resources Reconnaissance Series Report 6, 60 p., with 1 plate.

Epstein, B., and J. Huntington, 2004, **Quantification of the uncertainty associated with estimates of precipitation and recharge in Nevada**, poster presented in the 2004 Nevada Water Resources Association Annual Conference.

Ertec Western, Inc., 1981, **MX Siting Investigation water resources program technical summary report**, vol. IIB, 131 p.

ESI (Environmental Simulations, Inc.), 2007, **Groundwater Vistas, version 5.0, user's guide**.

Fiero, W.R., 1968, **Potentiometric map of the Hot Creek Flow System**, University of Nevada, Desert Research Institute.

Finney, S.C., B.D. Perry, P. Emsbo, and R.J. Madrid, 1993, **Stratigraphy of the Roberts Mountains allochthon, Roberts Mountains and Shoshone Range, Nevada**, in *"Crustal Evolution of the Great Basin and Sierra Nevada"*, Geological Society of America Guidebook, pp. 197-230.

Flint, A.L., and L.E. Flint, 2007, **Application of the basin characterization model to estimate in-place recharge and runoff potential in the Basin and Range carbonate-rock aquifer system, White Pine County, Nevada, and adjacent areas in Nevada and Utah**, U.S. Geological Survey Scientific Investigations Report 2007-5099, 19 p.

Flint, A.L., L.E. Flint, J.A. Hevesi, and J.M. Blainey, 2004, **Fundamental concepts of recharge in the desert southwest: A regional modeling perspective,** in *"Ground-Water Recharge in a Desert Environment: The Southwestern United States"*, American Geophysical Union, ed. J. F. Hogan, F. M. Phillips, and B. R. Scanlon, Water Science and Application Series 9, pp. 159-184.

Flynn, T., and K. Buchanan, 1990, **Geothermal fluid genesis in the Great Basin, 1988-1990**, United States Department of the Interior, Idaho Operation Office, DE-FG07-88ID12784.

Franke, O.L., T.E. Reilly, and G.D. Bennett, 1984, **Definition of boundary and initial conditions in the analysis of saturated groundwater flow systems—an introduction**, U.S. Geological Survey Open-File Report 84-458, Reston, Virginia.

Freeze, R.A., and J.A. Cherry, 1979, **Groundwater**, Prentice-Hall, Inc. Publishers, New Jersey, 604 p.

Friedman, I., J.M. Harris, G.I. Smith, and C.A. Johnson, 2002, **Stable isotope composition of waters in the Great Basin, United States 1, Air-mass trajectories**, Journal of Geophysical Research, 107(D19).

Garside, L.J., and J.H. Schilling, 1979, **Thermal waters of Nevada**, Nevada Bureau of Mines and Geology, Bulletin 91.

Garside, L.J., R.H. Hess, K.L. Fleming, and B.S. Weimer, 1988, **Oil and gas developments in Nevada**, Nevada Bureau of Mines and Geology Bulletin 104, 136 p.

Gatewood, J.S, T.W. Robinson, B.R. Colby, J.D. Hem, and L.C. Halpenny, 1950, **Use of water by bottom-land vegetation in lower Safford valley, Arizona**, U.S. Geological Survey Water-Supply Paper 1103., 210 pp.

Gordon, I.R., 1990, **Sedimentation during the late Pliocene and early Pleistocene in the Pine Valley basin, northeast Nevada,** in *"Oil Fields and Geology of the Pine Valley, Eureka County Area, Nevada"*, Nevada Petroleum Society 1990 Fieldtrip Guidebook, ed. D. M. H. Flannigan, L. J. Garside, and M. W. Hansen, 74 p.

Great Basin Center for Geothermal Research, 2007, **Geographic information system spatial data.** http:/www.unr.edu/Geothermal/datalist.html, accessed July 2007.

Halepaska, John, C., and Associates, 2005, **Geological, geochemical, and hydrological investigations for Phase I Feasibility Study, Mount Hope Project**, 64 p.

Harbaugh, A.W., E.R. Banta, M.C. Hill, and M.G. McDonald, 2000, **MODFLOW-2000, U.S. Geological Survey Modular Ground-Water Model – user guide to modularization concepts and the ground-water flow process**, U.S. Geological Survey Open-File Report 00-92.

Hardman, George, 1936, **Nevada precipitation and acreages of land by rainfall zones**, Nevada University Agricultural Experiment Station Report and Map.

Hardman, George, Vic Kral, Jack Haffey, et al., 1965, **Nevada precipitation map**, University Agricultural Experiment Station, no scale provided, 1 plate.

Harrill, J.R., 1968, **Hydrologic response to irrigation pumping in Diamond Valley, Eureka and Elko counties, Nevada, 1950-65, with a section on surface water by R.D. Lamke**: State of Nevada Department of Conservation and Natural Resources, Water Resources Bulletin No. 35, 85 p.

Harrill, J.R., J.S. Gates, and J.M. Thomas, 1988, **Major ground-water flow systems in the Great Basin region of Nevada, Utah, and adjacent states**, U.S. Geological Survey Hydrologic-Investigations Atlas HA--694--C.

Harrill, J.R., and D.E. Prudic, 1998, **Aquifer systems in the Great Basin region of Nevada, Utah, and adjacent states, summary report**, U.S. Geological Survey Professional Paper, 1409-A, 66 p. with plates.

Hay, R.L., and S.G. Guldman, 1987, **Diagenetic alteration of silicic ash in Searles Lake, California**, Clay and Clay Minerals, vol. 35, no. 6, pp. 449-457.

Heath, R.C., 1989, **Basic ground-water hydrology**, U.S. Geological Survey Water-Supply Paper 2220, 84 p.

Hedman, E.R., 1970, **Mean annual runoff as related to channel geometry in selected streams in California**, U.S. Geological Survey Water-Supply Paper 1999-E, 17 p.

Hedman, E.R., D.O. Moore, and R.K. Livingston, 1972, **Selected stream-flow characteristics as related to channel geometry of perennial streams in Colorado**, U.S. Geological Survey Open-File Report, 14 p.

Hedman, E.R., W.M. Kastner, and H.R. Hejl, Jr., 1974, **Kansas stream-flow characteristics—part 10, Selected streamflow characteristics as related to active-channel geometry of streams in Kansas**, Kansas Water Resources Board Technical Report No. 10, 21 p.

Hedman, E.R., and W.R. Osterkamp, 1982, **Streamflow characteristics related to channel geometry of streams in the western United States**, U.S. Geological Survey, Water Supply Report.

Helm, D.C., 1978, **Field verification of a one-dimensional mathematical model for transient compaction and expansion of a confined aquifer system**, American Society of Civil Engineers, Specialty Conference on Verification of Mathematical and Physical Models in Hydraulic Engineering, College Park, MD, August 1978, Proceedings, pp. 189 – 196.

Hevesi, J.W., A.L. Flint, and L.E. Flint, 2003, **Simulation of net infiltration using a distributed parameter watershed model for the Death Valley regional flow system, Nevada and California**, U.S. Geological Survey Water-Resources Investigations Report, 03-4090, 104 p.

Hoffman, J., and H.A. Zebker, 2001, **Seasonal subsidence and rebound in Las Vegas Valley, Nevada observed by synthetic aperture radar interferometry**, Water Resources Research, vol. 37, no. 6, pp. 1551-1566.

Hose, R.K., A.K. Armstrong, and A.G. Harris, 1982, **Devonian and Mississippian rocks of the northern Antelope Range, Eureka County, Nevada**, U.S. Geological Survey Professional Paper 1182, 19 p.

Houng-Ming, J., J.H. Trimmer, and R. Jewell, 1983, **Nevada Watershed Studies, 1963 – 1980**, United States Department of the Interior, Bureau of Land Management, Technical Publication BLMNVPT830014340, variably paginated.

Hsieh, P., and J. Freckleton, 1993, **Documentation of a computer program to simulate horizontal-flow barriers using the USGS MODFLOW Model**, U.S. Geological Survey Open File Report 92-477.

Huntington, J.L., and R.G. Allen, 2010, **Evapotranspiration and net irrigation water requirements for Nevada**, Nevada Division of Water Resources, 260 p.

HydroGeoLogic, Inc., 1996, **MODFLOW-SURFACT: Version 3.0**, HydroGeoLogic Inc., Herndon, Virginia.

Hydro-Search, Inc., 1982, **Hydrology resources technical report no. 4, Mount Hope Molybdenum Project**, Volume I of II, variably paginated.

Independent Mining Consultants, 2007, unpublished consultant report prepared for Idaho General Mines, Inc.

Interflow Hydrology, Inc., and T. Buqo, Consulting Hydrogeologist, 2007, unpublished consultant report, Kobeh Valley Central Well Field Aquifer Testing Plan, June 2007, 9 p.

Interflow Hydrology, Inc., 2010, **Kobeh Valley Well Field data summary report: A summary of geologic and hydrogeologic data for the Kobeh Valley Well Field area of the Mount Hope project, Eureka County, Nevada**, prepared for General Moly, Inc., March 8, 2010.

Jacob, C.E., 1940, **On the flow of water in an elastic artesian aquifer**, American Geophysical Union Transmittal 21st Annual Meeting, part 2, pp. 674-686.

_____, 1946, **Drawdown test to determine effective radius of artesian wells**: Am. Soc. Civil Eng. Proc., vol. 72, no. 5, pp. 629-646.

Jeton, A.E., S.A. Watkins, T.J. Lopes, and J. Huntington, 2005, **Evaluation of precipitation estimates from PRISM for the 1961-1990 and 1971-2000 data sets, Nevada**, U.S. Geological Survey Scientific Investigations Report 2005-5291.

Johannesen and Cole, 1990, **Blackburn Oil Field, Eureka County, Nevada** in *"Oil Fields and Geology of the Pine Valley, Eureka County Area, Nevada"*, Nevada Petroleum Society 1990 Fieldtrip Guidebook, ed. D. M. H. Flanigan, L. J. Garside, and Mike Hansen.

Katzer, T., and D. Donovan, 2003, **Surface-water resources and basin water budget for Spring Valley, White Pine and Lincoln Counties, Nevada**, Southern Nevada Water Authority – Las Vegas Valley Water District publication, 70 p.

Ketner, K.B., 1998, **The nature and timing of tectonism in the western facies terrain of Nevada and California – An outline of evidence and interpretations derived from geologic maps of key areas**, U.S. Geological Survey Professional Paper 1592, 17 p.

Konikow, L.F., 1978, **Calibration of groundwater models**, in *"Proceedings of the Specialty Conferences on Verification of Mathematical and Physical Models in Hydraulic Engineering"*, College Park, Maryland, August 9-11, 1978.

Kruseman, G.P., and N.A. De Ridder, 1990, **Analysis and evaluation of pumping test data**, Publication 47, Second Edition, International Institute for Land Reclamation and Improvement, Wageningen, The Netherlands.

Laczniak, R.J., L.J. Smith, and G.A. DeMeo, 2006, **Annual ground-water discharge by evapotranspiration from areas of spring-fed riparian vegetation along the eastern margin of Death Valley, 2000-02, Nevada and California**, U.S. Geological Survey Water-Resources Investigations Report 2006-5145, 46 p.

Larson, E.R., and J.F. Riva, 1963, **Preliminary geologic map of the Diamond Springs Quadrangle, Nevada**, Nevada Bureau of Mines, Map 20.

Leake, S.A., and D.E. Prudic, 1991, **Documentation of a computer program to simulate aquifer-system compaction using the modular finite-difference ground-water flow model**, USGS Techniques of Water Resource Investigations Report, Book 6, Chapter A2.

Lee, C.H., 1912, **An intensive study of the water resources of a part of Owens Valley, California**, U.S. Geological Survey Water-Supply Paper 294, 135 p.

Leopold, L.B., and T. Maddock, Jr., 1953, **The hydraulic geometry of stream channels and some physiographic implications**, U.S. Geological Survey Professional Paper 252, 57 p.

Linacre, E.T., 1994, **Estimating U.S. Class A pan evaporation from few climate data**, Water International, Vol. 19, pp. 5-14.

Lopes, T.J., and D.M. Evetts, 2004, **Ground-water pumpage and artificial recharge estimates for calendar year 2000 and average annual natural recharge and interbasin flow by hydrographic area, Nevada**, U.S. Geological Survey Scientific Investigations Report 2004-5239.

Lopes, T.J., S.G. Buto, J.L. Smith, and T.L. Welborn, 2006, **Water-table levels and gradients, Nevada, 1947-2004**, U.S. Geological Scientific Investigations Report 2006-5100.

M3 Engineering & Technology Corp., 2007, **Mount Hope Project, Molybdenum mine and process plant, bankable feasibility study**, revised report prepared for Idaho General Mines, Inc., September 11, 2007.

Malek, E., G.E. Bingham, and G.D. McCurdy, 1990, **Evapotranspiration from the margin and moist playa of a closed desert valley**, Journal of Hydrology, 120, pp. 15-34.

Mallory, Sheila, 2007, Personal Communication. Ms. Mallory works for the Battle Mountain BLM.

Mariner, R.H., J. B. Rapp, L.M. Willey, and T.S. Presser, 1974, **Chemical composition and estimated minimum thermal reservoir temperatures of the principal hot springs of northern and central Nevada**, U.S. Geological Survey open file report.

Mariner, R.H., T.S. Presser, and W.C. Evans, 1983, **Geochemistry of active geothermal systems in the northern Basin and Range Province**, Geothermal Resources Council, Special Report No. 13, pp. 95-120.

Maurer, D.K., T.J. Lopes, R.L. Medina, and J.L. Smith, 2004, **Hydrogeology and hydrologic landscape regions of Nevada**, U.S. Geological Survey Scientific Investigations Report, 2004-5131.

Maxey, G.B., and T.E. Eakin, 1949, **Groundwater in the White River Valley, White Pine, Nye, and Lincoln Counties, Nevada**, Nevada Department of Conservation and Natural Resources Bulletin 8.

Mazor, E., 1991, **Applied chemical and isotopic groundwater hydrology**, Halsted Press, New York.

McDonald, M.G., and A.W. Harbaugh, 1984, **A modular three-dimensional finite-difference ground-water flow model**, U.S. Geological Survey TWRI, Book 6, Chapter A1.

McKee, E.H., 1968, **Geologic map of the Ackerman Canyon Quadrangle, Lander and Eureka Counties, Nevada**: U.S. Geological Survey Geologic Quadrangle Map GQ-761, scale 1:62,500.

McKee, E.H., and J.E. Conrad, 1998, **Geologic map of the Frazier Creek Quadrangle, Nye County, Nevada**, Nevada Bureau of Mines and Geology Map FS-15, scale 1:24,000.

Meinzer, O.E., 1927, **Large springs in the United States**, U.S. Geological Survey Water Supply Paper no. 557, pp. 8-88.

Merriam, C.W., and C.A. Anderson, 1942, **Reconnaissance survey of the Roberts Mountains, Nevada**, Geological Society of America Bulletin, vol. 53, no. 12, 1 plate, pp. 1675-1727.

Mifflin, M.D., 1968, **Delineation of ground-water flow systems in Nevada**, University of Nevada, Reno, Desert Research Institute, Center for Water Resources Research Technical Report H-W, no. 4.

Mifflin, M.D., and M.M. Wheat, 1979, **Pluvial lakes and estimated pluvial climates of Nevada**, Nevada Bureau of Mines and Geology Bulletin 94, 57 p.

Moench, A.F., 1984, **Double-porosity models for a fissured groundwater reservoir with fracture skin**, American Geophysical Union Water Resources Research, vol. 20, no. 7, pp. 831-846.

_____, 1988, **The response of partially penetrating wells to pumpage from double-porosity aquifers**, Proceedings of the International Conference on Fluid Flow in Fractured Rocks, Atlanta, Georgia, May 16-18, 1988.

Montana Department of Environmental Quality, 2007, **General information regarding geothermal exploration and reservoirs**: http://www.deq.Mountgov/energy/geothermal/electric.asp.

Monteith, J.L., 1965, **Evaporation and environment, the state and movement of water in living organisms**, in *"Proceedings, Symposium No. 19"*, Society for Experimental Biology, ed G. E. Fogg, New York, Academic Press, pp. 205-234.

Montgomery & Associates, 2008, **Results of groundwater exploration and drilling investigation, Mount Hope area, Eureka County, Nevada**, prepared for Idaho General Mines, Inc.

_____, 2010a, **Data selection for pit area water level contours and steady-state local model target water levels, Mt. Hope Project, Eureka County, Nevada**, Technical Memorandum prepared for Itasca Denver, Inc., February 24, 2010.

_____, 2010b, **Hydrogeologic Characterization of Pit Area, Mt. Hope Project, Eureka County, Nevada**, report prepared for General Moly, Inc., March 2010.

Moore, D.O., 1968, **Estimating mean annual runoff in ungaged semi-arid areas**: International Association Scientific Hydrology, Bulletin 13, vol. 1, pp. 29-39. [Reprinted as Nevada Department of Conservation and Natural Resources, Water Resources Bulletin 36, pp. 36-39.]

Moreo, M.T., R.J. Laczniak, and D. I. Stannard, 2007, **Evapotranspiration rate measurements of vegetation typical of ground-water discharge areas in the Basin and Range carbonate-rock aquifer system, White Pine County, Nevada, and adjacent areas in Nevada and Utah, September 2005-August 2006**, U.S. Geological Survey Scientific Investigations Report 2007-5078, 36 p.

Morgan, D.S., and M.D. Dettinger, 1996, **Groundwater conditions in Las Vegas Valley, Clark County, Nevada, Part 2, hydrogeology and simulation of ground-water flow**, U.S. Geological Survey Water-Supply Paper 2320-B, 124 p.

Murphy, M.A., E.H. McKee, E.L. Winterer, J.C. Matti, and J.B. Dunham, 1978, **Preliminary geologic map of the Roberts Creek Mountain quadrangle, Nevada**, U.S. Geological Survey Open-File Report OF-78-376, scale 1:31250.

Murphy, M.A., E.H. McKee, E.L. Winterer, S.C. Finney, J.C. Matti, and J.B. Dunham, 2007, **Geologic map of the Cooper Peak Quadrangle, Eureka County, Nevada**, Nevada Bureau of Mines and Geology, scale 1:24,000.

National Water Information System (NWIS), 2007, **USGS Water Data for USA**, U.S. Geological Survey, http://waterdata.usgs.gov/nwis, accessed March 2007 through May 2008.

Nevada Bureau of Mines and Geology (NBMG), 2008-2009, **Databases and water rights report summaries**, available on line at http://www.nbmg.unr.edu/.

Nevada Department of Conservation and Natural Resources, Division of Water Resources, 1977, **Water for Nevada, Nevada's Water Resources**, 87 p.

Nevada Division of Water Resources, 2005a, **Water law – An overview and related issues, Interim Study Committee on the Use, Management and Allocation of Water Resources**, presentation by Tracy Taylor and Jason King, October 13, 2005.

_____, 2005b, **Designated groundwater basins of Nevada**, Office of the State Engineer, Carson City Nevada, 1 plate, scale 1:750,000.

_____, 2006, presentation including Perennial Yield in Nevada Hydrographic Basins.

_____, 2007, **Preliminary hydrographic basin summaries and water rights information**, http://water.nv.gov.

_____, 2008 and 2009, **Water rights abstract**, http://water.nv.gov, accessed May 2008 and May 2009.

_____, 2009, Ruling No. 5966, March 2009.

Nichols, W.D., 1992, **The uncertainty of water budget estimates in the Great Basin, in managing water resources during global change**, American Water Resources Association 28th Annual Conference and Symposium, Reno, Nevada, November 1-5, 1992, ed. R. Herrmann, pp. 309-317.

_____, W.D., 1993, **Estimating discharge of shallow groundwater by transpiration from greasewood in the northern Great Basin**, Water Resources Research, vol. 29, no. 8, pp. 2771-2778.

_____, W.D., 1994, **Groundwater discharge by phreatophyte shrubs in the Great Basin as related to depth to groundwater**, Water Resources Research, vol. 30, no. 12, pp. 3265-3274.

_____, W.D., 2000, **Regional ground-water evapotranspiration and ground-water budgets, Great Basin, Nevada**, U.S. Geological Survey Professional Paper 1628, 82 p. plus CD.

Nichols, W.D., and T.R. Rapp, 1996, **Micrometeorological data for energy-budget studies near Rogers Spring, Ash Meadows National Wildlife Refuge, Nye County, Nevada, 1994**, U.S. Geological Survey Open-File Report 96-170, 49 p.

Nichols, W.D., R.J. Laczniak, G.A. DeMeo, and T.R. Rapp, 1997, **Estimated ground-water discharge by evapotranspiration, Ash Meadows National Wildlife Refuge, Nye County, Nevada, 1994**, U.S. Geological Survey Water-Resources Investigations Report 97-4025, 13 p.

Noble, A.C., S. Brown, and R. Gowans, 2008, **Technical report on the Tonkin Project**, prepared for US Gold Corporation, May 16, 2008.

Nolan, T.B., C.W. Merriam, and J.S. Williams, 1956, **The stratigraphic section in the vicinity of Eureka, Nevada**, U.S. Geological Survey Professional Paper 276, 77 p.

Nolan, T.B., 1974, **Stratigraphic evidence on the age of the Roberts Mountains thrust, Eureka and White Pine Counties, Nevada**, U.S. Geological Survey Journal of Research of the U.S. Geological Survey V.2-4, scale 1:370,000.

Nolan, T.B., C.W. Merriam, M.C. Blake, Jr., 1974, **Geologic map of the Pinto Summit Quadrangle, Eureka and White Pine Counties, Nevada**, U.S. Geological Survey Miscellaneous Investigations Series Map I-793, scale 1:31,680.

Oregon State University (OSU), 2006, **Parameter regression on independence slope model (PRISM)**, http://prism.oregonstate.edu/products/, accessed March 2007.

Osterkamp, W.R., and E.R. Hedman, 1977, **Variation of width and discharge for natural high-gradient stream channels**, Water Resources Research, vol. 13, no. 2, pp. 256-258.

Pennington, R.W., 1980, **Evaluation of empirical methods for estimating crop water consumptive use for selected sites in Nevada**, NDWR, Division of Water Planning Information Series, Water Planning Report No. 3.

Philbin, F.W., J.L. Meuschke, and W.E. McCaslin, 1963, **Aeromagnetic map of the Roberts Mountains, central Nevada**, U.S. Geological Survey Open-File Map, March 7, 1963, scale 1:25,000.

Plume, R.W., 1996, **Hydrogeologic framework of the Great Basin region of Nevada, Utah, and adjacent states**, U.S. Geological Survey Professional Paper 1409–B, 64 p.

Plume, R.W., and S.M. Carlton, 1988, **Hydrogeology of the Great Basin region of Nevada, Utah, and adjacent states**, U.S. Geological Survey Hydrologic Atlas 694-A., 1 plate.

Ponce, D.A., 1997, **Digital data of Nevada**, U.S. Geological Survey Digital Data Series DDS-42.

Ponce, D.A., J.M.G. Glen, 2002, **Relationship of epithermal gold deposits to large-scale fractures in northern Nevada**, Economic Geology, vol. 97, 2002, pp. 3–9.

Prudic, D.E., J.R. Harrill, and T.J. Burbey, 1995, **Conceptual evaluation of regional ground-water flow in the carbonate-rock province of the Great Basin, Nevada, Utah, and adjacent states**, U.S. Geological Survey Professional Paper 1409-D, 102 p.

PTI Environmental Services, Inc., 1994, **The hydrogeochemistry of the Robinson Mining District, White Pine County, Nevada**, prepared for Magma Mining Company, Tucson, Arizona, 8 numbered sections, 1 appendix.

_____, 1997, **Effects of pumping the proposed Olinghouse Mine supply well on Dodge Flat and the Truckee River, Washoe County, Nevada**, prepared for Bureau of Land Management, Carson City Field Office, PTI Contract CV1T, 02--01, PTI Environmental Services, Boulder, Colorado, 19 p.

Pugsley, M., and S. Robinson, 1981, **Geothermal Resource Area 6, Lander and Eureka Counties, area development plan**, Nevada Department of Energy plan DOE/RA/50075-T9.

Raines, G.L., K.A. Connors, L.A. Moyer, and R.J. Miller, 2003, **Spatial digital database for the geologic map of Nevada**, U.S. Geological Survey Open File Report 03-66, Digital database version 3.0.

Redsteer, M. Hiza, R.E. Anderson, and M.N. Machette, 2000, **Fault number 1211, Western Diamond Mountains fault zone,** in Quaternary fault and fold database of the United States, U.S. Geological Survey website: http://earthquakes.usgs.gov/regional/qfaults, 04/08/2008, 04:36 PM.

Reed, M.J., R.H. Mariner, C.A. Brook, and M.L. Sorey, 1983, **Selected data for low-temperature (less than 90 degrees C) geothermal systems in the United States (reference data for USGS Circular 892)**, U.S. Geological Survey Open-File Report 83-250, 129 p.

Reheis, Marith, 1999, **Extent of Pleistocene lakes in the western Great Basin**, U.S. Geological Survey Miscellaneous Field Studies Map, MF-2323.

Ricci, H., 2001, **Nevada water laws**, published by the Nevada Division of Water Resources.

Roberts, R.J., P.E. Hotz, J. Gilluly, and H.G. Ferguson, 1958, **Paleozoic rocks of north-central Nevada**, American Association of Petroleum Geologists Bull., vol. 46, no. 11, pp. 2033-2056.

Roberts, R.J., K.M. Montgomery, and R.E. Lehner, 1967, **Geology and mineral resources of Eureka County**, Nevada Bureau of Mines and Geology, Bulletin 64.

Robinson, T.W., 1970, **Evapotranspiration by woody phreatophytes in the Humboldt River Valley near Winnemucca, Nevada**, U.S. Geological Survey Professional Paper 491-D, 41 p.

Robinson, B.P., W. Thordarson, and W.A. Beetam, 1967, **Hydrologic and chemical data for wells, springs, and streams in central Nevada, Townships 1 – 21 North and Ranges 41 – 57 East**, U.S. Geological Survey Open-File Report TEI-871, 61 p.

Rumbaugh, J.O., and D.B. Rumbaugh, 2007, **Groundwater Vistas (Version 5.21)**, Environmental Simulations Inc., Reinholds, Pennsylvania.

Rush, E.F., and D.E. Everett, 1964, **Ground-water appraisal of Monitor, Antelope, and Kobeh Valleys, Nevada**, U.S. Geological Survey Ground-Water Resources Reconnaissance Series Report 30, 45 p.

_____, 1966, **Water-resources appraisal of Little Fish Lake, Hot Creek, and Little Smoky Valleys, Nevada**, U.S. Geological Survey Water Resources-Reconnaissance Series Report 38, 37 p. with 1 plate.

Rush, F.E., B.R. Scott, A.S. Van Denburgh, and B.J. Vasey, 1971, **State of Nevada water resources and inter-basin flows**, U.S. Geological Survey Field Studies Map, scale 1:750,000.

Russell, C.E., and T. Minor, 2002, **Reconnaissance estimates of recharge based on an elevation-dependent chloride mass-balance approach**, Nevada Nuclear Security Administration, USDOE, Publication No. 45164.

Saltus, R.W., and R.C. Jachens, 1995, **Gravity and basin-depth maps of the Basin and Range Province, western United States**, U.S. Geological Survey Geophysical Investigations Map GP-1012, 1:2,500,000.

Sandberg, C.A., J.R. Morrow, and F.G. Poole, 2001, **Significance of type Devils Gate Limestone on Devonian proto-Antler forebulge, west of Eureka, Nevada**, Nevada Petroleum Society 2001 Summer Field Trip, Structure and Stratigraphy of the Eureka, Nevada Area, pp. 59-71.

Schaefer, D.H., S.A. Thiros, and M.R. Rosen, 2005, **Ground-water quality in the carbonate-rock aquifer of the Great Basin, Nevada and Utah, 2003**, U.S. Geological Survey Scientific Investigations Report, 2005-5232.

Scott, B.R., T.J. Smales, F.E. Rush, and A.S. Van Denburgh, 1971, **Nevada's water resources**, Nevada Division of Water Resources, Water for Nevada Report 3, 87 p.

Shepherd Miller Inc., 1997, **Baseline geochemistry and hydrology for the proposed Olinghouse open-pit gold mine, Washoe County, Nevada**, prepared for Alta Gold Company, Shepherd Miller Inc., Fort Collins, Colorado, 9 numbered sections, 10 appendices.

Shevenell, L., and L. Garside, 2005, **Nevada geothermal resources**, 2nd edition, Nevada Bureau of Mines and Geology Map 141.

Singer, D.A., ed., 1996, **An analysis of Nevada's metal-bearing mineral resources**, Nevada Bureau of Mines and Geology Open-File Report 96-2, scale 1:1,000,000.

Smith, J.L., R.J. Laczniak, M.T. Moreo, and T.L. Welborn, 2007, **Mapping evapotranspiration units in the Basin and Range carbonate-rock aquifer system, White Pine County, Nevada, and adjacent parts of Nevada and Utah**, U.S. Geological Survey Scientific Investigations Report 2007-5087, 20 p.

Sneed, Michelle, 2001, **Hydraulic and mechanical properties affecting ground-water flow and aquifer-system compaction, San Joaquin Valley, California**, U.S. Geological Survey Open-File Report 01-35.

Soil Conservation Service, 1981, **Nevada irrigation guide**, USDA document NV210-VI-NVIG.

SRK Consulting, 2008a, **Mount Hope Project, Baseline surface water and groundwater report**, BLM Review Draft January 11, 2008, 50 p. and appendices.

_____, 2008b, **Mount Hope Project, Regional spring and seep inventory, Fall 2007, January 2008**, BLM review draft, 9 p. and appendices.

_____, 2010, **Mount Hope Project, Plan of Operations and Reclamation Permit Application NVN - 082096**, January 2010.

Stearns, N.D., H.T. Stearns, and G.A. Waring, 1937, **Thermal springs in the United States**, U.S. Geological Survey Water-Supply Paper 679-B.

Stewart, J.H., and J.E. Carlson, 1974, **Preliminary geologic map of Nevada**, U.S. Geological Survey Miscellaneous Field Studies MF-609, scale 1:500,000.

Stewart, J.H., and J.E. Carlson, 1978, **Geologic map of Nevada in spatial digital database for the geologic map of Nevada**, ed. G.L. Raines, K.A. Connors, L.A. Moyer, and R.J. Miller, U.S. Geological Survey Open File Report 03-66, 2003, Digital database version 3.0.

Stewart, J.H., 1980, **Geology of Nevada, A discussion to accompany the geologic map of Nevada**, Nevada Bureau of Mines and Geology Special Publication 4, 120 p.

Stone, D.B., C.L. Moomaw, and A. Davis, 2001, **Estimating recharge distribution by incorporating runoff from mountainous areas in an alluvial basin in the Great Basin region of the southwestern United States**, Ground Water, Journal of the Association of Ground Water Scientists and Engineers, vol. 39, no. 6, pp. 807-818.

Tanner, C.B., 1960, **Energy balance approach to evapotranspiration from crops**, Soil Sci. Soc. Am. Proc., 24, pp. 1-9.

Terzaghi, K., 1925, **Principles of soil mechanics, IV, Settlement and consolidation of clay**, Engineering News-Record 95, no. 22:874-878.

Theis, C.V., 1935, **The relationship between the lowering of the piezometric surface and the rate and duration of discharge of a well using ground-water storage:** American Geophysical Union, Transactions, vol. 16, pp. 519-524; reprinted in Society of Petroleum Engineers, Pressure Transient Testing Methods, SPE Reprint Series (14), pp. 27-32, Dallas, Texas.

Thomas, J.M., J.L. Mason, and J.D. Crabtree, 1986, **Ground-water levels in the Great Basin region of Nevada, Utah, and adjacent states**, U.S. Geological Survey Hydrologic Investigations Atlas HA-694-B, scale 1:1,000,000.

Thomas, J.M., A.H. Welch, and M.D. Dettinger, 1997, **Geochemistry and isotope hydrology of representative aquifers in the Great Basin region of Nevada, Utah, and adjacent states**, U.S. Geological Survey Professional Paper 1409-C.

Todd, D.K., 1980, **Groundwater hydrology**, 2nd Edition, John Wiley & Sons Publishers, New York, 535 p.

Tosdal, R.M., 2000, **Reactivation of Neoproterozoic continental rift faults during formation of Eocene sedimentary rock-hosted Au deposits in Nevada (U.S.A.)**, Canadian Society of Economic Geologists, Abstracts with Programs.

Tumbusch, M.L., and R.W. Plume, 2006, **Hydrogeologic framework and ground water in basin-fill deposits of the Diamond Valley Flow System, central Nevada**, U.S. Geological Survey Scientific Investigations Report 2006-5249, 38 p. with 1 plate.

U.S. Geological Survey (USGS), 2009, **The numeric time scale**, downloaded from http://pubs.usgs.gov/gip/fossils/fig15.gif.

Walker, L.G., 1962, **Geology of the Mount Hope area, Garden Valley quadrangle, Nevada**, M.S. thesis, Univ. California, Los Angeles, scale 1:24,000.

Walton, W.C., 1962, **Selected analytical methods for well and aquifer evaluation**, Illinois State Water Survey, Board of Natural Resources and Conservation, Bulletin 49, 17 p.

_____, W.C., 1987, **Ground-water pumping test, design and analysis**, Lewis Publishers Inc., Chelsea, Michigan, 201 p.

Waring, G.A., 1965, **Thermal springs of the United States and other countries of the world**, U.S. Geological Survey Professional Paper 492.

Watermark Numerical Computing, 2002, **PEST Model-Independent Parameter Estimation Model User's Guide**, 275 p.

Watson, P., P. Sinclair, and R. Waggoner, 1976, **Quantitative evaluation of a method for estimating recharge to the desert basins of Nevada**, Journal of Hydrology 31, pp. 335-357.

Weeks, E.P., H.L. Weaver, G.S. Campbell, and B.T. Tanner, **Water use by saltcedar and by replacement vegetation in the Pecos River floodplain between Acme and Artesia, New Mexico**, U.S. Geological Survey Professional Paper 491-G, 33 p.

Western Regional Climate Center (WRCC), 2008, **Desert Research Institute**, online database at: http://www.wrcc.dri.edu/, accessed March 2008 through January 2009.

Welch, A.H., Bright, D.J., Knochenmus, L.A., 2007, **Water resources of the Basin and Range carbonate-rock aquifer system, White Pine County, Nevada, and adjacent areas in Nevada and Utah**, U.S. Geological Survey Scientific Investigations Report, 2007-5261.

White, D.E., 1955, **Thermal springs and epithermal ore deposits**, Economic Geology, Fiftieth Anniversary Volume, pp. 100-154.

White, W.N., 1932, **A Method of estimating ground-water supplies based on discharge by plants and evaporation from soil - Results of investigations in Escalante Valley, Utah**, in *"Contributions to the Hydrology of the United States, 1932"*, U.S. Geological Survey Water-Supply Paper 659A, pp. 1-105.

Yigit, O., Nelson, E.P., Hitzman, M.W. and Hofstra, A.H., 2003, **Structural controls on Carlin-type gold mineralization in the Gold Bar district, Eureka County, Nevada**, *Economic Geology*, vol.98, pp.1173-1188.

Zoback, M.C., Zoback, M.D., Schiltz, M.E., 1984, **Index of stress data for the North American and parts of the Pacific Plate**, U.S. Geological Survey Open-File Report 84-157, 62 p.

No Tables in Chapter 1

TABLE 2.0-1 UNDERGROUND WATER RIGHTS COMMITMENT STATUS BY HYDROGRAPHIC BASIN

HYDROGRAPHIC BASIN AND NDWR BASIN NO.	MANNER OF USE*	MARCH 2010 COMMITTED DUTY (AF/yr)	EST. PERENNIAL YIELD (AF/yr)	REFERENCE FOR PERENNIAL YIELD
Kobeh (No. 139)	ALL Uses	12,583	16,000	Rush and Everett (1964)
	IRR	1,044		
	MM	11,300		
	STK	239		
Antelope (No. 151)	ALL Uses	3,080	4,000	Rush and Everett (1964)
	IRR	2,906		
	STK	175		
Diamond (No. 153)	ALL Uses	132,136	30,000	Harrill (1968)
	IRR	126,973		
	MM	2,000		
	MUN	1,679		
	QM	508		
	STK	940		
	COM	3		
	DOM	34		
Pine Valley (No. 53)	ALL Uses	15,361	20,000	Eakin (1961)
	IRR	14,210		
	MM	928		
	STK	222		

AF/yr = acre-feet per year

(*) IRR = irrigation
MM = mining and milling
STK = stock watering
MUN = municipal
QM = quasi-municipal
COM = commercial
DOM = domestic
ALL = All manners of use for the basin

TABLE 3.1-1 2009 GEOLOGIC TIME SCALE

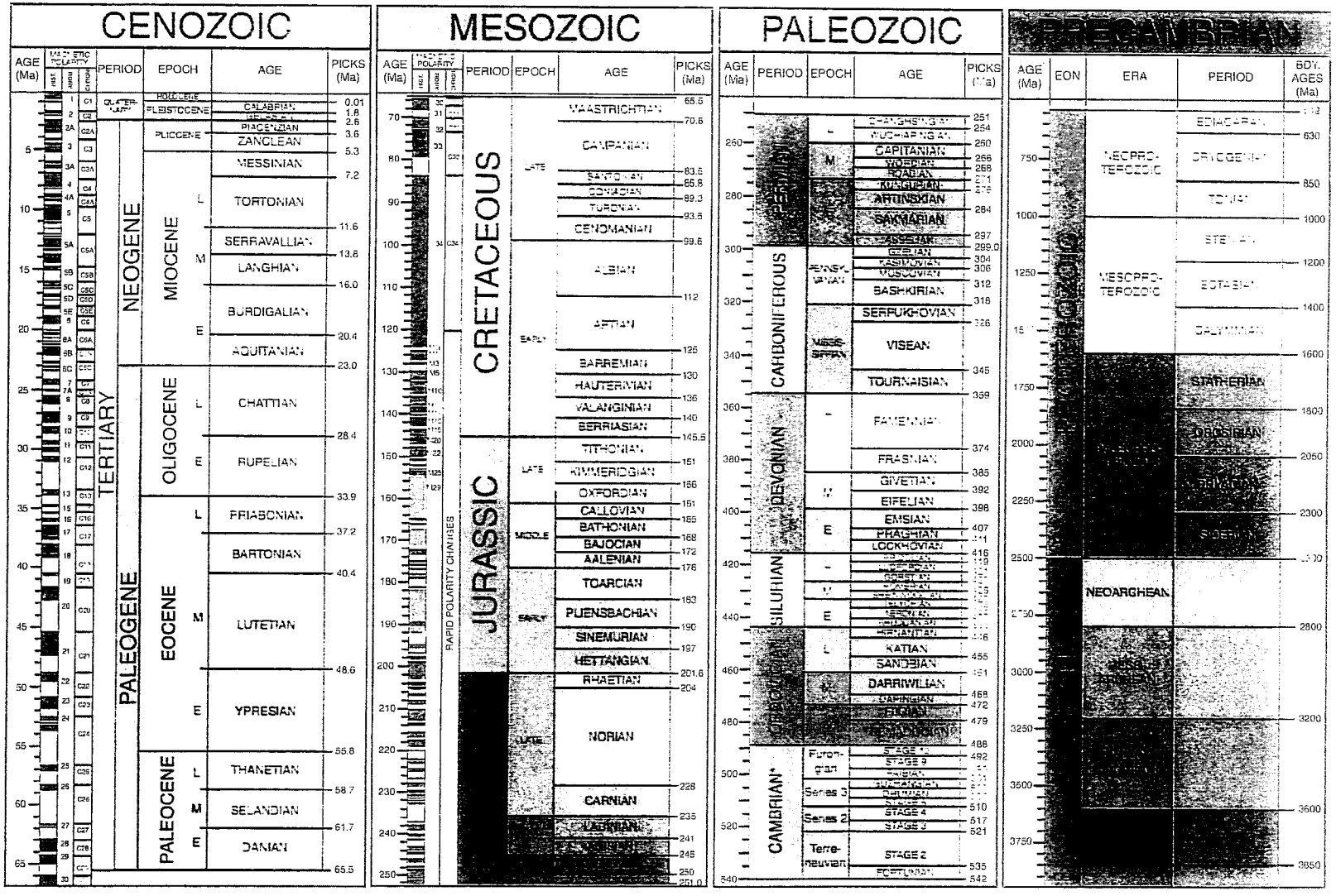

*International ages have not been fully established. These are current names as reported by the International Commission on Stratigraphy.

Sources for nomenclature and ages are primarily from Gradstein, F., Ogg, J., Smith, A., et al., 2004, A Geologic Time Scale 2004: Cambridge University Press, 589 p. Modifications to the Triassic after: Furin, S., Preto, N., Rigo, M., Roghi, G., Gianolla, P., Crowley, J.L., and Bowring, S.A., 2006, High-precision U-Pb zircon age from the Triassic of Italy: Implications for the Triassic time scale and the Carnian origin of calcareous nannoplankton and dinosaurs: Geology, v. 34, p. 1009–1012, doi: 10.1130/G22967A.1; and Kent, D.V., and Olsen, P.E., 2008, Early Jurassic magnetostratigraphy and paleolatitudes from the Hartford continental rift basin (eastern North America): Testing for polarity bias and abrupt polar wander in association with the central Atlantic magmatic province: Journal of Geophysical Research, v. 113, B06105, doi: 10.1029/2007JB005407.

THE GEOLOGICAL SOCIETY OF AMERICA®

TABLE 3.1-2 GEOLOGIC AND HYDROSTRATIGRAPHIC UNITS IN THE STUDY AREA

Group Name		HSU	Map Symbol	General Geological Characteristics
	Younger Valley-Fill	VF1		Valley-fill deposits - Thickness ranges from 0 ft along mountain fronts to more than 6,700 ft. in central Kobeh Valley. Younger alluvium comprises unconsolidated sand and gravel deposits ranging in thickness from 150 to 200 ft and is considered to have moderate to high production potential. Younger and Older alluvium may be consolidated and cemented, with low to moderate production potential.
	Older Valley-Fill			
	Volcaniclastic Sediments	VF2		Volcaniclastic sediments include re-worked ash-flow tuffs interbedded with the lacustrine sediments; the thickness of tuff units ranges from 10 ft to about 370 ft. Although usually not exposed at land surface in many locations, these rocks have been penetrated in the structural basins. Hydraulic properties of these units are not known but the production potential is likely low to moderate, and the units may likely be aquitards.
	Lacustrine Sediments	VF3		Lacustrine sediments include claystone, sandstone, freshwater limestone, and conglomerate with thicknesses of individual lithologies ranging from a few tens of feet to more than 260 ft, and with limited water production potential. Conglomerates are generally considered aquitard units except where intensely fractured. Minerals exploration holes in the vicinity of Lone Mountain have penetrated lost-circulation zones in the lower valley-fill units that may be productive horizons.
	Conglomerate			
	Basalt	VOL1		Extrusive Igneous/Volcanic Rocks: Numerous mafic dike swarms intrude the Paleozoic rocks and older volcanic rocks in the northern Nevada rift portions of the Roberts Mountains. Associated with these intrusive dikes are numerous basalt and andesite/dacite flows along the flanks of the rift may have moderate production potential at the base of flows or where intensely fractured. The rhyolite, andesite, and tuff units total as much as 1,000 ft. In general, the production potential of these units depends on the degree of welding, post-depositional deformation, and the degrees of mineralization and fracture filling. Because of the limited extent of these units in the Kobeh Valley watershed, they are not considered a primary target for development but may augment yields from wells drilled into underlying Paleozoic rocks.
	Rhyolite, Tuffs			
	Intrusive Igneous Rocks	VOL2		Intrusive Igneous Rocks: Intrusive igneous rocks occur at Mount Hope (quartz porphyry) and Whistler Mountains (alaskite), and are generally not prolific aquifer units.
	Garden Valley Formation	AQT1		Siliciclastic Rocks: The Garden Valley Fm is limited in to the west slopes of the Sulfur Springs Mountains and a small portion of the western Roberts Mountians where the upper 1,000 ft thick silica cemented conglomerate member likely forms an effective flow barrier between portions of Pine and Kobeh Valley and Diamond Valley. The Vinini and Webb Fms outcrop in the Roberts and Sulfur Spring Mountains, and at Whistler Mountain, and may be as much as 2,000 feet thick. The lower Vinini comprises fine grained limestone, quartzite, and calcareous sandstone, the upper Vinini includes chert and shale. Likely only moderate production potential for development.
	Vinini and Webb Formations			
	Devils Gate Limestone	CA1		Carbonate Rocks: The Devils Gate LS is a thick-bedded limestone that can be more than 2,000 ft thick, outcropping in the Roberts Mountains, Devils Gate area, and the Mahogany Hills. Where fractured and dissolved, and not intruded, the Devils Gate LS may be very productive.
	Denay Limestone	CA2		Carbonate Units: These Paleozoic carbonates outcrop in the Roberts Mountains, the Sulfur Spring Range, and Lone Mountain areas, and in general have more dolomite and mudstone content than the overlying Devils Gate Limestone. Where sufficiently faulted, karsted, or fractured, the units may provide large quantities of water to wells.
	McColley Canyon Formation			
	Nevada Formation			
	Lone Mountain Dolomite	CA3		Dolomitic Units: The Roberts Mountains Fm and the Lone Mountain Dolomite are about 1,900-2,200 ft thick. Although they may be a productive aquifer where fractured and dissolved, they are not widespread at shallow depths in the Kobeh Valley watershed portion of the Roberts Mountains.
	Roberts Mountains Formation			
	Lower Eastern Assemblage	CA4		Siliciclastics and some Carbonate Rocks: The Lower Eastern Assemblage includes the Eureka Quartzite, Pogonip Group, and Hamburg Dolomite and, in Kobeh Valley is only exposed at Lone Mountain. These units are deeply buried in most of Kobeh Valley. Where sufficiently fractured, they may be water bearing.

HSU: Hydrostratigraphic Unit, Map Symbol refers to Appendix A of Kobeh Valley Well Field Data Summary Report, Interflow, 2010

TABLE 3.1-3 PETROLEUM LOGS FROM THE STUDY AREA

WELL NO. (Figure 3.1-4)	WELL NAME	AMERICAN PETROLEUM INSTITUTE NUMBER	ELEVATION (feet)	TOTAL DEPTH (feet)	DEPTH (feet)	UNIT	THICKNESS (feet)	UTM EASTING (feet)	UTM NORTHING (feet)
DIAMOND VALLEY									
1	Diamond Valley Federal No. 1–24	27-011-05206	5,780	8,900	0	Basin fill deposits	1,070	1932813.676	14510660.05
					1,070	Volcanic rocks	6,285		
					7,355	Carbonate rocks			
2	Diamond Valley Unit No. 1	27-011-05056	5,800	8,042	0	Basin fill deposits	7,500	1940032.732	14473415.93
					7,500	Carbonate rocks			
3	Walter L. Plaskett No. 1	27-011-05204	5,881	10,600	0	Basin fill deposits	1,070	1936611.046	14426233.95
					1,070	Volcanic rocks	6,285		
					7,355	Carbonate rocks			
4	Diamond Valley No. 1–11	27-011-05224	5,880	6,552	0	Basin fill deposits	2,248	1931362.447	14420710.2
					2,248	Volcanic rocks	2,132		
					4,380	Clastic sedimentary rocks	1,830		
					6,210	Carbonate rocks			
5	Black Point No. 6–41	27-011-05251	5,893	8,600	0	Basin fill deposits	4,242	1941768.875	14426092.76
					4,242	Volcanic rocks	530		
					4,773	Carbonate rocks			
6	Monte Federal No. 1–4	27-011-05287	5,900	4,055	0	Basin fill deposits	3,850	1951164.837	14424385.91
						Carbonate rocks			

TABLE 3.1-3 PETROLEUM LOGS FROM THE STUDY AREA

WELL NO. (Figure 3.1-4)	WELL NAME	AMERICAN PETROLEUM INSTITUTE NUMBER	ELEVATION (feet)	TOTAL DEPTH (feet)	DEPTH (feet)	UNIT	THICKNESS (feet)	UTM EASTING (feet)	UTM NORTHING (feet)
KOBEH VALLEY									
7	Willow Wash Federal No. 42–24	27-011-05225	6,210	7,834	0	Basin fill deposits	685	1808548.708	14407353.6
					685	Tuff/Volcanic Rocks	824		
					1,380	Clastic Sedimentary Rocks	1080		
					2,460	Volcanic Rocks	640		
					3,100	Carbonate Rocks	5336		
					7,796	Clastic Sedimentary Rocks			
8	N. Kobeh Valley Federal No. 13–10	27-011-05242	6,263	6,462	0	Basin fill deposits	830	1806879.907	14411489.61
					830	Volcanic rocks	746		
					1,576	Clastic sedimentary rocks	1,036		
					2,750	Carbonate rocks			
9	Lone Mountain Federal No. 15–1	27-011-05243	6,132	5,201	0	Basin fill deposits	1,400	1830707.912	14381616.72
					1,400	Carbonate rocks			
10	Stoneberger Creek Federal A No. 1–35	27-015-05006	6,267	5,050	0	Basin fill deposits	390	1741865.768	14330837.24
					390	Volcanic rocks	3,206		
					3,596	Clastic sedimentary rocks			
11	Twin Springs Federal No. 10–6	27-011-05247	6,270	8,031	0	Basin fill deposits	1,820	1828925.169	14326579.5
					1,820	Volcanic rocks	4,804		
					6,624	Carbonate rocks			

TABLE 3.1-3 PETROLEUM LOGS FROM THE STUDY AREA

WELL NO. (Figure 3.1-4)	WELL NAME	AMERICAN PETROLEUM INSTITUTE NUMBER	ELEVATION (feet)	TOTAL DEPTH (feet)	DEPTH (feet)	UNIT	THICKNESS (feet)	UTM EASTING (feet)	UTM NORTHING (feet)
12	Hot Creek Wash Federal No. 15–1	27-011-05286	6,316	5,940	0	Basin fill deposits	1,535	1828043.033	14318582.5
					1,535	Volcanic rocks	4,325		
					5,860	Carbonate rocks			
13	Silver State Federal No. 33–18	27-011-5208	5,875	9,120	0	Basin fill deposits	2,960	1813564	14385898
					2,960	Volcanic rocks	3,760		
					6,720	Carbonate rocks	892		
					7,512	Lower Eastern Assemblage	1,608		
ANTELOPE VALLEY									
14	Cedar Creek No. 2–1	27-011-05284	6,283	5,660	0	Basin fill deposits	1,860	1840886.239	14301384.45
					1,860	Volcanic rocks	3,402		
					5,262	Clastic sedimentary rocks			
PINE VALLEY									
15	Blackburn No. 12	27-011-05218	5,275	8426	0	Basin fill deposits	3,362	1879416.217	14614491.08
					3,362	Volcanic rocks	4,341		
					7,703	Carbonate rocks			
16	Blackburn No. 1	27-011-05205	5,454	4893	0	Basin fill deposits	2,745	1880704.655	14601554.6
					2,745	Volcanic rocks			
17	Blackburn No. 6	27-011-05214	5,335	7651	0	Basin fill deposits	3,371	1882351.768	14607640.44
					3,371	Volcanic rocks	1,164		
					4,535	Tertiary basin fill	2,880		
					7,415	Granitic rocks			

Data from Nevada Bureau of Mines and Geology: <*http://www.nbmg.unr.edu/lists/oil/oil.htm*>. Modified from Tumbusch and Plume, 2006

TABLE 3.2-1 COMPARISON OF DRAINAGE AREAS IN AND ADJACENT TO THE STUDY AREA

BASIN NAME	BASIN NUMBER	AREA (ACRES)[1] TUMBUSCH AND PLUME (2006)	AREA (ACRES)[1] RECONNAISSANCE SERIES REPORTS	AREA (ACRES)[1] THIS STUDY
Antelope Valley	151	288,000	292,000	287,000
Diamond Valley	153	480,000	550,000	479,000
Kobeh Valley	139	550,000	560,000	552,000
North Monitor Valley	140A	339,000	335,000	337,000
Pine Valley	053	---	638,000	640,000
Pine Valley (minus Garden)	---	---	---	562,000
Garden Valley	---	---	---	78,000

[1]Rounded to nearest 1,000 acres

TABLE 3.2-2 PRECIPITATION STATION AVERAGES IN AND NEAR THE STUDY AREA

STATION	STATION ID[1]	UTM EASTING[1] (feet)	UTM NORTHING[1] (feet)	STATION AVERAGE PRECIPITATION[1] (inches per year)	ELEVATION[1] (feet, amsl)[3]	30-YEAR 1971-2000 NWS, NORMAL PRECIPITATION[2] (inches per year)
Austin	260507	1621436	14344546	13.02	6,600	14.33
Eureka	262708	1931877	14352142	12.02	6,540	12.06
Beowawe	260795	1788623	14739545	8.69	4,700	8.84
Beowawe UNR	260800	1757233	14490488	10.63	5,740	11.04
Jiggs	264086	2015994	14693455	11.09	5,420	---
Jiggs Zaga	264095	2025848	14657173	14.28	5,800	13.35
Pine Valley Bailey	266242	1886189	14685795	10.57	5,050	10.24
Snowball Ranch	267640	1867571	14175755	9.02	7,160	8.81
Diamond USDA	262296	1912388	14412864	9.14	5,970	9.14
Ruby Lake	267123	2059185	14602970	12.93	6,010	13.66
Fish Creek Ranch	262860	1923180	14261408	4.82	6,050	---
Cortez Mine	261975	1742093	14593668	9.61	4,910	---

[1]Data from Jeton et al. (2005), from PRISM datasets 1961-1990 and 1971-2000
[2]Data from Western Regional Climate Center (2008)
[3]feet, amsl = feet above mean sea level
--- = not available

TABLE 3.2-3 SUMMARY OF BLM COILS CREEK WATERSHED PRECIPITATION DATA 1963 TO 1980

BLM SITE 6-2 CAN NO.	UTM EASTING (feet)	UTM NORTHING (feet)	ELEVATION (feet, amsl)	AVERAGE ANNUAL PRECIPITATION (inches)
1	1804760	14448901	6,800	10.86
2	1796857	14439747	6,520	10.78
3	1912397	14212833	7,820	11.58
4	1917503	14212705	7,160	12.42
5	1885164	14208736	6,560	11.29
6	1877729	14215342	6,800	11.45
7	1774880	14164416	7,400	11.09
8	1877308	14163330	6,810	11.30
9	1887781	14221748	6,620	11.26
10	1888062	14172777	6,750	11.15
11	1878308	14183305	7,000	11.96
12	1916902	14180595	6,750	9.38
13	1880074	14186720	7,200	11.99
14	1890788	14184515	7,060	11.02
15	1898817	14171850	7,080	10.51
16	1906760	14163678	7,480	12.31
17	1899563	14163544	7,020	12.85
18	1902055	14216609	7,000	11.83
19	NR	NR	7,060	11.71
20	NR	NR	6,440	11.39

NR = not reported
feet, amsl = feet above mean sea level

TABLE 3.2-4 COMPARISON OF ANNUAL PRECIPITATION DETERMINED BY USGS RECONNAISSANCE REPORT STUDIES AND THIS STUDY FOR MT. HOPE STUDY AREA BASINS

BASIN NAME	USGS INVESTIGATOR	USGS METHOD	USGS REPORTED VOLUME OF ANNUAL PRECIPITATION[1] (AF/yr)	VOLUME OF ANNUAL PRECIPITATION USING 1971-2000 PRISM DATA[1] (AF/yr) THIS STUDY	PERCENT DIFFERENCE
Kobeh Valley	Rush and Everett (1964)	Hardman Map	460,000	544,200	+18.3
North Monitor Valley	Rush and Everett (1964)	Hardman Map	230,000	388,000	+68.7
Antelope Valley	Rush and Everett (1964)	Hardman Map	190,000	255,600	+34.5
Pine Valley	Eakin (1961)	Hardman Map	654,200	668,200	+2.1
Pine Valley	Berger (2000a)	PRISM, 1961-1990	688,000	668,200	-2.9
Garden Valley part of Pine Valley	Harrill (1968)	Hardman Map	97,000	91,400	-5.8
Diamond Valley	Harrill (1968), Eakin (1962)	Hardman Map	409,900	503,500	+22.8
MEAN					**+19.7**

[1]Rounded to nearest 100 AF/yr
AF/yr = acre-feet per year

TABLE 3.2-5 HYDROLOGIC COMPONENTS OF THE USGS AND STATE OF NEVADA GROUNDWATER BUDGETS FOR VALLEYS IN AND NEAR THE STUDY AREA

HYDROGRAPHIC AREA	AREA, IN ACRES/PRECIPITATION (AF/yr)		POTENTIAL GROUNDWATER RECHARGE (AF/yr)	ET (AF/yr)	GROUNDWATER MOVEMENT DIRECTION AND VOLUME (AF/yr)	MOUNTAIN FRONT RUNOFF[5] (AF/yr)
	<7,000 feet, amsl	>7,000 feet, amsl				
Monitor Valley South[1]	86,200/43,000	255,800/ 237,000	15,000	9,200	2,000 to N.	44,000
North Monitor Valley[1]	140,000/70,000	215,000/ 160,000	6,300 + 2,000 from Monitor S.	2,000	N. to Kobeh, 6,000	23,000
Antelope Valley[1]	161,000/80,000	131,000/ 110,000	4,100	4,200	0	14,000
Stevens Basin[1]	- 0 -	11,800/ 8,500	200	0	200 to Antelope or Diamond	500
Kobeh Valley[1]	470,000/350,000	90,000/ 74,000	11,000 + 6,000 from Monitor N.	15,000	< 100 to Diamond	9,000
Garden Valley[2]	80,100/97,000	ND	10,000	1,000	9,000 E. to Diamond[4]	ND
Pine Valley[2,3]	All precipitation is effective	638,000/ 654,800[2] 645,000/ 688,000[3]	46,000[2] 52,500-79,300[3]	24,000[2] 45,000[3]	N. to the Humboldt 300[2]	31,000, outflow = 8,000[3]
Diamond Valley North Sub-Area[4]	< 5,840' elevation 119,300/76,000	> 5,840' elevation 75,500/ 89,600	9,000	29,000	NA	1,400
Diamond Valley South Sub-Area[4]	< 6,000' elevation 17,400/10,000	> 6,000' elevation 258,400/ 234,300	12,000	1,400	11,000 to N. Diamond	4,400

[1] Rush and Everett (1964)
[2] Eakin (1961) included Garden Valley with Pine Valley
[3] Berger (2000a) included Garden with Pine
[4] Harrill (1968: Table 7)
[5] Scott et al. (1971) provide mountain-front runoff calculations except for Diamond Valley, which is provided in Harrill (1968)
feet amsl = feet above mean sea level
AF/yr = acre-feet per year
ET = evapotranspiration
ND = not determined
NA = not applicable

TABLE 3.2-6 CHECK OF MAXEY-EAKIN RECHARGE ESTIMATES IN USGS RECONNAISSANCE SERIES REPORTS

BASIN NAME	ELEVATION ZONE (feet amsl)	ACRES (THIS STUDY)	USGS ANNUAL PRECIP. (feet)	TOTAL PRECIP. (AF/yr)	USGS ASSUMED RECHARGE EFFICIENCY	RECHARGE ESTIMATE (THIS STUDY) USING MAXEY-EAKIN METHOD (AF/yr)	USGS REPORTED RECHARGE (AF/yr)
Kobeh Valley	5,000-6,000	3,571	0.4	1,500	0%	0	
	6,000-7,000	428,377	0.8	321,282	0%	0	
	7,000-8,000	96,006	1.1	107,526	7%	7,527	
	8,000-9,000	21,564	1.5	31,484	15%	4,723	
	9,000-10,000	2,349	1.8	4,111	25%	1,028	
	10,000-11,000	98	1.8	171	25%	43	
	Total	**551,965**			**Total**	**13,321**	11,000
Antelope Valley	6,000-7,000	158,122	0.5	79,061	0%	0	
	7,000-8,000	86,468	0.7	60,528	2%	1,211	
	8,000-9,000	36,947	1.0	36,947	5%	1,847	
	9,000-10,000	5,464	1.4	7,650	12%	918	
	10,000-11,000	103	1.7	175	22%	39	
	Total	**287,104**			**Total**	**4,015**	4,100
Pine Valley (Model Area Only, includes Garden Valley)	5,000-6,000	199,076	0.8	165,233	3%	4,957	
	6,000-7,000	187,110	1.1	209,563	7%	14,669	
	7,000-8,000	60,411	1.5	88,200	15%	13,230	
	8,000-9,000	8,237	1.8	14,416	25%	3,604	
	9,000-10,000	1,525	1.8	2,670	25%	667	
	Total	**456,359**			**Total**	**37,127***	46,000
	* For southern portion of Pine Valley only – not the total basin as reported in USGS Reconnaissance Series Report						
Garden Valley	5,000-6,000	62	0.8	49	3%	1	
	6,000-7,000	56,991	1.1	62,690	7%	4,388	
	7,000-8,000	18,150	1.5	27,225	15%	4,084	
	8,000-9,000	2,597	1.8	4,674	25%	1,169	
	9,000-10,000	548	1.8	987	25%	247	
	Total	**78,348**			**Total**	**9,889**	10,000
North Diamond Valley Subarea	<5840	107,430	0.6	64,458	0%	0	
	5,800-6,000	23,073	0.8	18,458	3%	554	
	6,000-7,000	48,620	1.1	53,482	7%	3,744	
	7,000-8,000	16,050	1.5	24,075	15%	3,611	
	>8000	5,223	1.8	9,401	25%	2,350	
	Total	**200,396**			**Total**	**10,259**	9,000
South Diamond Valley Subarea	5,000-6,000	118,402	0.6	71,041	0%	0	
	6,000-7,000	97,422	0.8	77,938	3%	2,338	
	7,000-8,000	47,733	1.1	52,507	7%	3,675	
	8,000-9,000	12,492	1.5	18,739	15%	2,811	
	9,000-10,000	2,066	1.8	3,719	25%	930	
	10,000-11,000	148	1.8	266	25%	67	
	Total	**278,263**			**Total**	**9,821**	12,400

Data Source: Maxey and Eakin (1949)
AF/yr = acre-feet per year

1212.1/Report/Tables/Tbl3.2-6_Makey-EakinRechargeEst.doc/21Apr2010

TABLE 3.3-1 HISTORIC SPRING DISCHARGE MEASUREMENTS FOR THE STUDY AREA

SPRING NO. (APPENDIX B)	SPRING NAME	BASIN NAME	UTM EASTING (feet)	UTM NORTHING (feet)	DATE	DISCHARGE (cfs)
542	Tule Dam Springs[1]	Diamond Valley	1903405	14471488	11/16/1965	0.12
560, 562, 564, 567, 570	Sulphur Springs[1]	Diamond Valley	1902211	14466316	11/18/1965	0.09
185, 187	Flynn Ranch Springs[1]	Diamond Valley	1910044	14557348	9/22/1965	0.02
330	Shipley Hot Spring[1]	Diamond Valley	1900352	14495127	9/22/1965	7.19
330	Shipley Hot Spring[1]	Diamond Valley	1900352	14495127	4/1/1965	7.01
330	Shipley Hot Spring[1]	Diamond Valley	1900352	14495127	10/19/1966	6.20
330	Shipley Hot Spring[3]	Diamond Valley	1900352	14495127	1977	5.58
330	Shipley Hot Spring[3]	Diamond Valley	1900352	14495127	1982	6.03
330	Shipley Hot Spring[3]	Diamond Valley	1900352	14495127	Jan-84	8.26
330	Shipley Hot Spring[3]	Diamond Valley	1900352	14495127	Oct-84	6.03
330	Shipley Hot Spring[3]	Diamond Valley	1900352	14495127	Jan-85	5.92
330	Shipley Hot Spring[3]	Diamond Valley	1900352	14495127	Mar-85	5.36
330	Shipley Hot Spring[3]	Diamond Valley	1900352	14495127	Jan-86	5.13
330	Shipley Hot Spring[3]	Diamond Valley	1900352	14495127	May-86	5.36
330	Shipley Hot Spring[3]	Diamond Valley	1900352	14495127	Jun-87	7.81
330	Shipley Hot Spring[3]	Diamond Valley	1900352	14495127	Jan-88	6.03
330	Shipley Hot Spring[3]	Diamond Valley	1900352	14495127	Apr-89	8.26
330	Shipley Hot Spring[3]	Diamond Valley	1900352	14495127	Apr-90	7.59
330	Shipley Hot Spring[3]	Diamond Valley	1900352	14495127	Jan-91	8.04
330	Shipley Hot Spring[3]	Diamond Valley	1900352	14495127	5/7/2008	3.56
288	Siri Ranch Spring[1]	Diamond Valley	1908062	14524546	12/7/1965	0.66
288	Siri Ranch Spring[1]	Diamond Valley	1908062	14524546	4/1/1965	0.82

TABLE 3.3-1 HISTORIC SPRING DISCHARGE MEASUREMENTS FOR THE STUDY AREA

SPRING NO. (APPENDIX B)	SPRING NAME	BASIN NAME	UTM EASTING (feet)	UTM NORTHING (feet)	DATE	DISCHARGE (cfs)
357	Unnamed Spring at Bailey Ranch[1]	Diamond Valley	1901832	14495143	12/7/1965	1.14
285	Siri Ranch Spring[1]	Diamond Valley	1908386	14523335	12/7/1965	0.58
352/353	Thompson Ranch Spring[1]	Diamond Valley	1957805	14492451	9/21/1965	1.14
352/353	Thompson Ranch Spring[1]	Diamond Valley	1957805	14492451	4/1/1966	0.58
352/353	Thompson Ranch Spring[1]	Diamond Valley	1957805	14492451	10/19/1966	2.06
352/353	Thompson Ranch Spring[3]	Diamond Valley	1957805	14492451	1981	0.04
352/353	Thompson Ranch Spring[3]	Diamond Valley	1957805	14492451	1982	0.28
352/353	Thompson Ranch Spring[3]	Diamond Valley	1957805	14492451	Oct-82	1 79
352/353	Thompson Ranch Spring[3]	Diamond Valley	1957805	14492451	1982	1.56
352/353	Thompson Ranch Spring[3]	Diamond Valley	1957805	14492451	Jun-82	1.34
352/353	Thompson Ranch Spring[3]	Diamond Valley	1957805	14492451	Jul-82	1 17
352/353	Thompson Ranch Spring[3]	Diamond Valley	1957805	14492451	Oct-82	0.56
352/353	Thompson Ranch Spring[3]	Diamond Valley	1957805	14492451	May-83	2.68
352/353	Thompson Ranch Spring[3]	Diamond Valley	1957805	14492451	Jul-83	4.23
352/353	Thompson Ranch Spring[3]	Diamond Valley	1957805	14492451	Mar-84	4.08
352/353	Thompson Ranch Spring[3]	Diamond Valley	1957805	14492451	Aug-84	3.13

TABLE 3.3-1 HISTORIC SPRING DISCHARGE MEASUREMENTS FOR THE STUDY AREA

SPRING NO. (APPENDIX B)	SPRING NAME	BASIN NAME	UTM EASTING (feet)	UTM NORTHING (feet)	DATE	DISCHARGE (cfs)
352/353	Thompson Ranch Spring[3]	Diamond Valley	1957805	14492451	Oct-84	3.35
352/353	Thompson Ranch Spring[3]	Diamond Valley	1957805	14492451	Oct-85	2.57
352/353	Thompson Ranch Spring[3]	Diamond Valley	1957805	14492451	Dec-85	2.46
352/353	Thompson Ranch Spring[3]	Diamond Valley	1957805	14492451	Jan-87	1.95
352/353	Thompson Ranch Spring[3]	Diamond Valley	1957805	14492451	Jul-87	0.84
352/353	Thompson Ranch Spring[3]	Diamond Valley	1957805	14492451	Feb-88	0.56
352/353	Thompson Ranch Spring[3]	Diamond Valley	1957805	14492451	Jan-89	0.51
352/353	Thompson Ranch Spring[3]	Diamond Valley	1957805	14492451	Feb-89	0.56
352/353	Thompson Ranch Spring[3]	Diamond Valley	1957805	14492451	Jul-90	0.11
352/353	Thompson Ranch Spring[3]	Diamond Valley	1957805	14492451	Oct-81	0.04
352/353	Thompson Ranch Spring[6]	Diamond Valley	1957805	14492451	7-Oct	0
930	Klobe Spring[3]	Antelope Valley	1824003	14313192	4/1/1964	1.11
559	Jack Spring[4]	Kobeh Valley	1801823	14468707	Oct-80	dry
742	Lone Mountain Spring[4]	Kobeh Valley	1841235	14386250	Oct-80	dry
721	Mud Spring[4]	Kobeh Valley	1842433	14393036	Oct-80	dry
907	Jack Rabbit Spring[4]	Kobeh Valley	1778961	14328787	Oct-80	dry
824	Hot Spring Hill[4]	Kobeh Valley	1820728	14365562	Oct-80	0.004
845	Warm Springs[4]	Kobeh Valley	1812892	14354989	Oct-80	dry

TABLE 3.3-1 HISTORIC SPRING DISCHARGE MEASUREMENTS FOR THE STUDY AREA

SPRING NO. (APPENDIX B)	SPRING NAME	BASIN NAME	UTM EASTING (feet)	UTM NORTHING (feet)	DATE	DISCHARGE (cfs)
797	Unnamed Spring[4]	Kobeh Valley	1884103	14376760	Oct-80	0.03
912	Antelope Wash (aka Antelope Spring)[5]	Kobeh Valley/ Antelope Valley	1845028	14342786	Apr-64	dry
1038	Bald Mtn. Spring[4]	Antelope Valley	1796783	14273768	Sep-80	0.004
1067	Water Canyon Spring[4]	Antelope Valley	1843168	14221196	Sep-80	0.007
1039	Sullivan Spring[5]	Antelope Valley	1814318	14272162	Apr-64	dry
1060	Rye Grass Spring[4]	Antelope Valley	1800686	14227672	Sep-80	0.002
912	Springs at Kitchen Meadow	Antelope Valley	1899863	14488652	Apr-64	0.27
77	Bruffey's Hot Springs	Pine Valley	1899996	14607850	June 2007	0.11
83	Austin/ Edward's Spring[5]	Pine Valley	1898148	14603527	1960	1.0

[1] Harrill (1968)
[2] Rush and Everett (1964)
[3] Arteaga et al. (1995)
[4] Ertec Western (1981)
[5] Eakin(1962)
[6] This study
cfs = cubic feet per second

Note: Thompson Ranch Spring is also known as Taft Spring

TABLE 3.3-2 SUMMARY OF TONKIN AND SHIPLEY SPRING FLOW MEASUREMENTS, 2007-2009

SPRING NO. (APPENDIX B)	SPRING NAME	BASIN NAME	UTM EASTING (feet)	UTM NORTHING (feet)	DATE	DISCHARGE (cfs)
378	Tonkin Spring	Pine Valley	1803780	14490281	8/21/2007	2.42
378	Tonkin Spring	Pine Valley	1803780	14490281	10/11/2007	2.32
378	Tonkin Spring	Pine Valley	1803780	14490281	12/10/2007	2.07
378	Tonkin Spring	Pine Valley	1803780	14490281	4/15/2008	1.58
378	Tonkin Spring	Pine Valley	1803780	14490281	5/6/2008	1.64
378	Tonkin Spring	Pine Valley	1803780	14490281	8/21/2008	1.73
378	Tonkin Spring	Pine Valley	1803780	14490281	11/4/2008	2.01
378	Tonkin Spring	Pine Valley	1803780	14490281	1/6/2009	1.66
378	Tonkin Spring	Pine Valley	1803780	14490281	2/27/2009	1.59
378	Tonkin Spring	Pine Valley	1803780	14490281	3/31/2009	1.17
378	Tonkin Spring	Pine Valley	1803780	14490281	5/7/2009	1.53
378	Tonkin Spring	Pine Valley	1803780	14490281	6/22/2009	1.46
378	Tonkin Spring	Pine Valley	1803780	14490281	7/21/2009	1.60
378	Tonkin Spring	Pine Valley	1803780	14490281	8/21/2009	1.60
378	Tonkin Spring	Pine Valley	1803780	14490281	9/22/2009	1.64
330	Shipley Hot Spring	Diamond Valley	1900352	14495127	5/7/2008	3.56
330	Shipley Hot Spring	Diamond Valley	1900352	14495127	1/6/2009	3.00
330	Shipley Hot Spring	Diamond Valley	1900352	14495127	2/25/2009	3.11
330	Shipley Hot Spring	Diamond Valley	1900352	14495127	3/31/2009	2.08
330	Shipley Hot Spring	Diamond Valley	1900352	14495127	5/9/2009	2.90
330	Shipley Hot Spring	Diamond Valley	1900352	14495127	6/25/2009	2.88
330	Shipley Hot Spring	Diamond Valley	1900352	14495127	7/23/2009	2.36
330	Shipley Hot Spring	Diamond Valley	1900352	14495127	8/23/2009	3.06
330	Shipley Hot Spring	Diamond Valley	1900352	14495127	9/24/2009	2.56

cfs = cubic feet per second

TABLE 3.3-3 HISTORIC STREAM FLOW MEASUREMENTS IN THE STUDY AREA

STREAM NAME	BASIN NAME	UTM, EASTING (feet)	UTM, NORTHING (feet)	DATE	DISCHARGE (cfs)
Snow Water Canyon[1]	Kobeh Valley	1779584	14429227	May-64	2.5
Roberts Creek[2]	Kobeh Valley	1836428	14451050	Oct-80	0.9
Ackerman Canyon[2]	Kobeh Valley	1737610	14377548	Oct-80	0.002
Ackerman Canyon[2]	Kobeh Valley	1740355	14375941	Oct-80	0.04
Ackerman Canyon[3]	Kobeh Valley	1740355	14375941	May-64	0.5
Dagget Creek[3]	Kobeh Valley	1844904	14358160	May-64	1.5
Slough Creek[3]	Kobeh Valley	1866062	14374523	May-64	1.5
Slough Creek[3]	Kobeh Valley	1866062	14374523	May-64	2.46
Dry Creek[2]	Kobeh Valley	1710745	14357737	Oct-80	0.08
Willow Creek[3]	Kobeh Valley	1787087	14347342	May-64	1
Coils Creek[1]	Kobeh Valley	1794476	14433360	May-64	8
Nine Mile Creek[3]	Antelope Valley	1841714	14245964	May-64	1.5
Allison Creek[3]	Antelope Valley	1814440	14277321	Apr-64	1
Copenhagen Cyn[3]	Antelope Valley	1808760	14220846	May-64	2.01

[1] Rush and Everett (1964)
[2] Ertec Western (1981)
[3] Robinson et al. (1967)
cfs = cubic feet per second

TABLE 3.3-4 ROBERTS CREEK SEEPAGE RUN STATIONS AND DISCHARGE MEASUREMENTS

STATION NAME	STREAM/REACH NAME	UTM EASTING (feet)	UTM NORTHING (feet)	ELEVATION (feet, amsl)	DISCHARGE (cfs)	DATE
SR-1	Roberts Creek, Middle Fork	1831486.3	14461355	7,050	0.01	8/22/2007
SR-2	Roberts Creek, East Fork	1831887 7	14462718	7,130	0.24	8/22/2007
---	Roberts Creek, West Fork	1831486.3	14461355	7,050	0	8/22/2007
SR-3[1]	Roberts Creek	1834158.4	14457146	6,930	0.16	8/22/2007
					0.2	12/11/2007
SR-4	Roberts Creek	1835608	14452514	6,810	0.12	8/22/2007
SR-5	Roberts Creek	1836910.1	14448144	6,710	0.07	8/22/2007
SR-6	Roberts Creek	1837785.4	14442917	6,610	0.04	8/22/2007
					0.016	10/10/2007
					0	12/10/2007

[1] Recording gage installed 12/10/2007.
Elevations are approximate; obtained with handheld GPS
--- = No station name assigned
feet, amsl = feet above mean sea level
cfs = cubic feet per second

TABLE 3.3-5 HENDERSON CREEK SEEPAGE RUN DISCHARGE MEASUREMENTS

SITE	UTM EASTING (feet)	UTM NORTHING (feet)	DISCHARGE (cfs)	ELEVATION (feet, amsl)
Henderson Creek No. 1	1862273	14219998	0.06	7,120
No. 2	1860145	14464970	0.01	6,890
No. 3	1864277	14467574	0.01	6,720
No. 4	1866699	14469344	0	6,640

Measurements obtained 08/22/2007
cfs = cubic feet per second
feet, amsl = feet above mean sea level

TABLE 3.3-6 MISCELLANEOUS MEASUREMENTS OF DISCHARGE FOR SELECTED DRAINAGES IN STUDY AREA, 2007-2009

SITE	UTM EASTING (feet)	UTM NORTHING (feet)	DISCHARGE (cfs)	DATE
GARDEN VALLEY (Tributary to Pine Valley)				
Henderson Creek	1856762	14462707	0.06	8/22/2007
			0.09	10/11/2007
			0.08	12/11/2007
			0.3	5/8/2008
			0.07	2/26/2009
			0.32	3/2/2009
			0.35	5/8/2009
			1.12	7/22/2009
			0.07	8/22/2009
			0.08	9/23/2009
			0.15	10/28/2009
Henderson Creek, upper	1835686	14453280	0.08	12/11/2007
			0.4	5/8/2008
			0.13	7/22/2009
			0.08	9/23/2009
			0.11	10/28/2009
Vinini Creek	1864747	14475667	0	8/22/2007
			0	10/11/2007
			6.93	5/8/2008
			0.39	2/26/2009
			0.41	3/30/2009
			12.79	5/8/2009
			2.08	6/23/2009
			0.48	7/22/2009
			0.06	8/22/2009
			0.05	9/24/2009
			0.05	10/28/2009
Vinini Creek, upper	1851447	14480587	6.08	5/8/2008
			0.98	3/30/2009
			13.3	5/8/2009
			2.12	6/23/2009
			0.61	7/22/2009
			0.05	8/22/2009
			0.03	9/24/2009
			0.13	10/28/2009

TABLE 3.3-6 MISCELLANEOUS MEASUREMENTS OF DISCHARGE FOR SELECTED DRAINAGES IN STUDY AREA, 2007-2009

SITE	UTM EASTING (feet)	UTM NORTHING (feet)	DISCHARGE (cfs)	DATE
KOBEH VALLEY				
Water Canyon	1744013	14183490	0	6/21/2007
			0	12/10/2007
	1744014	14183491	0	4/15/2008
			1.0 *	2/25/2009
Roberts Creek, at gage	1837785	14442917	1.25	4/15/2008
			4.17	5/7/2008
			0.16	8/22/2007
			0.2	12/11/2007
			1.25	4/15/2008
			4.17	5/8/2008
			0.2	8/21/2008
			0.25	11/3/2008
			0.13	2/26/2009
			0.6	3/29/2009
			6.45	5/7/2009
			2.4	6/25/2009
			1.4	7/22/2009
			0.56	8/22/2009
			0.33	9/24/2009
			0.23	10/28/2009
Roberts Creek, above reservoir	1837785	14442917	0.04	8/22/2007
			0.16	10/10/2007
			0	12/10/2007
			0.01	2/26/2009
			0.26	3/29/2009
			5.62	5/7/2009
			3.06	6/25/2009
			1.6	7/22/2009
			0.71	8/22/2009
			0.28	9/24/2009
			0.23	10/28/2009
Allison Creek	1820479	14278870	< 0.25 *	6/22/2007
Ackerman Canyon	1743193	14369329	0	6/21/2007
			0.06	8/23/2007
	1740694	14372906	0	12/10/2007
			0	2/25/2009
Ferguson Creek	1759922	14420488	< 0.25 *	5/30/2007
	1759364	14420516	0	8/22/2007
Dry Canyon	1723015	14344963	0	6/21/2007
Rutabaga Creek	1810645	14437955	0.02	8/21/2007

TABLE 3.3-6 MISCELLANEOUS MEASUREMENTS OF DISCHARGE FOR SELECTED DRAINAGES IN STUDY AREA, 2007-2009

SITE	UTM EASTING (feet)	UTM NORTHING (feet)	DISCHARGE (cfs)	DATE
PINE VALLEY				
Pete Hanson Creek, at Mountain Front	1813856	14488822	0	8/21/2007
			0	2/27/2009
			6.61	5/8/2009
			2.28	6/22/2009
			0.79	7/22/2009
			0.35	8/22/2009
			0.17	9/22/2009
			0.31	10/28/2009
Pete Hanson, upper	1819470	14485652	0.6	2/27/2009
			0.67	3/30/2009
			7.93	5/8/2009
			2.46	6/22/2009
			1.02	7/22/2009
			0.59	8/22/2009
			0.31	9/22/2009
			0.4	10/28/2009
Birch Creek, at Mountain Front	1828741	14506405	0.11	2/26/2009
			0.33	3/30/2009
			7.66	5/8/2009
			0.88	6/22/2009
			0.25	7/22/2009
			0.09	8/22/2009
			0.05	9/23/2009
			0.09	10/28/2009
Birch Creek, upper	1830891	14502805	0.09	2/26/2009
			0.37	3/30/2009
			7.49	5/8/2009
			1.26	6/22/2009
			0.25	7/22/2009
			0.11	8/22/2009
			0.05	9/23/2009
			0.08	10/28/2009
Willow Creek, at Mountain Front	1833330	14507701	3.22	5/8/2009
			1.57	6/22/2009
			0.07	7/21/2009
			0.01	8/21/2009
			0.001	9/23/2009
			0.01	10/26/2009

TABLE 3.3-6 MISCELLANEOUS MEASUREMENTS OF DISCHARGE FOR SELECTED DRAINAGES IN STUDY AREA, 2007-2009

SITE	UTM EASTING (feet)	UTM NORTHING (feet)	DISCHARGE (cfs)	DATE
Willow Creek, upper	1833005	14508602	0.07	8/21/2007
			0.02	10/11/2007
			0.07	5/6/2008
			0.065	1/6/2009
			0.08	2/29/2009
			0.11	3/30/2009
			0.51	5/8/2009
			0.58	6/22/2009
			0.7	7/21/2009
			0.4	8/21/2009
			0.16	9/23/2009
			0.4	10/26/2009

cfs = cubic feet per second

* = estimated

TABLE 3.3-7 COMPARISON OF GAGED ANNUAL FLOW WITH CORRELATED ANNUAL FLOW USING REGRESSION ANALYSES AT THREE GAGING STATIONS IN MONITOR VALLEY

CREEK	USGS STATION ID	PERIOD OF RECORD	MEAN ANNUAL FLOW[1] (AF/yr)	CORRELATED WITH:	CORRELATED ANNUAL FLOW[1] (AF/yr)
Pine Creek near Belmont	10245900	1978-2005	3,980	South Twin River	3,820[2]
Mosquito Creek near Belmont	10245910	1978-2005	1,670	Pine Creek	1,710
Stoneberger Creek north of Austin	10245925	1978-1996	1,220	South Twin River	1,100

AF/yr = acre-feet per year
[1] Rounded to nearest 10 AF/yr
[2] Long-term average flow is about 5,000 AF/yr

TABLE 3.3-8 MEAN ANNUAL RUNOFF AT THREE GAGING STATIONS IN MONITOR VALLEY

SITE	ELEVATION RANGE (feet)	AREA[1] (acres)	SURFACE-WATER RUNOFF	
			feet/acre	AF/yr[2]
Pine Creek	11,000-12,000	1,260	1.5	1,900
	10,000-11,000	2,470	1.0	2,500
	9,000-10,000	2,400	0.58	1,400
	8,000-9,000	1,510	0.27	400
	7,000-8,000	110	0.04	4
	Total	**7,750**	---	**6,204**
Mosquito Creek	10,000-11,000	2,310	1.0	2,300
	9,000-10,000	4,430	0.58	2,600
	8,000-9,000	2,470	0.27	700
	7,000-8,000	400	0.04	20
	Total	**9,610**	---	**5,620**
Stoneberger Creek	10,000-11,000	100	1.0	100
	9,000-10,000	4,830	0.58	2,800
	8,000-9,000	11,600	0.27	3,100
	7,000-8,000	6,160	0.04	200
	6,000-7,000	300	0	0
	Total	**22,990**	---	**6,200**

[1] Values rounded to nearest 10

[2] AF/yr = acre-feet per year; values rounded to nearest 100; value not rounded when less than 10

Data Source: Moore (1968)

TABLE 3.3-9 COMPARISON OF ANNUAL DISCHARGE MEASURED BY GAGE IN MONITOR VALLEY TO ESTIMATES FROM HEDMAN-OSTERKAMP AND MOORE METHODS

BASIN NAME	GAGE STATION	LATITUDE/LONGITUDE (DD MM.MM)	SURFACE-WATER RUNOFF (AF/yr)[1]		
			CORRELATED GAGE RECORD	MOORE (1968) METHOD	HEDMAN-OSTERKAMP (1982) METHOD
Monitor	Pine Creek	38° 47.67' / 116° 51.22'	3,800	6,200	3,600
Monitor	Mosquito Creek	38° 48.37' / 116° 40.72'	1,700	5,600	1,900
Monitor	Stoneberger Creek	39° 08.40' / 116° 43.27'	1,100	6,200	1,100

[1] AF/yr = acre-feet per year; rounded to nearest 100

TABLE 3.3-10 HEDMAN-OSTERKAMP CHANNEL GEOMETRY SITE PARAMETERS IN STUDY AREA

SITE NO.	NAME	UTM EASTING (feet)	UTM NORTHING (feet)	EQUATION USED[1]	ACTIVE CHANNEL WIDTH (feet)	ANNUAL DISCHARGE (AF/yr)
K-27	Barley Creek	1774454.27	13996195.5	7	10	4,900
K-26	Ikes Canyon	1717805.22	14179594.3	7	2.5	260
K- 28	Potts Ranch	1742415.01	14194133.9	7	2.5	260
K-21	Stoneberger Wash	1734513.01	14253352.9	14	6	60
K-16	Stoneberger Wash	1738352.14	14333608.9	14	4	30
K-12	Ferguson Creek*	1758267.77	14420244.1	7	3	500
K-8	Coils Creek*	1791271.31	14442456.1	12	14	600
K-9	Coils Creek	1806187.84	14493560.3	12	4	90
K-29	Roberts Creek*	1838044.04	14442786	7	4	870
K-3	Roberts Creek	1833128.3	14399566.7	14	3	20
K-15	Dry Canyon*	1723014.7	14344963.1	12	3.5	70
K-14	Water Canyon*	1743279.07	14365536.6	7	4	870
K-13	Ackerman Canyon*	1757283.84	14369390.1	12	5.5	140
K-4**	Three Drainages	1849083.1	14361604.5	12	7	200
K- 30	Fenstermaker Wash	1877768.61	14261604.1	14	1	4
K-31	Fenstermaker Wash	1858760.72	14276169.8	14	3	20
K-19	Fenstermaker Wash	1858760.72	14276169.8	12	6	160
K-20	Antelope V Wash	1827540.68	14212785.9	12	5	120
K- 32	Unnamed tributary to Antelope V Wash	1806838.72	14282163.4	12	5	120
K-17	Allison Creek (@ Mount Front)	1820478.63	14278869.5	7	3	500
K-17a	Allison Creek (Valley Rd. xing)	1790648.17	14336594.9	7	2.5	360
K-18	Antelope V Wash	1790648.17	14336594.9	12	5.5	140
K-25	Denay Creek	1829875.41	14562542.3	12	2.5	40
K-33	Henderson Creek	1866637.63	14469385.7	7	4	870
K-34	Vinini Creek	1865323.19	14475091.2	7	6	1,860

[1]Hedman and Osterkamp (1982, Table 2, p. 13)

* Site used to estimate runoff into Kobeh Valley

** K4 is downstream of the confluences of Roberts Creek, Coils Creek, and Willow Wash; drainage is tributary to Slough Creek

AF/yr = acre-feet per year

TABLE 3.4-1 HISTORIC DISCHARGE MEASUREMENTS FROM FLOWING WELLS IN THE STUDY AREA

WELL ID	NAME	UTM NORTH (feet)	UTM EAST (feet)	DISCHARGE (ft^3/day)	DISCHARGE (gpm)	DATA SOURCE
587	153 N23 E52 131	14478088	1904450	44,850	233	Harrill (1968)
343	153 N24 E53 6BDAB	14524078	1909962	38,498	200	Harrill (1968)
583	N18 E51 30	14312344	1843843	32,723	170	Rush and Everett (1964)
495	Bartine Ranch Wells T19N R50E	14354048	1820661	29,834	155	Rush and Everett (1964)
338	153 N23 E52 13CDAC1	14480521	1902643	19,634	102	Harrill (1968)
586	153 23N 52E 25	14476304	1903518	15,591	81	Harrill (1968)
340	153 N23 E52 11ADAB	14488653	1899863	12,127	63	Harrill (1968)
585	153 T23N R52E 13AD2	14483769	1902386	6,352	33	Harrill (1968)
582	N18 E51 18CC	14319607	1843110	3,465	18	Rush and Everett (1964)
593	T28N R52E 22c1	14632627	1892428	3,456	18	Eakin (1961)
589	153 24N 51E 6b1	14595253	1845961	3,272	17	Harrill (1968)
337	153 N23 E52 13CDDB1	14481028	1902588	3,080	16	Harrill (1968)
590	153 T24N R53E 05	14554973	1914972	2,887	15	Harrill (1968)
584	N18 E51 30DA	14311126	1847052	962	5	Rush and Everett (1964)
594	Fera Well	14566214	1913369	unknown	unknown	GBCGR (2007)
162	139 N21 E49 25BBDA1	14404054	1804481	unknown	unknown	GBCGR (2007)
104	139 N20 E52 18BBBB1	14383265	1876332	unknown	unknown	GBCGR (2007)
7	139 N20 E52 18ABDB1	14382722	1879596	unknown	unknown	GBCGR (2007)
494	Treasure Well	14380963	1823992	unknown	unknown	GBCGR (2007)
54	153 N20 E53 31DAAC1	14364539	1912441	unknown	unknown	GBCGR (2007)
50	153 N19 E53 08AB 1	14359633	1915155	unknown	unknown	GBCGR (2007)
596	Garcia Well	14582168	1935334	unknown	unknown	GBCGR (2007)
596	unknown	14576066	1953021	unknown	unknown	GBCGR (2007)
382	unknown	14553086	1844756	unknown	unknown	GBCGR (2007)
351	IGM-152	14461518	1869315	unknown	unknown	GBCGR (2007)
597	Unknown petroleum test well	14576065	1953020	unknown	unknown	GBCGR (2007)

ft^3/day = cubic feet per day
gpm = gallons per minute

TABLE 3.4-2 TRANSMISSIVITY VALUES FROM BOBCAT RANCH AREA WELLS

NDWR WELL LOG	WELL NUMBER	PUMPING RATE (gpm)	DRAWDOWN (feet)	SPECIFIC CAPACITY (gpm/ft)	TRANSMISSIVITY[1] (gpd/ft)
33406	36	3,000	98	31	61,220
63775	42	2,000	175	11	22,860
27856	37	2,200	78	28	56,410
21365	38	4,000	85	47	94,120

Data Source: Driscoll (1986)
[1]Estimated transmissivity = specific capacity x 2000
gpm = gallons per minute
gpm/ft = gallons per minute per foot of drawdown
gpd/ft = gallons per day per foot

TABLE 3.4-3 EVAPOTRANSPIRATION RATES AND VOLUMES FOR PHREATOPHYTES IN THE STUDY AREA

PHREATOPHYTE	AREA (acres)	AREAL DENSITY (percent)	DEPTH TO SATURATED CONDITIONS (feet)	EVAPOTRANSPIRATION	
				ft/yr	AF/yr
North Monitor Valley[1]					
Greasewood, rabbitbrush, and	5,100	20 - 25	15 – 40	0.2	1,000
Saltgrass and wet meadow	800	---	< 10	1.25	1,000
TOTALS	**5,900**				**2,000**
Antelope Valley[1]					
Greasewood, rabbitbrush	11,000	10 - 25	5 – 40	0.2	2,200
Saltgrass and wet meadow	1,600	---	< 5	1.25	2,000
TOTALS	**12,600**				**4,200**
Kobeh Valley[1]					
Greasewood, rabbitbrush, and saltgrass	12,000	20 - 25	< 20	0.4	4,800
Greasewood and rabbitbrush	10,000	20 - 25	20-40	0.2	2,000
Saltgrass and wet meadow	6,500	---	< 5	1.25	8,100
TOTALS	**28,500**				**14,900**
Pine Valley[2]					
Meadow and pasture	6,850	0 - 5	---	1 or 1.25	8,000
Greasewood, rabbitbrush, and	26,600	~3 - 25	---	0.1 – 0.5	9,100
Correction for below average	---	---	---	---	2,000
Groundwater discharge to Pine	Not included in total				(5,000)
TOTALS	**33,450**				**19,100**
Pine Valley[3], 1989					
Phreatophytes, undifferentiated	15,360	< 10	Not listed	0.5	7,710
	9,450	10 - 20		1.35	12,720
	3,610	20 - 35		2.17	7,820
	1,990	35 - 50		2.55	5,080
	2,320	≥50		2.64	6,120
Bare soil	170	---		0.15	30
TOTALS	**32,900**				**39,480**
Pine Valley[3], 1995					
Phreatophytes, undifferentiated	5,500	< 10	Not listed	0.62	3,380
	17,530	10 - 20		1.36	23,810
	5,190	20 - 30		2.17	11,280
	3,130	35 - 50		2.55	7,980
	1,470	≥50		2.64	3,870
Bare soil	70	---		0.15	10
TOTALS	**32,890**				**50,330**
Diamond Valley[4]					
Greasewood, rabbitbrush, and saltgrass	47,000	Low to heavy	Maximum ~ 20 ft Average ~ 10 ft	0.3	14,100
Meadow and pasture grasses	4,600 1,000	---	shallow	1.25 3.0	5,800 3,000
Playa	49,000	---	?	?	?
TOTALS	**101,600**				**22,900**

TABLE 3.4-3 EVAPOTRANSPIRATION RATES AND VOLUMES FOR PHREATOPHYTES IN THE STUDY AREA

PHREATOPHYTE	AREA (acres)	AREAL DENSITY (percent)	DEPTH TO SATURATED CONDITIONS (feet)	EVAPOTRANSPIRATION	
				ft/yr	AF/yr
North Diamond Valley[5]					
Greasewood, rabbitbrush, and sparse saltgrass	46,000	Moderate to low	5 - 20	0.3	14,000
Meadowgrass, hay, some	4,500	---	< 5	1.2	5,400
Wet meadow, marsh, some	1,500	---	< 5	3.0	4,500
Bare soil - playa	50,000	---	< 5	0.1	5,000
SUBTOTALS	**102,000**				**28,900**
South Diamond Valley[5]					
Greasewood, rabbitbrush, and sparse saltgrass	4,000	Moderate to low	5 - 20	0.3	1,200
Meadowgrass and saltgrass	150	---	< 5	1.2	180
SUBTOTALS	**4,150**				**1,380**
North and South TOTAL	**106,150**				**30,280**

[1] Rush and Everett (1964)
[2] Eakin (1961); Total groundwater discharge equals 24,000 AF/yr.
[3] Berger (2000a)
[4] Eakin (1962); Eakin did not subdivide Diamond Valley into north and south as did Harrill (1968).
[5] Harrill (1968)

ft/yr = feet per year
AF/yr = acre-feet per year

TABLE 3.5-1 WATER BUDGET COMPONENTS BASED ON USGS RECONNAISSANCE SERIES REPORTS FOR VALLEYS IN AND NEAR THE STUDY AREA

HYDROGRAPHIC AREA	ESTIMATED GROUNDWATER RECHARGE (AF/yr)	ESTIMATED ET DISCHARGE (AF/yr)	INTERPRETED SUBSURFACE OUTFLOW (AF/yr)	SURFACE WATER RUNOFF GENERATED IN BASIN (AF/yr)
South Monitor Valley	15,000	9,200	2,000 to N.	44,000
North Monitor Valley	6,300 + 2,000 from Monitor S.	2,000	6,000 North to Kobeh	23,000
Antelope Valley	4,100	4,200	0	14,000
Stevens Basin	200	0	200 to Antelope	500
Kobeh Valley	11,000 + 6,000 inflow from Monitor Valley	15,000	Minor outflow to Diamond Valley at Devils Gate	9,000
Garden Valley	10,000	1,000	9,000 East to Diamond	---
Pine Valley	46,000	24,000	300 North to Humboldt	31,000
Diamond Valley N.	9,000	29,000	---	5,800
Diamond Valley S.	12,000	1,400	11,000 to North	---
Little Smoky N.	4,000	1,900	1,000 to Newark	4,000

AF/yr = acre-feet per year

TABLE 3.5-2 CONCEPTUAL MT. HOPE REGIONAL WATER BALANCE FOR PRE-GROUNDWATER DEVELOPMENT (PRE-1960) CONDITIONS

COMPONENT OF WATER BALANCE	QUANTITY (AF/yr)	NOTES
INFLOWS*		
Kobeh Valley		
GW Recharge – from Precipitation Falling on the Basin	13,320	Recharge total from Rush and Everett (1964) – 11,000, this study recalculated at 13,320 AF/yr
Subsurface Inflow – N. Monitor Valley	1,680	Rush and Everett (1964) had 6,000 AF/yr, this study 200 to 3,450 AF/yr
Subsurface Inflow – Antelope Valley	1,000	Zero in Rush and Everett (1964), 150 to 3,000 AF/yr in this study
Subtotal	***16,000***	Rush and Everett (1964) total recharge 17,000, perennial yield 16,000
Antelope Valley		
GW Recharge – from Precipitation Falling on the Basin	4,000	Recharge total from Rush and Everett (1964), 4,000 AF/yr
Subsurface Inflow	0	
Subtotal	***4,000***	
Diamond Valley – North Part		
GW Recharge – from Precipitation Falling on the Basin	9,000	Recharge total from Harrill (1968) is 9,000 AF/yr
Subsurface Inflow from Garden Valley	7,780	Harrill (1968) at 9,000 AF/yr – determined by difference to balance with estimated discharge
Subsurface Inflow from Southern DV	12,120	By difference with water budget in S. Diamond Valley
Subtotal	***28,900***	
Diamond Valley – South Part		
GW Recharge – from Precipitation Falling on the Basin	12,400	Recharge total from Harrill (1968) is 12,400 AF/yr
Subsurface Inflow from Kobeh	1,100	Devils Gate plus deep inflow
Subtotal	***13,500***	

TABLE 3.5-2 CONCEPTUAL MT. HOPE REGIONAL WATER BALANCE FOR PRE-GROUNDWATER DEVELOPMENT (PRE-1960) CONDITIONS

COMPONENT OF WATER BALANCE	QUANTITY (AF/yr)	NOTES
Pine Valley – Garden Valley Sub-basin		
GW Recharge – from Precipitation Falling on the Basin	10,000	Recharge to Garden Valley Subbasin = 10,000 AF/yr from Harrill (1968)
Subsurface Inflow	0	
Subtotal	***10,000***	
Pine Valley – Remaining Portion in Study Area		
GW Recharge Mountain Blocks	27,130	Total 37 130 AF/yr by Maxey-Eakin Method for Pine Valley and Garden Valley Sub-basin. Eakin (1961) estimated recharge for entire basin at 46,000 AF/yr less estimated recharge to the Garden Valley Sub-basin of 10,000 AF/yr
Subsurface Inflow	0	
Subtotal	***27,130***	
OUTFLOWS		
Kobeh Valley		ET total from Rush and Everett (1964) is 15,000 AF/yr
ET – Greasewood, Rabbitbrush	6,800	
ET – Meadow, Salt Grass	8,100	
Subsurface Outflow (Devils Gate)	40	Harrill (1968), 6 to 270 AF/yr this study
Subsurface Outflow – Deep carbonate and north of Whistler Peak to S. Diamond Valley	1,060	By difference to balance with inflows
Subtotal	***16,000***	
Antelope Valley		ET total from Rush and Everett (1964), reduced by 70% to accommodate outflow and maintain water balance with recharge
Greasewood, Rabbitbrush	1,600	2,200 AF/yr in Rush and Everett (1964)
Meadow, Salt Grass	1,400	2,000 AF/yr in Rush and Everett (1964)
Subsurface Outflow to Kobeh	1,000	Zero in Rush and Everett (1964)
Subtotal	***4,000***	

TABLE 3.5-2 CONCEPTUAL MT. HOPE REGIONAL WATER BALANCE FOR PRE-GROUNDWATER DEVELOPMENT (PRE-1960) CONDITIONS

COMPONENT OF WATER BALANCE	QUANTITY (AF/yr)	NOTES
Diamond Valley – North Part		ET from Harrill (1968)
Greasewood, Rabbitbrush	14,000	
Meadow, Salt Grass	9,900	
Playa	5,000	
Subtotal	***28,900***	
Diamond Valley – South Part		ET from Harrill (1968)
Greasewood, Rabbitbrush	1,200	
Meadow, Salt Grass	180	
Subsurface Outflow to North Part	12,120	By difference with inflow
Subtotal	***13,500***	
Pine Valley – Garden Valley Sub-basin		ET from Harrill (1968)
Greasewood, Rabbitbrush	210	
Meadow, Salt Grass	360	
Outflow to Pine and Diamond Valleys	9,430	Outflow 1,650 AF/yr to Pine by difference, 7,780 AF/yr to N. Diamond by difference in Diamond
Subtotal	***10,000***	
Pine Valley – Remaining Portion in Study Area		Total ET and subsurface outflow estimated by difference with recharge estimate. Eakin (1961) estimated ET at 24,000 AF/yr for entire basin including Garden Valley; there is a large imbalance with his recharge estimate of 46,000 AF/yr
Greasewood, Rabbitbrush	12,770	Estimate based on 53% from "native" vegetation based on Eakin (1961)
Meadow, Salt Grass	11,230	Estimate based on 47% ET from meadow and pasture based on Eakin (1961)
Subsurface Outflow to N. Pine Valley	3,130	By difference to produce 27,130 AF/yr
Subtotal	***27,130***	
Total with Garden Valley Sub-basin	***37,130***	

*Distribution method described in Section 3.2.2

GW = Groundwater

AF/yr = acre-feet per year

ET = evapotranspiration

TABLE 3.5-3 ESTIMATES OF PERENNIAL YIELD FOR STUDY AREA BASINS

BASIN	PERENNIAL YIELD (AF/yr)
Kobeh Valley	16,000[1]
Antelope Valley	4,000[1]
Diamond Valley	30,000[2]
Pine Valley	24,000[3]

[1]Rush and Everett (1964)
[2]Harrill (1968); Eakin (1962) estimate was 23,000 AF/yr
[3]Eakin (1961); Berger (2000a) suggests water budget and perennial yield may be significantly greater
AF/yr = acre-feet per year

TABLE 3.5-4 REPORTED AND ESTIMATED CROP CONSUMPTIVE USE DIAMOND AND KOBEH VALLEYS

	DIAMOND VALLEY			KOBEH VALLEY		
YEAR	NDWR INVENTORY (AF/yr)	CORRECTED AND ESTIMATED VALUES FOR THIS STUDY (AF/yr)	ADJUSTED TO 2.5 FT CONSUMPTION FOR ALFALFA (AF/yr)	NDWR INVENTORY (AF/yr)	CORRECTED AND ESTIMATED VALUES FOR THIS STUDY (AF/yr)	ADJUSTED TO 2.5 FT CONSUMPTION FOR ALFALFA (AF/yr)
1950	300	300	246	---	---	---
1951	600	600	492	---	---	---
1952	800	800	657	---	---	---
1953	800	800	657	---	---	---
1954	800	800	657	---	---	---
1955	1,000	1,000	821	---	---	---
1956	1,000	1,000	821	---	---	---
1957	1,200	1,200	985	---	---	---
1958	1,200	1,200	985	---	---	---
1959	1,800	1,800	1,477	---	---	---
1960	2,400	2,400	1,970	---	---	---
1961	6,100	6,100	5,006	---	---	---
1962	11,000	11,000	9,028	---	---	---
1963	9,700	9,700	7,961	600	600	498
1964	12,000	12,000	9,848	---	600	498
1965	16,000	16,000	13,131	---	600	498
1966	22,400	22,400	18,383	---	600	498
1967	19,400	19,400	15,921	---	600	498
1968	18,200	18,200	14,937	---	600	498
1969	22,900	22,900	18,794	---	800	664
1970	---	28,968	23,774	---	800	664
1971	---	32,198	26,424	---	800	664
1972	---	35,427	29,075	---	800	664
1973	---	38,657	31,725	---	800	664
1974	---	41,887	34,376	---	800	664
1975	46,278	53,388	41,429	---	1,000	830
1976	48,192	56,139	42,809	---	1,000	830
1977	42,471	52,141	44,701	---	1,000	830
1978	58,500	58,500	51,105	---	1,000	830
1979	60,970	61,009	53,088	---	1,000	830
1980	64,000	64,010	55,320	---	1,000	830
1981	71,700	71,050	60,734	---	1,000	830
1982	73,300	72,891	61,751	---	1,000	830
1983	71,900	75,772	64,083	---	1,000	830
1984	78,100	78,030	65,859	---	1,000	830
1985	78,100	78,030	65,859	---	1,200	996
1986	69,600	69,605	59,033	---	1,200	996
1987	66,000	66,028	55,980	---	1,200	996

TABLE 3.5-4 REPORTED AND ESTIMATED CROP CONSUMPTIVE USE DIAMOND AND KOBEH VALLEYS

	DIAMOND VALLEY			KOBEH VALLEY		
YEAR	NDWR INVENTORY (AF/yr)	CORRECTED AND ESTIMATED VALUES FOR THIS STUDY (AF/yr)	ADJUSTED TO 2.5 FT CONSUMPTION FOR ALFALFA (AF/yr)	NDWR INVENTORY (AF/yr)	CORRECTED AND ESTIMATED VALUES FOR THIS STUDY (AF/yr)	ADJUSTED TO 2.5 FT CONSUMPTION FOR ALFALFA (AF/yr)
1988	63,400	63,356	53,247	---	1,400	1,162
1989	66,700	66,354	56,472	---	1,400	1,162
1990	64,400	64,054	53,965	---	1,400	1,162
1991	---	63,309	53,066	---	1,600	1,328
1992	58,585	62,200	53,035	---	1,600	1,328
1993	60,478	60,478	51,660	1,815	1,815	1,506
1994	60,833	60,883	51,998	1,800	1,800	1,494
1995	55,140	55,140	47,320	2,445	2,445	2,029
1996	57,779	57,779	49,303	2,445	2,445	2,029
1997	55,140	52,795	45,468	2,445	2,445	2,029
1998	60,985	59,477	50,666	2,445	2,445	2,029
1999	68,883	68,998	58,212	2,740	2,740	2,274
2000	70,601	62,157	53,673	2,740	2,740	2,274
2001	---	63,028	54,182	2,740	2,740	2,274
2002	60,900	63,900	54,800	2,380	2,380	1,975
2003	60,900	63,900	54,805	2,380	2,380	1,975
2004	65,687	65,527	55,809	3,490	3,490	2,897
2005	65,687	65,527	55,811	3,490	3,490	2,897
2006	65,687	65,687	55,811	---	4,500	3,870
2007	65,737	65,737	55,853	5,272	5,272	4,533

AF/yr = acre-feet per year
Data Source: Huntington and Allen (2010)

TABLE 3.5-5 AVERAGE WELL DEPTHS, DEPTHS TO WATER, AND ESTIMATED WELL LIFESPAN FOR SELECTED AREAS IN DIAMOND VALLEY

WELLS	WELL DEPTH (feet)	AVERAGE DEPTH TO WATER PER TOWNSHIP (feet)	AVERAGE WATER DEPTH ABOVE WELL BOTTOM (feet)	YEARS UNTIL DRY (at 2 ft/yr decline)
Average Irrigation Well Depth	264	---	---	---
Median Irrigation Well Depth	240			
Average Irrigation Well Depth since 1980	357			
Average Well Depth in T21N, R53E	249	104	145	72.5
Average Well Depth in T21N, R54E	255	118	137	68.5
Average Well Depth in T22N, R54E	265	54	211	105.5
Deepest Irrigation Well	662	225	437	218.5

--- = Not applicable

TABLE 3.6-1 AVERAGE RANGE IN HYDRAULIC CONDUCTIVITY FOR BASIN-FILL SEDIMENTS IN NEVADA

GEOMORPHIC POSITION	RANGE IN HORIZONTAL HYDRAULIC CONDUCTIVITY (feet per day)
Fluvial deposits	4 to 2,200
Valley fill, undifferentiated	$1x10^{-3}$ to 590
Alluvial slope	10 to 30
Upper Alluvial Slope	0.5 to 140
Lower Alluvial Slope	$2x10^{-2}$ to 140
Undifferentiated	$2x10^{-4}$ to over 150
Valley floor	2 to 90
Playa	$3x10^{-5}$ to 2

Modified from Maurer et al. (2004)

TABLE 3.6-2 AVERAGE RANGE IN HYDRAULIC CONDUCTIVITY VALUES FOR UNCONSOLIDATED SEDIMENTS BY GEOGRAPHIC POSITION

DESCRIPTIVE CATEGORY	AVERAGE HYDRAULIC CONDUCTIVITY (feet per day)	CORRESPONDING SEDIMENT TYPE
Very high	20 to 30	Alluvial slope/dune sand
High	10 to 20	Alluvial slope/stream channel
Moderate	5 to 10	Valley floor alluvium
Low	1 to 5	Flood plain/lake deposits
Very low	0.02 to 1	Playa, tuffaceous sediments

Modified from Maurer et al (2004)

TABLE 3.6-3 RESULTS OF AQUIFER TESTING AT WELL KCT#1

WELL NAME	TYPE OF WELL	DEPTH OF WELL (feet)	TYPE OF ANALYSIS[1]	TRANSMISSIVITY (gpd/ft)	TRANSMISSIVITY (ft^2/d)	STORAGE COEFFICIENT
KCE #2	observation	1,100	Cooper-Jacob Semi-Log	28,600	3,823	0.00024
KCE #2	observation	1,100	Theis Semi-Log Recovery	16,100	2,152	0.0012
KCE #3	observation	640	Cooper-Jacob Semi-Log	---	---	---
KCE #4	observation	540	Cooper-Jacob Semi-Log	---	---	---
KCE #5	observation	500	Cooper-Jacob Semi-Log	---	---	---
KCE #6	observation	500	Cooper-Jacob Semi-Log	85,700	11,456	0.032
KCE #6	observation	500	Theis Semi-Log Recovery	73,400	9,812	0.027
KCT#1	pumped	845	Cooper-Jacob Semi-Log	700	94	---
KCT#1	pumped	845	Theis Semi-Log Recovery	12,000	1,604	---

[1]Theis (1935); Cooper and Jacob (1946)

Data Source: Hydro-Search (1982)
gpd/ft = gallons per day per foot
ft^2/d = square feet per day

TABLE 3.6-4 AQUIFER TESTING RESULTS FROM VALLEY-FILL WELLS KOBEH VALLEY

WELL	INITIAL STATIC WATER LEVEL (ft, bgs)	SATURATED THICKNESS (feet)	DURATION OF TEST (minutes)	AVERAGE PUMPING RATE (gpm)	MAXIMUM DRAWDOW (feet)	SPECIFIC CAPACITY (gpm/ft)	THEIS TRANSMISSIVITY DRAWDOWN (ft^2/d)	COOPER-JACOB TRANSMISSIVITY DRAWDOWN (ft^2/d)	TRANSMISSIVITY RECOVERY METHOD (ft^2/d)	AVERAGE HYDRAULIC CONDUCTIVITY (ft/d)
KV11	90.25	793	120	418	7.0	60	11,600	---	14,700	20
KV11	90.4	793	107	480	5.2	92	11,600	---	14,700	20
KV11	90.4	793	128	412	6.8	58	---	11,400	14,700	19
9211R	2.8	647	500	600	31	19.4	---	93,600	---	145
EW-1	131.55	750	1,479	490	490	82	---	3,200	2,700	4
EW-2	135.5	561	1,479	490	490	7	---	3,600	3,000	7
228T	276	550	7,200	451	76	5.9	2,700	---	---	5
229T	202	550	7,200	490	77	6.4	3,300	---	2,900	6
222T	77	690	10,080	600	33	18.2	12,900	---	12,900	19

Data Source: Montgomery & Associates (2008)
ft, bgs = feet below ground surface
gpm = gallons per minute
gpm/ft = gallons per minute per foot of drawdown
ft^2/d = square feet per day
ft/d = foot per day

TABLE 3.6-5 SUMMARY OF HYDRAULIC CONDUCTIVITY FOR MAJOR ROCK TYPES IN SOUTH CENTRAL NEVADA

LITHOLOGY	GEOMETRIC MEAN OF HYDRAULIC CONDUCTIVITY (ft/d)	ARITHMETIC MEAN OF HYDRAULIC CONDUCTIVITY (ft/d)	MINIMUM HYDRAULIC CONDUCTIVITY (ft/d)	MAXIMUM HYDRAULIC CONDUCTIVITY (ft/d)	95-PERCENT CONFIDENCE INTERVAL OF GEOMETRIC MEAN (ft/d)		NUMBER OF TESTS
					LOWER BOUND	UPPER BOUND	
Young Alluvium	6.6	36	3.0E-03	427	1.9	13.1	43
Average of Clastics	0.02	8.3	4.9E-04	8.9	3.0E-03	0.1	28
Shale	0.03	0.2	1.0E-03	1.3	7.0E-03	0.2	9
Quartzites	1.9E-06	0.7	9.8E-08	16.4	2.3E-07	1.6E-05	19
Carbonate Aquifer	1.9	295	3.3E-05	2,690	0.7	6.6	51
Faulted / Karsted	9.8	394	0.03	2,690	9.8	13.1	18
Unfaulted	0.3	6.6	3.3E-04	46	0.07	1.6	19
Tertiary Volcanics	0.3	13.1	3.3E-06	591	0.3	0.7	159

Data Source: Belcher et al. (2001)

ft/d = feet per day

TABLE 4.1-1 EVAPOTRANSPIRATION AREAS IN THE MT. HOPE REGIONAL MODEL

AREA & PLANT TYPE	MODEL ET ZONE	ET RATE (ft/d)*	EXTINCTION DEPTH (feet)**
Kobeh Valley			
Kobeh – Shrubs	6	0.0018	40
Kobeh – Grasses/Meadow	7	0.012	10
Antelope Valley			
Antelope – Shrubs	9	0.0018	40
Antelope – Grasses/Meadow	10	0.012	10
Diamond Valley			
N. & S. Diamond – Shrubs	2	0.00095	40
N & S. Diamond – Grasses/Meadow	5	0.012	10
N. Diamond Playa	8	0.0007	5
Pine Valley			
Pine - Garden Sub-basin - Shrubs	11	0.0024	40
Pine - Garden Sub-basin – Grasses/Meadow	12	0.013	10
Other Pine Valley			
Remaining Pine – Shrubs	3	0.0024	40
Remaining Pine – Grasses/Meadow	4	0.013	10

* Zero depth to groundwater ET rate

** Depth to groundwater at which the ET rate goes to zero

ft/d = feet per day

ET = evapotranspiration

TABLE 4.1-2 SIMULATED SPRINGS AND FLOWING ARTESIAN WELLS IN THE REGIONAL MODEL AREA

ID[a]	NAME	BASIN NAME	UTM NORTH (feet)	UTM EAST (feet)	DISCHARGE (ft^3/d)	DISCHARGE* (cfs)	TEMP	WELL DEPTH (feet)	MODEL LAYER
582	Flowing Well N18 E51 18CC	Antelope	14319606.59	1843109.83	3,465	0.04	warm	290	3
583	Flowing Well N18 E51 30	Antelope	14312344.42	1843843.28	32,723	0.38	warm	unknown	3
584	Flowing Well N18 E51 30DA	Antelope	14311125.60	1847051.76	962	0.01	hot	738	6
45	Klobe Hot Springs	Antelope	14311028.00	1824822.00	14,437	0.17	hot	NA	6
359	Springs at Kitchen Meadow	Antelope	14310846.00	1844661.00	119,342	1.38	cold	NA	3
340	Flowing Well 153 N23 E52 11ADAB	Diamond	14488652.83	1899863.27	12,127	0.14	cold	98	3
585	Flowing Well 153 T23N R52E 13AD2	Diamond	14483769.26	1902386.27	6,352	0.07	cold	unknown	3
337	Flowing Well 153 N23 E52 13CDDB1	Diamond	14481028.06	1902588.01	3,080	0.04	cold	unknown	3
338	Flowing Well 153 N23 E52 13CDAC1	Diamond	14480521.19	1902642.98	19,634	0.23	cold	unknown	3
586	Flowing Well 153 N23 E52 131	Diamond	14478088.41	1904450.09	44,850	0.52	cold	unknown	3
587	Flowing Well 153 23N 52E 25	Diamond	14476303.60	1903517.52	15,591	0.18	cold	unknown	3
588	Flowing Well 153 24N 51E 6b1	Diamond	14595253.03	1845960.84	3,272	0.04	cold	unknown	3
589	Flowing Well 153 N24 E53 6BDAB	Diamond	14524078.20	1909962.30	38,498	0.45	cold	unknown	3
343	Flowing Well 153 T24N R53E 05	Diamond	14554972.76	1914972.23	2,887	0.03	cold	unknown	3
62	Shipley Hot Spring	Diamond	14506611.41	1900216.02	520,180	6.02	warm	NA	3-6
238	Siri Ranch Spring	Diamond	14523993.26	1908128.57	50,110	0.58	warm	NA	3
286	Sulphur Spring	Diamond	14466974.02	1901953.01	7,776	0.09	warm	NA	3
361	Thompson Ranch Spring	Diamond	14493109.14	1957547.76	189,929	2.20	warm	NA	4
280	Tule Dam Spring	Diamond	14472146.25	1903145.39	10,370	0.12	cold	NA	3
242	Bailey Ranch Spring	Diamond	14496099.58	1901783.58	98,500	1.14	cold	NA	3
951, 961	Flynn Ranch Springs	Diamond	14557348.00	1910044.00	1,924	0.02	warm	NA	5
591	Bartine Ranch Flowing Wells T19N R50E	Kobeh	14354048.00	1820661.00	29,834	0.35	cold	124	3
337	Hot Spring Hill (aka Bartine Hot Spring)	Kobeh	14367258.00	1820643.00	964	0.01	hot	NA	6
590	Unnamed Spring at T20N R52E 20	Kobeh	1437676.00	1884103.00	2,309	0.03	cold	NA	3
593	Flowing Well T28N R52E 22c1	Pine	14632626.63	1892427.55	3,456	0.04	cold	unknown	3
140	Tonkin Springs	Pine	14490420.04	1803734.54	154,886	1.79	cold	NA	3-4
239	Bruffy Hot Springs	Pine	14607850.00	1899996.00	9,624	0.11	hot	NA	6

* see Tables 3.3-1 and 3.3-2

NA = not applicable

[a] Refers to ID numbers and Appendix E

ft^3/d = cubic feet per day

cfs = cubic feet per second

TABLE 4.1-3 SUMMARY OF RECHARGE DISTRIBUTION IN THE MT. HOPE REGIONAL MODEL BY MAJOR RECHARGE ZONES

MODEL ZONE	BASIN NAME	GEOGRAPHIC AREA	TOTAL RECHARGE* (AF/yr)
		KOBEH VALLEY	
1	Kobeh	Mountain Block – Monitor Range & Lone Mountain	1,238
2	Kobeh	Mountain Block – Simpson Park Range	2,788
3	Kobeh	Mountain Block – Roberts Mountains – Carbonate Rocks	2,220
4	Kobeh	Mountain Block – Whistler Mountain & Mahogany Hills	1,996
6	Kobeh	Mountain Block – Roberts Mountains – Clastic Rocks	588
Multiple	Kobeh	Local Model area	584
Subtotal Kobeh Valley Mountain Block			***9,414***
5, 15	Kobeh	Alluvial Fans	1,558
31	Kobeh	Piedmont – Roberts Creek	578
33	Kobeh	Piedmont – Rutabaga Creek	108
29	Kobeh	Piedmont – Coils Creek	327
36	Kobeh	Piedmont – Ferguson Creek	406
35	Kobeh	Piedmont – Water Canyon	707
34	Kobeh	Piedmont – Dry Creek	6
Subtotal Kobeh Valley Alluvial Fans and Streams			***3,690***
KOBEH VALLEY BASIN TOTAL			**13,104**
		ANTELOPE VALLEY	
7	Antelope	Mountain Block – Fish Creek and Antelope Range	579
8	Antelope	Mountain Block – Monitor Range	1,801
Subtotal Mountain Block			***2,380***
10	Antelope	Piedmont – Regional	925
28	Antelope	Antelope and Fenstermaker Wash	780
Subtotal Antelope Valley Streams			***1,705***
ANTELOPE VALLEY TOTAL			**4,085**
		SOUTH DIAMOND VALLEY	
23, portion 64	S. Diamond	Mountain Block – Diamond Mountains and Whistler Mountain	6,614
22, 25	S. Diamond	Combined Piedmont and Ephemeral Streams – Regional	4,346
multiple	S. Diamond	Local Model area	1,173
Subtotal South Diamond Valley			***12,133***

TABLE 4.1-3 SUMMARY OF RECHARGE DISTRIBUTION IN THE MT. HOPE REGIONAL MODEL BY MAJOR RECHARGE ZONES

MODEL ZONE	BASIN NAME	GEOGRAPHIC AREA	TOTAL RECHARGE* (AF/yr)
NORTH DIAMOND VALLEY			
19	N. Diamond	Mountain Block – Diamond Mountains and Sulphur Spring Range	5,510
18, 48	N. Diamond	Combined Piedmont and Ephemeral Streams – Regional	3,683
Subtotal North Diamond Valley			***9,193***
DIAMOND VALLEY TOTAL			**21,326**
PINE VALLEY AND GARDEN VALLEY			
40	Pine w/o Garden	Mountain Block – Roberts Mountains	7,425
14, 44	Pine w/o Garden	Simpson Park Mountains, Cortez Range, and Sulphur Spring Range	6,510
11	Pine w/o Garden	Piedmont – Regional	5,515
32	Pine w/o Garden	Pine Creek, Denay Creek, and Henderson Creek	4,853
Subtotal Pine Valley			***24,303***
63	Garden portion of Pine	Mountain Block – Roberts Mountains	3,051
64	Garden portion of Pine	Mountain Block – Sulphur Spring Range	2,702
multiple	Garden portion of Pine	Local Model area	120
61	Garden portion of Pine	Piedmont – Valley Floor	1,899
62	Garden portion of Pine	Henderson Creek	3,041
Subtotal Garden Valley			***10,813***
PINE VALLEY AND GARDEN VALLEY TOTAL			**35,116**

* Some zones cross hydrographic basin divides. For more precise accounting of recharge on a basin scale see Table 4.1-5.

AF/yr = acre-feet per year

TABLE 4.1-4 RECHARGE DISTRIBUTION BY GEOGRAPHIC AREAS WITHIN THE MT. HOPE REGIONAL MODEL

HYDROGRAPHIC BASIN	GEOGRAPHIC AREA	PERCENT OF TOTAL HYDROGRAPHIC BASIN RECHARGE
Kobeh Valley	Mountain Blocks	72
	Alluvial Fans	12
	Ephemeral Streams	16
Antelope Valley	Mountain Blocks	58
	Alluvial Fans	23
	Ephemeral Streams	19
Diamond Valley (South Subarea)	Mountain Blocks	64
	Alluvial Fans and Ephemeral Streams Combined	36
Diamond Valley (North Subarea	Mountain Blocks	60
	Alluvial Fans and Ephemeral Streams Combined	40
Pine Valley – Garden Valley Subarea	Mountain Blocks	54
	Alluvial Fans	18
	Ephemeral Streams	28
Pine Valley – Remaining Area (all except Garden Valley Sub-area)	Mountain Blocks	57
	Alluvial Fans	23
	Ephemeral Streams	20

TABLE 4.1-5 RECHARGE DISTRIBUTION IN THE MT. HOPE REGIONAL MODEL BY HYDROGRAPHIC AREA

MODEL ZONE	HYDROGRAPHIC BASIN	INPUT RECHARGE (AF/yr)	CONCEPTUAL WATER BUDGET RECHARGE (AF/yr)*
1	Kobeh Valley	13,212	13,320
2	Antelope Valley	4,094	4,100
3	Diamond Valley – South	12,366	12,400
4	Diamond Valley – North	9,000	9,000
5	Pine Valley (w/o Garden)	24,182	27,130
6	Garden Subarea	10,678	10,000

AF/yr = acre-feet per year

*Refer to Table 3.5-2; Rush and Everett (1964); Harrill (1968)

TABLE 4.1-6 HYDRAULIC CONDUCTIVITY VALUES IN MT. HOPE REGIONAL MODEL

K ZONE	K_{X-Y} (ft/d)	K_Z (ft/d)	HYDROSTRATIGRAPHIC UNIT*
2	2.00E-06	2.00E-06	Siliciclastic Rocks – AQT1
11	1.53E+01	1.61E+00	Young Valley Fill – VF1
12	2.94E+01	1.01E+00	Young Valley Fill – VF1
13	2.90E+00	2.00E-01	Young Valley Fill – VF1
15	4.54E+01	6.89E-01	Siliciclastic Rocks – AQT1
16	3.05E+01	1.01E-01	Older Valley Fill – VF1, VF2, VF3
17	2.00E+00	1.00E-01	Older Valley Fill – VF1, VF2, VF3
18	4.88E+00	2.00E-01	Older Valley Fill – VF1, VF2, VF3
20	1.00E+00	1.00E-01	Young Valley Fill – VF1
21	4.74E+00	7.84E-01	Young Valley Fill – VF1
22	2.27E-01	1.86E-01	Older Valley Fill – VF1, VF2, VF3
23	2.25E-01	3.20E-02	Older Valley Fill – VF1, VF2, VF3
24	1.51E+00	1.37E-01	Older Valley Fill – VF1, VF2, VF3
25	1.00E+01	2.00E-01	Young Valley Fill – VF1
27	5.00E+00	5.00E-01	Young Valley Fill – VF1
28	4.34E+01	2.03E+00	Young Valley Fill – VF1
29	1.00E-01	1.23E-02	Basalt/Volcanic – VOL1
30	6.50E+00	6.50E-01	Young Valley Fill – VF1
31	1.31E+01	7.42E-03	Playa Deposits – VF3
32	2.10E+01	8.50E-01	Young Valley Fill – VF1
33	2.70E+01	1.35E-01	Young Valley Fill – VF1
34	6.15E-01	2.46E-02	Older Valley Fill – VF1
35	7.81E-01	2.29E-01	Older Valley Fill – VF1, VF2, VF3
37	5.34E+01	2.28E-01	Young Valley Fill – VF1
38	6.00E-01	3.00E-02	Extrusive Igneous Rocks – VOL1
39	3.50E-01	7.00E-02	Extrusive Igneous Rocks – VOL1
40	3.99E-01	1.01E-01	Carbonate and Dolomite Units – CA1, CA2, CA3
41	1.01E-02	2.27E-04	Extrusive Igneous Rocks – VOL1
42	5.38E-03	7.69E-04	Siliciclastic Rocks – AQT1
43	1.57E-02	8.76E-03	Intrusive Rocks – VOL2
44	3.05E+01	6.00E-01	Extrusive Igneous Rocks – VOL1
45	1.00E-01	1.00E-02	Extrusive Igneous Rocks – VOL1
47	3.00E-01	5.85E-02	Extrusive Igneous Rocks – VOL1
48	3.00E-02	3.00E-03	Mixed Carbonate and Siliciclastic – CA4
50	5.00E+00	2.73E-01	Young Valley Fill – VF1
51	8.64E-01	4.97E-01	Older Valley Fill – VF1
53	4.49E+01	1.59E+01	Young Valley Fill – VF1
54	4.03E+00	1.12E+00	Older Valley Fill – VF1, VF2, VF3

in **Appendix B** of the "Hydrogeologic Characterization of Pit Area" report (Montgomery & Associates, 2010b).

Hydraulic heads measured at multi-level grouted piezometers in 2009 indicated there was a component of the vertical hydraulic gradient directed downward in the pit area. However, at piezometer IGM 152 completed at a depth of 460 feet bgs, hydraulic head was nearly 200 feet als, indicating that hydraulic head in an area north of the proposed pit may have an upward gradient. The hydraulic head at piezometer 152 is believed to result from penetration of a fault or fracture zone which is in hydraulic communication with faults or fractures in rock units at higher elevations on the mountain slope. A slight upward hydraulic gradient was also apparent at the paired shallow and deep piezometers IGM-MH-226P and IGM-MH-227P.

4.2.4.2 GROUNDWATER MOVEMENT: The regional occurrence and movement of groundwater are presented in greater detail in **Section 3.4**. **Figure 4.2-9** shows the general direction of groundwater movement within the Local Model domain. Groundwater level contours indicate that groundwater moves from areas of recharge in the vicinity of Mt. Hope and the Roberts Mountains toward Diamond, Pine, and Kobeh Valleys. Groundwater hydraulic gradient within the Local Model domain ranges from 0.21 (1,100 feet per mile) on the eastern slope of Mt. Hope to 0.015 (80 feet per mile) on the eastern boundary of the Local Model domain in Diamond Valley. Current direction of groundwater movement in the proposed pit area is generally east in the north and east parts of the pit, and south to southeast in the south part of the pit area. Groundwater elevation and direction of movement in the pit area appears to be strongly influenced by topography; hydraulic gradients are steep where topography is steep and gentler in the flatter areas. Horizontal hydraulic gradient is steeper in the east and southeast areas of Mt. Hope compared with the surrounding area, flattening toward the Roberts Mountains (northwest of Mt. Hope) and to the east and southwest in Diamond and Kobeh Valleys.

4.2.4.3 RECHARGE AND EVAPOTRANSPIRATION: Recharge in the Mt. Hope area occurs from infiltration of precipitation in the mountains and alluvial fans. Precipitation and recharge in the Mt. Hope area are summarized in **Section 3.2**. The rates and distribution of recharge in the Local Model domain were derived by applying an estimated precipitation-recharge relationship to an elevation-precipitation model. The elevation-precipitation model used for this analysis, and for the Regional Model, was the national PRISM precipitation dataset (OSU, 2006). The PRISM dataset provided an estimated distribution of precipitation in the model domain at grid spacing of 800 meters. PRISM uses topographic information (elevation, slope, and aspect) to determine variations in precipitation as a function of elevation; orographic effects, including rain shadows, are explicitly integrated into PRISM's precipitation distribution algorithms. Zones of equal precipitation determined from the PRISM analysis were delineated for the model area. A precipitation-recharge relationship developed by USGS (Nichols, 2000) was applied to the PRISM precipitation distribution to estimate the percentage of precipitation in each precipitation zone that enters the groundwater system as recharge. A uniform recharge rate was specified for model grid cells within each zone. The USGS (Nichols, 2000) precipitation-recharge relationship was predicated on the assumption that areas receiving more precipitation have a higher ratio of recharge to precipitation, as shown in **Table 4.2-2**.

According to the PRISM dataset, precipitation within the Local Model domain ranges from a low of 10.00 inches per year (in/yr) on the eastern boundary of the model domain to a high of 16.29 in/yr at the summit of Mt. Hope. Precipitation at the center of the proposed pit is estimated to be 14.94 in/yr. Correspondingly, estimated recharge values within the model domain range from 0.084 in/yr on the eastern edge of the model domain to 2.3 in/yr at the summit of Mt. Hope.

Phreatophyte ET and spring/seep discharge are not believed to be a significant component of groundwater discharge in the Local Model area. Seeps and springs in the Mt. Hope area are documented in **Section 3.3**. Approximately seven springs and seeps have

been documented at Mt. Hope or near the flanks of Mt. Hope, including the Zinc Adit (SRK, 2008b). Discharges from identified springs are monitored by EMLLC. Spring resources are summarized in **Section 3.3.1**, mapped on **Plate 2**, and tabulated in detail in **Appendix E**. A total of 10 springs have been identified within the Local Model domain (**Plate 2**); discharges range from negligible to as much as 8 gpm from the Zinc Adit. Conditions of these springs have been observed to be seasonal in nature. None of the springs have been interpreted to represent a significant source of discharge of deep circulation groundwater. These springs are not specifically represented in the Local Model due to the limited magnitudes of discharge and negligible significance to the simulated water budget.

4.2.5 Aquifer Properties

A hydraulic testing program was conducted by EMLLC in 2007 through 2009 using slug tests, packer tests, and short-term and long-term pumping tests with multiple observation wells to provide aquifer characteristics and to constrain hydraulic conductivity and storage values for use in the Local Model. Locations of wells and piezometers utilized in the derivation and interpretation of data during these tests are shown on **Figure 4.2-10**. The March 2010 "Hydrogeologic Characterization of Pit Area" report (Montgomery & Associates, 2010b) provides detailed construction and testing data, analytical procedures, and results of the hydraulic testing programs. **Tables 4.2-3 through 4.2-5** summarize results of hydraulic testing. Five dominant lithologies have been encountered in the vicinity of Mt. Hope and have been investigated for their hydraulic properties using the hydraulic testing methods described above. The lithologies are Vinini Formation, hornfels, rhyolite tuff, and potassic or silicic quartz porphyry. The estimated range of values for hydraulic conductivity for the various lithologies and test methods are shown on **Figure 4.2-11**.

4.2.5.1 SLUG TESTING: A total of 17 falling head slug tests were conducted in 2-inch piezometers between December 2007 and March 2008. Interpretation of some slug tests were problematic due to issues related to well construction, test procedures, or data

quality. Highest quality tests are judged to have been conducted at piezometers IGMI-MH-220P, 227P, 228P, 230P, 231P, 232P, and 233P (Montgomery & Associates, 2010b) **(Table 4.2-3, Figure 4.2-10)**. These tests provide hydraulic conductivity estimates for the Vinini Formation, hornfels, and rhyolite tuff. Piezometers 228P, 231P, and 232P were screened in an unaltered portion of Vinini Formation to the east-southeast and northeast of the proposed pit area, with 228P and 232P distant from mapped fault structures and 231P located just north of a fault associated with the northwest-southeast-trending Corridor Trend **(Figure 4.2-3)**. Estimated hydraulic conductivity values from slug tests for the Vinini Formation ranged from 1.9E-04 ft/d at 232P to 1.5E-01 ft/d at 231P. Estimated hydraulic conductivity for the hornfels is 1.6E-02 ft/d at 220PB. Estimated hydraulic conductivity for the rhyolite tuff ranged from 2.7E-06 ft/d at 227P to 9.4E-05 ft/d at 233P; these three piezometers are distant from mapped fault structures.

4.2.5.2 PACKER TESTING: A total of 31 injection and air-lift packer tests were conducted by SRK, Inc. at coreholes MH2009-246, 247, and 248 in May and June 2009 **(Table 4.2-4, Figure 4.2-10)**. Descriptions of the packer tests have been presented previously (Montgomery & Associates, 2010b, **Appendix D**). Coreholes 246 and 247 are located near the center of the proposed pit in high-angle near continuous fault zones; rocks are predominantly composed of mineralized and fractured potassic or silicic quartz porphyry and hornfels. Hydraulic conductivity estimates for these packer tests ranged from 1E-4 ft/d for upper (potassic quartz porphyry) tests, to 1E-1 ft/d for lower (silicic quarz porphyry) tests. Corehole 248 is located northwest of the proposed pit, distant from mapped structures, in rocks composed predominantly of non-mineralized Vinini Formation. Hydraulic conductivity estimates for packer tests conducted in corehole 248 ranged from less than 1E-05 (possibly as low as 1.0E-7) to 1.2E00 ft/d and generally decrease with increasing depth. Aquifer parameters in the model were adjusted during calibration to approximate the measured conductivity data from the three packer tests.

4.2.5.3 PUMPING TESTS: Descriptions of pumping tests have been presented previously (Montgomery & Associates 2010b). The most commonly applied analytical methods for pumping tests in the study area, Theis (1935), Cooper and Jacob (1946), and Moench (1984 and 1988), assume an aquifer of uniform thickness and infinite areal extent, with radial flow occurring at least during late stages of pumping. Following methods described by Kruseman and De Ridder (1990), long-term pumping periods were required to attain at least "pseudo-radial" flow, so that once attained, these analytical methods were applicable (Montgomery & Associates, 2010b).

Short-term pumping tests were conducted in May and June 2009 at wells PDT2009-240, 241, 244, and 245 (**Table 4.2-5, Figure 4.2-10**). Length of pumping period ranged from 0.048 days (69 minutes) at well 240 to 0.5 days (720 minutes) at wells 241 and 245. Analyses included transmissivity using the semi-logarithmic Cooper-Jacob (1946) and Theis (1935) analytical drawdown methods. Results indicated transmissivity ranges from 0.4 ft^2/d at well 240 to 180 ft^2/d at well 244.

Long-term pumping tests were conducted in May, June, and July 2009 using pilot dewatering test wells GMI-PDT-1, PDT-2, PDT-3B, which are located along the southwest, northwest, and northeast boundaries of the proposed pit area, respectively (**Figure 4.2-10, Table 4.2-5**). Length of pumping period ranged from 7.3 days for the PDT-1 test to 26 days for the PDT-3B test. Observation well response was observed at wells 225P, 240, 178P, 242, 245, 244, and 221P. Results were analyzed for fracture and matrix hydraulic conductivity and specific storage using the Moench (date) log-log drawdown and recovery method. The model was calibrated to the observed drawdown response for the tests.

Lithology at PDT-1 is unaltered Vinini Formation with some hornfels; the well is screened in these units. Analysis of long-term pumping test data indicated that fracture hydraulic conductivity values for PDT-1 were in the range of 2.4E-03 to 7.1E-03 ft/d, and matrix hydraulic conductivity values were in the range of 6.8E-06 to 9.6E-04 ft/d. Fracture

specific storage for PDT-1 was in the range of 3.7E-10 to 3.5E-06 ft-1, and matrix specific storage was in the range of 2.9E-06 to 2.3E-03 ft-1.

Lithology at PDT-2 is rhyolite tuff, Vinini Formation, hornfels, and quartz porphyry; the well is screened in hornfels. Analysis of long-term pumping test data indicated that fracture hydraulic conductivity values for PDT-2 were in the range of 1.5E-01 to 3.3E-01 ft/d, and matrix hydraulic conductivity values were in the range of 1.4E-07 to 2.6E-04 ft/d; fracture specific storage was in the range of 3.7E-07 to 9.4E-05 ft-1, and matrix specific storage was in the range of 9.8E-04 to 5.8E-03 ft-1.

Lithology at PDT-3B is rhyolite tuff, hornfels, and quartz porphyry; the well is screened in hornfels with minor quartz porphyry. Analysis of long-term pumping test data indicated that fracture hydraulic conductivity values for PDT-3B were in the range of 1.1E-01 to 1.6E-01 ft/d, and matrix hydraulic conductivity values are in the range of 1.9E-08 to 1.9E-05 ft/d; fracture-specific storage was in the range of 1.7E-07 to 1.7E-05 ft^{-1}, and matrix-specific storage was in the range of 8.2E-07 to 2.3E-04 ft^{-1}.

4.2.6 Conceptual Model

A conceptual model of the groundwater flow system in the Mt. Hope area was developed based on available data, including the site-specific hydraulic properties described above, and knowledge of groundwater flow in fractured and porous rock media. The conceptual model provides the basis for development of the numerical model. Important components of the conceptual model are described as follows:

- Hydrogeologic characterization and hydraulic testing throughout the proposed Mt. Hope mine pit area supports the assumption that the rocks are sufficiently fractured and interconnected so that the system can be treated as an equivalent porous medium (EPM). The EPM concept assumes that for the time and distance scales of interest (years to decades, and thousands of feet), the fractured bedrock

flow system behaves as an interconnected continuous medium and representative behavior can be modeled using average hydraulic properties. These average hydraulic properties can be varied on a local scale to approximate flow system heterogeneities in the rocks.

- Faulting has been observed on the surface and in cores; however, the character of discrete faults was difficult to define during hydrogeologic investigations and relationships have not been identified between mapped fault features and observed water levels or aquifer test responses. The influence of faulting may contribute to the observed aquifer testing responses; simulated hydraulic conductivity distributions are adjusted to represent macro-scale features which may include faults and fractures.
- Hydraulic conductivity is primarily a function of fracture intensity and type of alteration, and is highly variable.
- Abundant sub-vertical fracturing is present within the proposed pit and is associated with mineralization. Hydraulic conductivity in fractured quartz porphyry within the pit is relatively large where silicic alteration has resulted in brittle rocks with little alteration or clay filling within fractures. Hydraulic conductivity in fractured quartz porphyry within the pit is lower where potassic alteration is present.
- Rocks surrounding the proposed pit are largely composed of Vinini Formation and overlying volcanic tuff. Results of testing indicate that hydraulic conductivity of Vinini Formation is highly variable.
- Groundwater recharge in the higher elevations of Mt. Hope, combined with low-permeability bedrock, sustains the higher groundwater levels observed in the proposed pit area; groundwater moves radially and downward away from the higher elevations in the area of the proposed pit. Groundwater recharge creates a downward vertical component of hydraulic gradient in the proposed pit area.
- The steep eastward groundwater level gradient in the eastern portion of the proposed pit area indicates a relatively low permeability flow system.

4.2.7 Numerical Model Construction

The Mt. Hope Local Model was constructed using the finite-difference model code MODFLOW-SURFACT Version 3.0 (HydroGeoLogic Inc., 1996) and Groundwater Vistas, a graphical modeling interface (Rumbaugh and Rumbaugh, 2007). The Local Model is a nested model located entirely within the Regional Model domain and was developed concurrently with the Regional Model using TMR. Solution of the Regional Model is used to define the lateral boundary conditions for the Local Model.

4.2.7.1 MODEL GRID: The finite-difference grid and boundary conditions for the Local Model are shown on **Figure 4.2-12**. The model covers an area of 28 square miles and consists of 19 layers with 90 rows and 118 columns. Grid cell dimensions range from 100 feet by 100 feet in the pit area to 800 feet by 800 feet at the edge of the model. There are 201,780 active model cells.

Lateral model boundaries are specified head (**Section 4.1**). For the initial steady-state condition, heads at the Local Model boundary were determined from the Regional Model and represent either inflow or outflow relative to the Local Model. For the transient model simulation representing pit dewatering and post-project pit-lake formation, the specified head boundary conditions are constant during each stress period but vary over time from one stress period to the next. They were determined through a coupling process between the Regional and Local Models. The coupling process is described in **Section 4.2.9**.

The base of the Local Model was specified at an elevation of mean sea level (0 feet, amsl) to be consistent with the Regional Model. Model layers are flat in the pit area to facilitate implementation of the lake software package used to simulate the possible formation of a pit lake following the cessation of mining activities. The bottom of model layer 1 in the pit area was set at an elevation of 6,350 feet, amsl, approximately 500 feet below the lowest pit area land surface elevation. Due to the lower elevations in the valley

floor areas in the eastern portion of the model domain, model layer bottoms would intersect land surface if model layers were maintained flat throughout the model domain. To avoid this situation, the bottom of model layer 1 east of the pit boundary was adjusted to slope to the east to a minimum of 90 feet below the lowest point in the surrounding valleys. Model layer 1 ranges in thickness from approximately 90 to 2,044 feet, with the thickest area under Mt. Hope and the thinnest area along the eastern model boundary. Model layer 2 varies in thickness from 75 to 350 feet. Model layers 3 through 15 vary in thickness from 75 to 100 feet. Model layers 16 through 19 are uniformly 1,175 feet in thickness.

4.2.7.2 SIMULATION PERIODS: The Local Model was constructed with a steady-state simulation calibrated to observed 2009 conditions, as historical data for groundwater levels in the pit area are too sparse for calibration purposes. Available historical data indicate regional pumping has not affected pit area water levels and the 2009 simulated steady-state water levels are considered representative of 1955 conditions. The simulated steady-state water levels served as initial conditions for the subsequent Local Model transient historical simulation from 1956 through 2010, followed by a 33-year dewatering simulation period of pre-mining (1 year) and pit advancement (32 years), followed by a 1,580-year post-project pit lake formation period. The 33-year simulation period of pre-mining and pit advancement was divided into eleven stress periods of 1 year each, four stress periods of 5 years each, and a final stress period of 2 years as defined by mine-plan pit shells provided in electronic format by Independent Mining Consultants, Inc. (2007). The 1,580-year length of the simulated post-project pit-lake development period was determined based on projected pit lake equilibrium estimates (**Section 4.5.3.2**), and is sufficient for pit lake projections to approach equilibrium; stress periods for the pit lake simulation were 1 year in length for the first 100 years, and 10 years for the remainder.

4.2.7.3 SIMULATED RECHARGE: Simulated recharge distribution in the Local Model is shown on **Figure 4.2-13**. Recharge was determined based on the PRISM elevation-precipitation model and the precipitation-recharge relationship developed by USGS (Nichols,

2000), as described in **Section 4.2.4.3**. Simulated recharge at the center of the proposed mine pit for both the Local and Regional Models is approximately 2 in/yr.

4.2.7.4 SIMULATED HYDRAULIC PARAMETERS: Hydraulic parameters specified for model layers were horizontal and vertical hydraulic conductivity, specific yield, and specific storage. Results of hydraulic testing, interpretation of geologic data by EMLLC and Montgomery & Associates, and interpretation of observed groundwater level conditions were used to characterize hydrogeologic zones in the Local Model. Interpretations from hydraulic testing combined with information collected during drilling and geologic mapping were used to develop hydraulic conductivities. Hydrogeologic zones incorporated in the model are described in **Section 4.2.3** and shown on **Figures 4.2-4 through 4.2-8**. The eight hydrogeologic zones represent a generalized approximation of zonal variation in hydraulic properties in the model study area. The hydraulic conductivity and storage values within these zones were adjusted to match measured steady-state groundwater levels and to groundwater level response observed during aquifer testing. PEST (Doherty, 2005), an automated inverse parameter estimation program, was used for varying hydraulic conductivity during the steady-state and transient calibration matching, and for varying storage values during the transient calibration matching. For the inverse calibration matching hydraulic conductivity parameters were permitted to vary within a range based on hydraulic testing data; storage values were permitted to vary within a range determined from hydraulic testing and based on available data for similar rock types.

4.2.7.4.1 Hydraulic Conductivity Distribution: Hydraulic conductivity values were permitted to vary both between the zones and within the zones, resulting in representation of the final horizontal and vertical distribution of hydraulic conductivity as a continuous field. A continuous field distribution smoothes out natural variation within hydrogeologic zones, including variation of fracture occurrence, density, and permeability in the bedrock areas, as well as the boundaries between hydrogeologic zones. Therefore, a continuous field varies a hydraulic parameter throughout an area in a geostatistical manner,

typically using kriging, rather than as discrete zones that define one average hydraulic parameter. The continuous field representation resulted in a reasonable match to observed groundwater levels while incorporating results from pumping tests. The horizontal to vertical hydraulic conductivity ratio distribution was assumed to be variable; ratio of horizontal to vertical hydraulic conductivity was fixed within the hydrogeologic zones, with the exception of the Paleozoic carbonate unit.

Final distribution of simulated hydraulic conductivity, and ratios of horizontal to vertical hydraulic conductivities, for model layers 1 though 19 are shown on **Figures 4.2-4 through 4.2-8**. Vertical sections of simulated hydraulic conductivities are shown on **Figures 4.2-14 and 4.2-15**; locations of the sections are shown on **Figures 4.2-4 through 4.2-8**. Hydraulic conductivities specified in the model are summarized in **Table 4.2-6**, with ratios of horizontal to vertical conductivities summarized in **Table 4.2.7**. Simulated hydraulic conductivity distribution by hydrogeologic zone is describes as follows:

Potassic quartz porphyry (Tqpp) – Present in layers 1 through 19; values range from 1.94E-04 to 4.54E-01 ft/d. Potassic Quartz Porphyry is assigned to hydrostratigraphic unit "VOL1" of the Regional Model (**Table 3.1-2**).

Silicic Quartz Porphyry (Tqps) – Present in layers 1 through 19; values range from 4.63E-03 to 1.47E-02 ft/d. Silicic Quartz Porphyry is assigned to hydrostratigraphic unit "VOL1" of the Regional Model (**Table 3.1-2**).

Hornfels (Hf) – Present in layers 1 through 15; values range from 1.11E-04 to 5.11E-01 ft/d. Hornfels is not described as a separate hydrogeologic unit in the Regional Model.

Rhyolite tuff (Tv) – Present in layers 1 through 7; values range from 1.07E-04 to 5.21E-01 ft/d. In general, hydraulic conductivity values within the zone are lowest in the northwestern portions of the zone and grade to the highest values in the southeastern

portions. Rhyolite tuff is assigned to hydrostratigraphic unit "VOL1" of the Regional Model (**Table 3.1-2**).

Vinini Formation (Ov) – Present in layers 1 through 16; values range from 1.00E-06 to 7.08E-01 ft/d. The lowest simulated hydraulic conductivity for the Vinini Formation is associated with the packer test MH2009-248 location. Vinini Formation is assigned to hydrostratigraphic unit "AQT1" of the Regional Model.

Garden Valley Formation (Pgl) – Present in layers 1 through 16; values range from 5.92E-03 to 7.28E-03 ft/d, with an average value of 1.49E-02 ft/d. Garden Valley Formation is assigned to hydrostratigraphic unit "AQT1" of the Regional Model.

Paleozoic carbonates (Pzca) – Present in layers 1 through 19; values set to 4.0 ft/d in layer 1, 0.421 ft/d in layers 2 through 16, 3.99E-03 ft/d in layer 17, and 1.00E-03 and 1.15E-01 ft/d in layers 18 and 19, as specified in the Regional Model. Paleozoic Carbonates are assigned to hydrostratigraphic units "CA1", "CA2", or CA3" of the Regional Model.

Paleozoic clastics (Pzcl) – Present in layer 17; value set to 5.38E-02 ft/d. Paleozoic Clastics are assigned to hydrostratigraphic units "CA2", "CA3" or CA4" of the Regional Model.

Simulated hydraulic conductivity values in the Local Model domain tend to decrease at depth where faulting and fracturing are interpreted to be reduced. Hydraulic conductivity within the Local Model domain is lowest in the proposed pit area, particularly in the lower portions of the quartz porphyry (Tqp) and hornfels (Hf) units in layers 6 through 19. Hydraulic conductivity values in the upper portions (layers 1 through 6) of the quartz porphyry and hornfels approximately parallel simulated values for the adjacent rhyolite tuff (Tv) and Vinini Formation (Ov) zones. Hydraulic conductivity in the Garden Valley Formation (Pgl) was constrained to a relatively small range of values and tended to match values in the northern portion of the adjacent Vinini Formation. The highest hydraulic conductivity values in the Vinini Formation occur south and northeast of the proposed pit area, in model layers 2 through 5.

Vertical distribution of simulated and measured hydraulic conductivities at the MH2009-246, 247, and 248 packer test locations are shown on **Figures 4.2-16, 4.2-17, and 4.2-18**, respectively. The hydraulic conductivity match at all three locations is considered acceptable for purposes of representing local-scale aquifer properties at the packer test locations.

4.2.7.4.2 Storage Distribution: Distribution of simulated specific yield for all the model layers is shown on **Figures 4.2-19 through 4.2-23**. Specific yield values in the pit area were estimated from calibration to pumping tests and literature values and range from 0.00024 to 0.025, with the lowest value (0.00024) specified in the hornfels and the highest value (0.025) specified in the quartz porphyry. Specific yield values for the carbonates on the eastern edge of the model and in the deeper layers were taken from the Regional Model and modified as necessary; they ranged from 0.01 to 0.03. Specific storage values were based on the long-term pumping tests (**Table 4.2-5**); simulated specific storage values range from 3.7E-10 ft-1 in the Vinini Formation to 5.0E-6 ft-1 in the Paleozoic Carbonates. For each model layer, change in storage was simulated by using specific yield when groundwater levels were below the top of a model layer and by using specific storage when groundwater levels were above the top of a model layer.

4.2.8 Results of Steady-State Model Simulation and Sensitivity Analysis

Groundwater levels in the Local Model area are considered to be in steady-state equilibrium, allowing measured March and May 2009 groundwater levels to be used for calibrating the steady-state model. A total of 33 groundwater elevations from both piezometers and completed wells were defined as calibration targets in the model and used in the steady-state calibration (**Table 4.2-1**). All targets are located in the upper 8 model layers (corresponding to the upper 1,800 feet of the planned pit depth); 88 percent (29) of the targets are located in model layers 1 and 2 (corresponding to the upper 1,250 feet of the planned pit depth), while the remaining targets are located in model layers 3 through 8.

Specified heads along the Local Model boundary match corresponding heads in the Regional Model.

4.2.8.1 STEADY-STATE CALIBRATION RESULTS: Simulated groundwater level elevations match observed values near the proposed pit area within reasonable limits. Contours of simulated groundwater level elevation for the steady-state simulation and the residual are shown on **Figure 4.2-24**. The residual was calculated by subtracting the simulated groundwater elevation from the observed groundwater elevation at each target location. The residual mean, the average difference between observed and simulated groundwater elevations, is 14.5 feet. As the residual mean approaches zero the simulated groundwater elevations match the observed conditions more closely, on average. The standard deviation is 31.6 feet, and the standard deviation divided by the range of observed data is 2.2 percent. A standard deviation divided by the observed data range of less than 5 percent was targeted for the model calibration. The absolute residual mean, the average of the absolute value of the difference between observed and simulated groundwater elevations, is 29.2 feet and represents the magnitude of the difference between observed and simulated groundwater elevations. The largest difference between simulated and observed groundwater elevations occurs both southeast of the proposed pit within layer 1, where the simulated groundwater elevation is 63 feet lower than the observed elevation, and northeast of the proposed pit in layer 8, where simulated groundwater level is 63 feet above the observed elevation. A graph of observed versus simulated groundwater elevations is shown on **Figure 4.2-25**. Data points for the target locations are grouped around the 45-degree line, indicating a good calibration. **Table 4.2-1** lists the target (observed) values, simulated values and the residual difference.

The simulated groundwater balance for the steady-state simulation is summarized as follows:

Groundwater Inflow

- Constant Head Inflow – 33,490 af/yr (20,748 gpm)
- Recharge – 1,663 af/yr (1,030 gpm)
- **Total In – 35,153 AF/yr (21,779 gpm)**

Groundwater Outflow

- Constant Head Outflow – 35,153 AF/yr (21,779 gpm)
- **Total In – 35,153 AF/yr (21,779 gpm)**

4.2.8.2 STEADY-STATE SENSITIVITY ANALYSIS: Analyses were conducted to evaluate sensitivity of the model calibration to variations in model parameters. Sensitivity was measured using the standard deviation. The standard deviation for the calibrated steady-state simulation is 31.6 feet. For the sensitivity analysis horizontal and vertical hydraulic conductivity were varied individually by hydrogeologic zone, and recharge rate was varied uniformly across the entire Local Model domain. Values were individually increased and decreased by 50 percent from the base simulation, in 10 percent increments. Results of varying these parameters are shown on **Figures 4.2-26, 4.2-27, and 4.2-28** and described as follows:

- The model calibration is very sensitive to increases and decreases to horizontal hydraulic conductivity changes in the Vinini and Rhyolitic Tuff hydrogeologic zones. The model is the most sensitive to increases and decreases to the Vinini resulting in standard deviation increasing to 64 and 51.8 feet, respectively.
- The model calibration is very sensitive to increases and decreases to vertical hydraulic conductivity changes in the Vinini hydrogeologic zone, resulting in standard deviation increasing to 54.6 and 39.1 feet, respectively.
- The model is very sensitive to increases and decreases in recharge rate, resulting in standard deviation increasing to 111.5 and 95 feet, respectively.

Sensitivity analyses provide guidance for determining which parameters substantially influence the model's ability to accurately represent observed conditions and which may

substantially influence the model's ability to predict future conditions. Investigations for data acquisition and data analysis are typically focused on those parameters which substantially influence model results. The analysis indicates model results are sensitive to changes in recharge and horizontal hydraulic conductivity. Recharge values were obtained from published data as described in **Sections 3.2.2 and 3.2.3**. Hydraulic conductivity data were obtained from published and field-acquired data (Interflow, 2010; Montgomery & Associates, 2010b). Determination of vertical hydraulic conductivity from testing is difficult; however, the results are less sensitive to changes in this parameter and the values used in the model are consistent with the understanding of the groundwater system and with values used to characterize similar types of fracture rock flow systems.

4.2.9 Transient Model Calibration to Pumping Test Responses

The model was calibrated to measured groundwater response for three separate long-term pumping tests conducted at pilot dewatering test wells GMI-PDT-1, PDT-2, and PDT-3. Results of the pumping tests are given in March 2010 report "Hydrogeologic Characterization of Pit Area" report (Montgomery & Associates, 2010b). Summaries of the tests are as follows:

- PDT-1 test commenced on May 28, 1009, for an approximate 7.33-day pumping period at an average rate of 60 gpm. Monitored observation wells included PDT2009-240, 241, IGMI-MH-225P, IGM-169, and multi-level grouted piezometers IGMI-MH183, 185, 187, and 196. Measurable groundwater level drawdown response occurred at wells 225P and 240 and these wells were used for transient model calibration. No discernable response was measured at well 169. Well 241 was not equilibrated from construction and short-term testing. Multi-level grouted piezometers were strongly affected by nearby core drilling and did show discernable response to PDT-1 pumping.

- PDT-2 test commenced on July 8, 2009, for an approximate 12.17-day pumping period at an average rate of 121 gpm. Monitored observation wells included GMI-178P, 179P, 222P, 223P, PDT-2009-242 and 244, and multi-level grouted piezometer MH2009-248. Measurable groundwater level drawdown response occurred at wells 178P and 242 and these wells were used for transient calibration; analysis for well 242 required removal of large antecedent trend. No discernable response was observed at wells 222P, 223P or 244. Well 179P and multi-level grouted piezometer 248 had not equilibrated from construction prior to PDT-2 testing.
- PDT-3 test commenced on June 6, 2009, for an approximate 26-day pumping period at an average rate of 70 gpm. Monitored observation wells included IGMI-MH-221P, 222P, 223P, 224P, 232P, 233P, PDT2009-244 and 245. Measurable groundwater level drawdown response occurred at wells 221P, 244, and 245 and these wells were used for transient calibration. Well 223P was strongly influenced by construction of nearby well 244 and had not equilibrated prior to testing. No discernable response was observed at well 223P or at other observation wells.

PEST (Doherty, 2005) was used to vary horizontal and vertical hydraulic conductivity, and specific yield, to inversely match measured groundwater level drawdown at pumping test observation wells. Observation wells with response and observation wells without response were equally weighted in the calibration process. No attempt was made to calibrate to measured response in the pumping wells as turbulent well losses and point drawdown at the pumping well can not be accurately reproduced using the model. The steady-state model calibration was maintained during the transient calibration process, as well as the match to measured hydraulic conductivities from packer tests MH2009-246, 247, and 248.

Results of calibration at observation wells 225P and 240 for the PDT-1 pumping test are presented on **Figures 4.2-29 and 4.2-30**, respectively. Timeline on the figures is displayed from start of the PDT-1 aquifer test which began May 29, 2009. Individual observation well simulated and measured responses are described as follows:

- Observation well 225P: simulated drawdown occurs at a similar time to measured drawdown. Maximum simulated drawdown is approximately 10 feet more than observed. Simulated recovery occurs earlier than measured recovery.
- Observation well 240: simulated drawdown occurs at a similar time to measured drawdown. Maximum simulated drawdown is approximately 7 feet less than observed. Simulated recovery occurs earlier than measured recovery.
- Results of calibration at observation wells 178P, and 242 for the PDT-2 pumping test are presented on **Figures 4.2-31 and 4.2-32**, respectively. Individual observation well simulated and measured responses are described as follows:
- Observation well 178P: simulated drawdown occurs at a similar time to measured drawdown. Maximum simulated drawdown is approximately 2 feet less than observed. Simulated recovery occurs at a similar rate compared to measured recovery.
- Observation well 242: simulated drawdown occurs faster compared to measured drawdown. Maximum simulated drawdown is approximately 7.5 feet more than observed. Recovery in 242 was not observed, simulated recovery occurs very slowly. An extended model simulation was conducted and demonstrates that recovery eventually occurs.
- Results of calibration at observation wells 221P, 244, and 245 for the PDT-3B pumping test are presented on **Figures 4.2-33, 4.2-34, and 4.2-35**, respectively. Individual observation well simulated and measured responses are described as follows:

- Observation well 221P: simulated drawdown occurs faster compared to measured drawdown. Maximum simulated drawdown is approximately 7 feet more than observed. Recovery was not observed in 221.
- Observation well 244: simulated drawdown occurs at a similar time compared to measured drawdown, however a change in slope is not represent by the model. Maximum simulated drawdown is approximately 6 feet more than observed. Simulated recovery occurs more slowly than measured recovery.
- Observation well 245: simulated drawdown occurs faster compared to measured drawdown. Maximum simulated drawdown is approximately 21 feet more than observed. Simulated recovery occurs faster than measured recovery.

Overall, the calibrated transient model shows a reasonable representation of local-scale aquifer behavior in the area of the pumping tests, while also maintaining a reasonable steady-state calibration. Some matches of simulated to measured responses were poor due to incomplete equilibration of some observation wells prior to pumping tests, and due to heterogeneities or hydraulic features which are not defined or poorly understood. These phenomena cannot be defensibly represented in the model.

4.3 MODEL ASSUMPTIONS AND UNCERTAINTY

Model results should be interpreted with knowledge of the uncertainties and conservative approximations inherent in the model. The following section discusses sources of uncertainty and potential effects on model results and interpretation.

4.3.1 Conceptual Hydrogeologic Framework

The local and regional models represent a simplification of the geologic structure of the subsurface, and in the regional flow model, the geology is simplified into hydrogeologic

units to create a conceptual basis for flow modeling. Real-world geology almost certainly differs from that depicted in the model, particularly at great depth where uncertainty inherently increases. Hydraulic property distributions are not available for all subsurface units, and therefore, the model relies upon the calibration process to arrive at reasonable hydraulic parameters for any given hydrogeologic unit.

By definition, a numeric flow model is a simplification of complex processes and geologic conditions. Even in the areas with refined geologic detail, the models still represent simplifications of actual conditions, which can vary significantly over very small distances. At the scales at which numeric flow modeling can be undertaken, the relevant equivalent volume approach has to be applied, whereby, on a regional basis, the hydraulic properties generally represent a generalization of more intricately distributed hydraulic conditions. This is the only practical way to approach numeric flow modeling, and as such, modeling results must be viewed as approximations.

4.3.2 Field Data and Model Input

The accuracy of the calibration process depends on data collected in the field and distributions of water budget parameters, including recharge and discharge from the basins within the Study Area. Potential errors in these data can affect model results and interpretation.

Data available to constrain and calibrate the flow models vary spatially within the model domains. For example, databases have been developed at Mt. Hope and in the proposed Kobeh Valley wellfield area through EMLLC exploration and drilling efforts. Studies by others in Diamond Valley have produced a substantial dataset in the vicinity of the agricultural development. Some portions of the model domain have sparse data, due to the limited development and scientific study. The data collection efforts, including well

construction and testing in the proposed EMLLC Kobeh Valley wellfield and proposed Mt. Hope mining area, have enhanced confidence in model results in those areas.

4.3.2.1 FIELD WATER LEVEL DATA: Field measurements of water level in the Study Area provide the basis for calibration of the numerical model described in this report. In the Regional Model, the majority of well and water level data were obtained from the USGS NWIS database with additional measurements from Tumbusch and Plume (2006), the NDWR, and EMLLC. Well locations and elevation datums in the proposed Kobeh Valley wellfield have been surveyed. In the Local Model, well locations and water level measurement datums have been surveyed for all wells used as calibration targets.

Quantifiable parameters of water level data that can be used to improve and verify accuracy include land surface elevation, proximity to nearby pumping sources (relevant for steady-state targets), accuracy of measurement, accuracy of well identification, and natural temporal variations including barometric pressure variations and the seasonal influences of recharge and ET discharge. Water levels in many wells may fluctuate a few to several feet, in response to discrete, seasonal, or climatic events. The temporal nature of the fluctuation and accuracy of measurements may cause differences in the measured and model-estimated values of head during both steady-state and transient calibrations.

4.3.2.2 PUMPING RECORDS: Precise records of pumping are not available for the Study Area. Pumping estimates were generated from published sources and crop inventories provided by NDWR that apply a duty of water to a known or estimated acreage of irrigated land. To the extent that estimated pumping and consumptive use is different from the actual consumptive use, the calibration will be affected.

4.3.2.3 POTENTIAL ERRORS ASSOCIATED WITH WATER BALANCE ESTIMATES: This model utilizes basin water balances provided in the Nevada Reconnaissance Series Reports published by the USGS (Eakin, 1961 and 1962; Rush and

Everett, 1964; Harrill, 1968) because these published values are more acceptable and defensible, given a lack of site-specific studies. The authors of the basin Reconnaissance Series Reports cited use of the classic Maxey-Eakin technique in developing recharge estimates for each basin, though the actual implementation of the technique differed in Antelope, Kobeh, Pine, and Diamond Valleys. All the authors modified their techniques to account for estimates of recharge within basins and sub-basins with differing perceived elevation-precipitation-recharge relationships, presumably to balance the water budget for a particular basin or group of basins. In many basins within Nevada (Avon and Durbin, 1994; NDWR, 2006), more recent water balance studies have found that older applied techniques can produce lower values of groundwater recharge and discharge. Simulating proposed pumping impacts using a model calibrated to a low water balance would tend to produce more extensive projected drawdown and would therefore be considered a conservative approach. This is the case for the model presented in this report.

4.3.2.4 RECHARGE DISTRIBUTION: The Regional Model input includes recharge distributed among the mountain blocks, alluvial fans, and ephemeral segments of major stream channels. The Regional Model uses a zone-based approach to distribute recharge to these areas. The Local Model, which represents predominantly a mountainous area, applies a more refined distribution of recharge, based on a percentage of precipitation estimated to fall at various elevations in the model domain. Both the precipitation quantity and recharge percentage increase with elevation in the Local Model. The recharge distributions used for the numeric flow models have resulted in satisfactory calibration results; however, other distributions may exist that would provide an equally satisfactory numeric result. Because of the difficulties in quantifying recharge and the associated model sensitivity, recharge distribution assumptions could introduce some uncertainty into model results. In reality, recharge is a complex phenomenon which must be simplified in the modeling process and is a function of precipitation and other factors, for which data are sparse in the model domains.

4.3.2.5 EVAPOTRANSPIRATION: ET within the Study Area has been estimated based on reconnaissance-scale distribution mapping of vegetation and by applying assumed annual volumes of consumptive groundwater uptake by various species. The ET volumes used in the regional flow model are consistent with data from the USGS Reconnaissance Series Reports (Eakin, 1961 and 1962; Rush and Everett, 1964; Harrill, 1968). Variables of maximum ET rate and extinction depth, required for simulation of the ET process, were derived based upon physical observations and measured rates from other basins in Great Basin region (White, 1932; Eakin et al., 1951; Robinson, 1970; Nichols, 1994; Nichols, 2000). None of the authors of the USGS Reconnaissance Series Reports physically measured ET rates in the basins, and therefore, ET can be considered a source of error in the water budgets, potentially affecting model calibration.

4.3.2.6 PIT LATE EVAPORATION: Pit lake evaporation rate has been estimated based on Class A Pan evaporation rates recorded at two meteorological stations: Ruby Lake, located 25 miles northwest of Diamond Valley (elevation 6,010 feet, amsl, 59-year average rate 51.46 inches) and the UNR Beowawe Experiment Station farm located in Grass Valley, located west of Kobeh Valley (elevation 5,745 feet, amsl, 35-year average rate 51.17 inches) (WRCC, 2008). Actual evaporation in the pit lake will be dependent on the unique environment of the steep-walled pit where conditions of temperature and wind across the lake surface may differ from conditions at the meteorological stations.

4.3.2.7 PIT RUNOFF: Runoff for the maximum pit catchment area is calculated by the LAK2 software package based on an estimated runoff coefficient. The base case scenario runoff coefficient is assumed to be 0.3. There could be considerable variation in the actual runoff coefficient due to such factors as the actual condition and slope of the pit walls. It is expected that, over time, the pit walls will change from vertical rock surfaces, hard-packed benches, and haul roads to collapsed walls with variable slope and grain size. Therefore, this parameter could vary over time and could introduce a source of error in the simulation of pit lake recovery in the Local Model.

4.3.2.8 HYDRAULIC PROPERTIES: Distribution of hydraulic properties in the flow models is input on a cell by cell basis, with each model cell having defined hydraulic conductivity and storage parameters. In the Regional Model, groups of cells with the same hydraulic parameters are lumped together into large areas or zones. Properties assigned to the cells are adjusted during calibration but are constrained by available data and geologic interpretations. In some portions of the models, available data are sparse and general assumptions are applied to constrain the values. In areas where aquifer testing has been conducted, aquifer test results are used to constrain the input parameters.

In nature, aquifer properties are more variable than can be represented at the scale of numerical models. The models utilize the concept of equivalent porous medium to represent hydraulic properties on a cell- or zone-sized area over which the model input values are representing average hydraulic properties.

Distributions of hydraulic properties in the model are non-unique, in that there may be more than one combination of hydraulic properties that could be input in the model to achieve an equivalent calibration result. Uncertainty in the model is reduced where aquifer testing (Kobeh Valley wellfield and Mt. Hope mine area) and responses to long-term pumping (Diamond Valley) have allowed for more precise quantification of hydraulic properties.

4.3.3 Wellfield Pumping Uncertainty

The location of pumping, in both historic and future pumping simulations, is represented by approximate well locations. For historic pumping, wells are simulated in the center of cells in which water use has been documented, primarily using NDWR crop inventory data. Simulation of EMLLC wellfield pumping is based on the wellfield development plans, developed in part from data collected in exploration drilling and aquifer testing. The exact number, location, well depths, and well pumping rates have a degree of

uncertainty which will remain until production wells are constructed and actual pumping rates determined. Simulation of wellfield pumping assumes 10 production wells sited along the wellfield pipeline corridor defined in the current Plan of Operations for the mine (SRK, 2010). Pumping is simulated as a constant rate for each year through the planned 44-year mine life. Pumping distribution varies by well, and the total volume pumped annually varies based on projected water supply contributions from pit dewatering. In reality, pumping may be rotated among wells, with some wells off-line for a period of time, and wells could be added or abandoned in the wellfield over the course of the 44-year mine life. Two modified pumping distributions were simulated, with pumping shifted more to the north or south as compared with the base case wellfield pumping configuration (**Section 4.4.4.4**). The differences in projected drawdown imposed by the shifts in pumping within the planned wellfield area brackets the uncertainty related to geographical and temporal pumping distribution in the wellfield.

4.3.4 Model Grid and Cell Size Resolution

The Mt. Hope Project numeric flow models have been developed as tools to reasonably and effectively simulate regional groundwater conditions and are specifically constructed for use in simulating impacts resulting from proposed wellfield pumping and pit dewatering. The level of discretization of the model grid varies by area. In the Regional Model, locations with coarse grid size (5,000 x 5,000 feet) will provide an average head value over a specific grid cell, rather than at a discrete location within the cell. Higher levels of discretization in the Regional Model, particularly in the proposed wellfield and Mt. Hope pit areas, provide increased resolution, with a minimum grid size of 1,000 x 1,000 feet. In the Local Model, the grid is further refined to 100 feet by 100 feet for increased resolution in simulating pit dewatering and development of a post-project pit lake. Water level and drawdown predictions are inherently tied to grid resolution limitations. The model grid also establishes layers of vertical discretization. Accurate simulation of near-well drawdown is based on grid spacing, and simulated drawdown within the pumping cell is an average

drawdown over the cell. Effects of well efficiency on water level drawdown in the pumping wells are not incorporated in the numeric flow model, nor are the near-well formation head losses associated with radial flow into the well. The model will therefore tend to under-predict drawdown near pumping wells; however, the model grid discretization more accurately simulates drawdown on a regional basis.

4.4 PREDICTIVE MODEL SIMULATIONS

Predictive model simulations were conducted to project regional drawdown impacts from proposed Mt. Hope mining operations, including open pit dewatering and subsequent pit lake formation, and mine water supply pumping from the Kobeh Valley Central Wellfield (KVCWF). The simulation period was from 2010 through 2455. The simulation length was chosen to be sufficiently long so as to demonstrate maximum regional extent of the 10-foot drawdown contour resulting from proposed mining activities. For the predictive simulations, the calibrated MODFLOW-SURFACT Regional Model (**Section 4.1**), consisting of a 1955 steady-state simulation and a 1956 through 2006 transient simulation, was extended to simulate groundwater flow through 2009 to establish initial conditions for the predictive modeling period. The Regional Model and Local Model were coupled to evaluate regional impacts from the 33-year pit dewatering and subsequent pit lake formation period. Components of the Regional Model steady-state, transient, and predictive simulations are presented in a schematic timeline shown on **Figure 4.4-1**. **Appendix L** provides the MODFLOW-SURFACT and Groundwater Vistas files for these simulations.

As part of the EIS analysis, three predictive model scenarios, No Action Alternative, Cumulative Action Scenario, and Proposed Action Alternative, were evaluated. Groundwater withdrawals simulated for the three scenarios are summarized in **Table 4.4-1** and described as follows:

The No Action Alternative:

- Diamond Valley agricultural consumptive use continues at 2009 rates (55,800 AF/yr) through 2105, and then is reduced by 60 percent to 22,320 AF/yr.
- Kobeh Valley agricultural consumptive use is at the 2006 rate of 2,900 AF/yr (Bobcat Ranch) through 2011, and increases to 3,570 AF/yr in 2012 (Bobcat Ranch and 3F Ranch).
- Eureka municipal water supply pumping continues at 2006 rate of 300 AF/yr; Ruby Hill mine use pumping continues at 2006 rate of 450 AF/yr terminating at the end of 2012.
- Projected water table drawdown for the No Action Alternative is computed by subtracting projected water level elevations at end of year 2055 from simulated groundwater levels at end of 2009, thus illustrating only projected future drawdown.

The Cumulative Action Scenario:

- Diamond Valley agricultural consumptive use continues at 2009 rates (55,800 AF/yr) through 2105, and then is reduced by 60 percent to 22,320 AF/yr.
- Kobeh Valley agricultural consumptive use is at the 2006 rate of 2,900 AF/yr (Bobcat Ranch) through 2011, and increases to 3,570 AF/yr in 2012 (Bobcat Ranch and 3F Ranch).
- Construction water supply is pumped from 2 wells in the tailings storage facility area, for year 2011 only at a combined rate of 480 AF/yr.
- Pit dewatering begins in year 2012 and continues for 32 years of mining. Water from the pit will be used at the mine and will supplement KVCWF water supply.
- Pit lake formation begins in year 2044.
- KVCWF pumping begins in 2012, and continues for 44 years. The wellfield pumping rate is 11,300 AF/yr, less water from pit dewatering.

- Eureka municipal water supply pumping continues at 2006 rate of 300 AF/yr; Ruby Hill mine use pumping continues at 2006 rate of 450 AF/yr terminating at the end of 2012.
- Projected water table drawdown for the Cumulative Action Scenario is computed by subtracting projected water level elevations at end of year 2055 from quasi steady-state (1955) pre-development levels, and illustrates total historical drawdown plus projected future drawdown.

The Proposed Action Alternative:

- The Proposed Action Alternative examines only the drawdown resulting from the Kobeh Valley Central Wellfield pumping, construction water supply, mine dewatering, and pit lake formation.
- Projected drawdown for the Proposed Action Alternative is computed by subtracting the simulated No Action Alternative water levels from the simulated Cumulative Action Scenario levels.

4.4.1 Predictive Model Boundary Conditions

Calibrated model boundary conditions described in **Section 4.1.3.3** which are unchanged for the predictive simulation include: constant head and general head boundaries, drains simulating springs and artesian wells, HFB boundaries, and ET. Predictive model withdrawals were changed from simulated historic rates as described above for the three predictive model scenarios. Recharge from precipitation was modified in the area of the potentially acid-generating waste rock (PAG) and low grade ore (LGO), because recharge area will not occur at the lined stockpiles.

4.4.1.1 DIAMOND VALLEY SIMULATED AGRICULTURAL PUMPING:

Well withdrawals and consumptive groundwater use by irrigation in Diamond Valley are assumed to continue at a total consumptive use of approximately 55,800 AF/yr (**Section**

3.5.3.1) through 2105. Pumping in Diamond Valley was reduced by 60 percent (from 55,800 to 22,320 AF/yr) beginning in year 2106 through end of simulations. This was implemented to constrain drawdown in Diamond Valley to approximately 300 feet in the agricultural area. This drawdown is consistent with irrigation well depths in Diamond Valley, and represents a sustainable withdrawal rate for modeling purposes. A hydrograph of simulated pumping for Diamond Valley agricultural pumping is shown on **Figure 4.4-2**.

4.4.1.2 KOBEH VALLEY SIMULATED AGRICULTURAL PUMPING: In Kobeh Valley, simulated pumping at the Bobcat Ranch was extended through the mining and post-project simulations at a rate similar to that of historical pumping through 2012 at the 2006 simulated rate of 2,900 AF/yr. Simulated pumping from 2012 forward assumes approximately 3,570 AF/yr of agricultural consumptive use. The pumping was equally distributed among five wells, four of which are located at the Bobcat Ranch and one of which is located at the 3F Ranch. Kobeh Valley Ranch LLC has applied for water rights to continue agriculture at the Bobcat and 3F Ranches. For the predictive simulations, it is assumed that the state would grant the pending applications for a total consumptive use of 3,570 AF/yr. The No Action Alternative and the Cumulative Action Scenario both include the 2012 increased pumping at the 3F Ranch. A hydrograph of simulated pumping for Kobeh Valley agricultural pumping is shown on **Figure 4.4-2**.

4.4.1.3 SIMULATED PIT DEWATERING AND PIT LAKE FORMATION: Pit dewatering is simulated using drains which progress in lateral extent and depth based on the mining plan over the 1-year pre-strip and 32-year pit excavation period (total of 33 years). Pit dewatering is simulated to commence in 2012 (**Figure 4.4-1**). The drains are specified in layers 1 through 5 of the Regional Model and are consistent with the drain configuration used in the Local Model (**Section 4.5.1**). Coupling of the Local Model with the Regional Model is discussed in **Section 4.5.3** followed by simulation of a pit lake (**Section 4.5.4.2**). Water balance for the pit lake is simulated with the Local Model (**Section 4.5.3.1**). The net pit lake fluxes vary annually and were computed using the Local Model. The pit inflows

computed using the Local Model from the base case recovery simulation start at 460 AF/yr (average over the first year of pit lake formation, year 2044) and decrease to 158 AF/yr at equilibrium. The groundwater inflow to the pit lake computed from the Local Model is specified in the Regional Model using wells. The Regional and Local Models are coupled during the pit lake formation, as discussed in **Section 4.2**.

4.4.1.4 DISTRIBUTION OF PUMPING IN THE KOBEH VALLEY CENTRAL WELLFIELD: Pumping from the proposed KVCWF is simulated to begin in 2012 and continue for the 32-year open pit mine excavation and 12-year low-grade ore processing (total project life of 44 years) (**Figures 4.4-1 and 4.4-2**). Pumping is simulated from ten wells situated along the Plan of Operations (SRK, 2010) wellfield pipeline corridor (**Figure 1.1-2, Appendix B**). Simulated pumping distribution is given in **Table 4.4-2**. The well pumping rates simulated in the model are continuous flow rates, ranging from 350 to 1,260 gpm. The combined pumping from the KVCWF wellfield, plus simulated Local Model pit dewatering, totals approximately 11,300 AF/yr, or a continuous flow of approximately 7,000 gpm.

Table 4.4-3 summarizes the annual pumping rate distribution in the wellfield during the 44-year mine life, including small reductions in KVCWF pumping due to availability of water from the pit. When pit dewatering is ongoing, the total pumped volume from the wellfield varies each year depending on the volume of water produced by pit dewatering, the sum equaling the total process water demand of 7,000 gpm

The distribution of pumping among the ten simulated KVCWF wells is based on results of exploration drilling and aquifer testing (Interflow et al., 2010). Analytical evaluations of long-term drawdown using the Theis equation were used to establish a preliminary but conservative range of potential long-term pumping rates for each production well site. **Appendix B** contains a summary of the evaluations made in consideration of the pumping rate distribution.

4.4.2 Model Stress Periods

The calibrated Regional Model simulation was extended from 2006 to 2009 using annual stress periods, allowing for updating of actual annual pumping and other groundwater stresses for that period. Simulated 2009 groundwater conditions were used as initial conditions for the predictive simulation period. For the predictive period, annual stress periods were specified for the period 2010 through 2145 and 10-year stress periods were specified for the period 2146 through 2455.

4.4.3 Simulated Current Conditions (2009)

Water level contours and drawdown from pumping that has occurred from 1955 through 2009 are presented on **Figures 4.4-3 and 4.4-4**. Groundwater inflows and outflows are summarized in **Table 4.4-4**.

Model simulations indicate that up to approximately 30 feet of drawdown has occurred in southwestern Kobeh Valley due to historic pumping at the Bobcat Ranch (**Figure 4.4-4**), which compares well with the degree of drawdown thought to have occurred in the area (**Section 3.5.3.2.1**).

Drawdown in southern Diamond Valley is over 100 feet, and the 10-foot drawdown contour extends north to the vicinity of the playa edge. As discussed in more detail in **Section 4.1.4.5**, and illustrated on **Figures 4.1-33 through 4.1-46**, simulated drawdown in Diamond Valley is approximately 10 to 20 feet greater than observed for some portions of the agricultural area, and is associated with a reduction of drawdown for a period from the mid 1980s to early 1990s. Drawdown trends continued after this time period at similar rates as observed in pre-1980s conditions. However, the lack of observed drawdown during this timeframe results in a slight overprediction of drawdown in the agricultural area for current (2009) conditions.

ET in Kobeh Valley is diminished by approximately 238 AF/yr (1.4 percent) over pre-development conditions, and in Diamond Valley ET (North and South subareas) is diminished by approximately 12,848 AF/yr (47 percent) (**Table 4.4-4**). Simulated subsurface inflows to Diamond Valley from Kobeh Valley and Garden Valley are increased by 418 AF/yr and 92 AF/yr, respectively, as a result of increasing gradients between the basins as drawdown occurs in Diamond Valley.

4.4.4 Predictive Simulation Results

4.4.4.1 NO ACTION ALTERNATIVE: Projected 2055 water level contours and drawdown for the No Action Alternative are shown on **Figure 4.4-5 and Figure 4.4-6**; simulated drawdown on **Figure 4.4-6** is computed by subtracting projected 2055 water levels from current (2009) water levels. Water resource attributes (springs, wells, and water rights) within the projected extent of 10-foot drawdown for year 2055 are shown on **Figure 4.4-7**. The simulation indicates 211 springs, 282 wells, and 542 active water rights sites are within the 10-foot drawdown contour (**Appendix M**). Most of these locations are within Diamond Valley. Reporting of drawdown for springs, wells, and water rights in **Appendix M** is by zones. Six drawdown zones were selected (**Figure 4.4-7**) based on geographic location and proximity to pumping stresses. Projected drawdown is reported in **Appendix M** as the range of projected drawdown in the zone, and as the arithmetic mean of predicted drawdown within the zone. Drawdown values for springs, wells, and water rights outside of the zones are reported as a single value.

Under the No Action Alternative, drawdown continues to increase in Diamond Valley. Simulated year 2055 drawdown increases in Diamond Valley by greater than 100 feet compared to simulated 2009 water levels. Simulated year 2055 drawdown in southwest Kobeh Valley (Bobcat Ranch) is increased by more than 20 feet compared to simulated 2009 water levels, with a small localized drawdown area of 40 feet east of the Bobcat Ranch area.

Table 4.4-5 presents a comparison of major water balance flows in the No Action Alternative at simulation year 2055 (same stress period as Mine Year 44) and simulation year 2105 (same stress period as post-project year 50), to current (2009) conditions.

4.4.4.2 CUMULATIVE ACTION SCENARIO: Projected 2055 water level contours and drawdown for the Cumulative Action Scenario are shown on **Figure 4.4-8** and **Figure 4.4-9**; simulated drawdown on **Figure 4.4-9** is computed as the cumulative drawdown from 1955 to 2055, including all major agricultural, industrial, and municipal, pumping, and pumping under the Proposed Action Scenario. Water resource attributes (springs, wells and water rights) within the predicted extent of 10-foot drawdown for year 2055 are shown on **Figure 4.4-10**. The simulation indicates 243 springs, 290 wells, and 575 water rights sites are within the 10-foot drawdown contour (**Appendix M**). Most of these locations are within Diamond Valley.

Under the Cumulative Action Scenario, drawdown continues to increase in Diamond Valley. Simulated year 2055 drawdown in Diamond Valley is more than 200 feet compared to simulated 1955 water levels. Simulated year 2055 drawdown in Kobeh Valley at Bobcat Ranch is more than 30 feet, and drawdown near the center of the KVCWF is more than 100 feet compared to simulated 1955 water levels. Water level drawdown also propagates vertically in the model domain, into model areas representing bedrock that underlies the alluvial materials in the KVCWF. **Figure 4.4-11** shows simulated Cumulative Action Scenario water table elevation for year 2055 for a cross-section through the KVCWF.

Table 4.4-6 presents a comparison of major water balance flows in the Cumulative Action Scenario at simulation year 2055 (same stress period as Mine Year 44) and simulation year 2105 (same stress period as post-project year 50), to pre-development conditions (1955).

4.4.4.3 PROPOSED ACTION ALTERNATIVE: Projected water level drawdown contours for the Proposed Action Alternative for years 2020, 2030, 2040, and 2055 are

shown on **Figures 4.4-12 and 4.4-13**. These drawdown results are generated by subtracting projected No Action Alternative water levels from the projected Cumulative Action Scenario water levels. **Table 4.4-7** presents a comparison of major water balance components of the No Action Alternative and the Cumulative Action Scenario.

Drawdown in the EMLLC Kobeh Valley Central Wellfield (KVCWF) ranges from approximately 100 to 130 feet in the northern portion of the wellfield and 30 to 80 feet in the southern portion **(Figure 4.4-13)** by the end of mine life (Project Year 44, simulation year 2055). The total change in subsurface outflow from Kobeh Valley to Diamond Valley as simulated in Mine Year 44 (2055) is a net gain of 15 AF/yr (Table 4.4-7). The net gain is a result of additional inflow to Diamond Valley near the pit of approximately 40 AF/yr, offset in part by a simulated reduction in subsurface flow through the Whistler Range and Devils Gate of 25 AF/yr. Since the additional inflow of 40 AF/yr near the pit is comsumed by the evaporation at the pit and does not flow through or past the pit, the impact to available Diamond Valley groundwater resources caused by the Proposed Action is a reduction of 25 Af/yr of subsurface flow (about 1 percent of the total simulated subsurface flow) that would otherwise flow through the Whister Range and Devils Gate into Diamond Valley.

Figure 4.4-14a presents a hydrograph of projected water table drawdown for the Proposed Action Alternative at several geographic locations in Kobeh Valley **(Figures 4.4-12 and 4.4-13)**. **Figure 4.4-14b** presents simulated water table drawdown for the No Action, Cumulative Action, and Proposed Action alternatives for phreatophyte areas in Kobeh Valley. For project year 44 (2055), Proposed Action projected drawdown in the central valley floor phreatophyte area, between Lone Mountain and Bean Flat, is about 8 feet. Water level recovery is projected to begin soon after end of wellfield pumping. For project year 44 (2055), Proposed Action projected drawdown in the Bean Flat area is about 3 feet, and projected drawdown increases to a maximum of about 4 feet around year 2080, followed by slow recovery.

The maximum lateral extent of water level drawdown is simulated to occur between approximately 2 and 30 years following cessation of mine pumping ("post-project"), as illustrated on **Figure 4.4-15**. The timing of the occurrence of the maximum lateral extent of drawdown varies spatially over the area of influence. The drawdown influence is simulated to expand and contract more slowly on the western side of Kobeh Valley and in the Roberts Mountains than in the central and eastern areas of Kobeh Valley.

Drawdown in the Roberts Mountains to the north of the KVCWF is projected due to the fact that the model has hydraulic connection between the valley fill materials and shallow carbonate rocks tapped by the wells in the KVCWF and the carbonate rocks that comprise the Roberts Mountains. Representation of an identified fault barrier at the base of the Roberts Mountains constrains the propagation of drawdown to the north, but does not preclude the occurrence of drawdown. Projected water table drawdown at the LRCMW and MRCMW (existing lower and upper Roberts Creek monitoring wells) is approximately 20 and 15 feet, respectively, at the end of project life (**Figure 4.4-15**).

Figure 4.4-16 shows the extent of the simulated 10-foot drawdown surrounding the pit for post-project years 10, 50, 100, 150, 200, 250, 300, 350, and 400. Drawdown impacts around the pit take a much longer time to equilibrate due to the low permeability conditions near Mt. Hope (**Section 4.5.4.2**). The maximum lateral extent of water table drawdown is simulated to occur at approximately 100 to 200 years after cessation of mining.

Figure 4.4-17 shows simulated drawdown in upper Henderson Creek and upper Vinini Creek, using simulated groundwater withdrawals for the No Action and Proposed Action Alternatives, and for the Cumulative Action Scenario. For purposes of **Figure 4.4-17**, the drawdown has been computed relative to 1955 pre-development conditions. Maximum drawdown for the Proposed Action Alternative is approximately 5 feet, and occurs approximately 150 to 200 years post-project. Simulated maximum

drawdowns for the No Action Alternative and Cumulative Scenario are about 16 feet and 23 feet, respectively, and occur approximately 150 to 200 years post-project.

Figure 4.4-18 shows simulated ET discharge of groundwater in Kobeh valley for the No Action, Cumulative Action, and Proposed Action Alternatives. The occurrence time for the projected maximum reduction in ET varies between 1 and 16 years after cessation of KVCWF pumping ("post-project") for shrub and salt grass phreatophyte types, respectively. ET discharge in project year 44 totals 11,016 AF/yr for the Cumulative Action Scenario (**Table 4.4-7**), which is a decrease of 4,015 AF/yr from the No Action Alternative. Projected maximum reduction in total Kobeh Valley ET occurs in post-project year 4 and is slightly greater than 4,015 AF/yr.

Figure 4.4-19 shows simulated discharge (Cumulative Action Scenario) for Tonkin Spring, Shipley Spring, and Thompson Ranch Springs, and for southern Diamond Valley Playa springs and ET. Simulated discharge for Thompson Spring, and southern Diamond Valley Playa springs and ET cease prior to initiation of the Proposed Action Alternative. Historical records demonstrate that Thompson Spring and Souther Diamond Valley Playa springs have already ceased to discharge (**Table 3.3-1**). Simulated discharge for Shipley Spring is also shown for the No Action Alternative. Projected Shipley Spring discharge for the No Action Alternative and Cumulative Action Scenario are identical, demonstrating that the Proposed Action Alternative has no effect on Shipely Spring discharge. **Tables 4.4-8 through 4.4-10** summarize the known wells, water rights, and spring resources within the area of the projected maximum extent of 10-foot drawdown, as shown on **Figure 4.4-20**. Nine wells not belonging to EMLLC have been identified within the 10-foot drawdown extent; seven of these have existing water rights for stock water supply (**Table 4.4-8**). Twenty-five existing water rights that are not part of the EMLLC project and have points of diversion within the simulated 10-foot drawdown area; many of these have designated uses for stock watering associated with a spring water source (**Table 4.4-9**).

Twenty-nine springs from the comprehensive spring dataset prepared for this study are identified as being within the area of simulated 10-foot water table drawdown (**Table 4.4-10**). EMLLC has collected baseline spring flow measurements throughout the area of projected maximum extent of 10-foot drawdown (**Appendix E**).

Tables 4.4-8 through 4.4-10 include projected drawdowns at water right locations and springs through 400 years post-project. No additional non-project wells are affected within this time period. A discussion of predicted impacts is provided in **Section 4.4.4.5**.

4.4.4.4 ALTERNATIVE WELLFIELD PUMPING SCENARIOS: Although the most likely pumping distribution within the KVCWF has been evaluated (**Section 4.3.11**), two alternative pumping scenarios have also been simulated, as summarized in **Table 4.4-11**. **Appendix L** includes the MODFLOW and Groundwater Vistas model input files for these simulations. The alternative distributions shift pumping more to the north or south within the wellfield as compared with the base case pumping distribution simulated in the Cumulative Pumping Scenario and Proposed Action Alternative. Pumping is simulated from the same ten production well locations as used in the base case. In the northern shift scenario, carbonate aquifer pumping is increased to 17 percent of total pumping, and greater pumping is simulated from northern valley fill wells. In the southern shift scenario, pumping from the carbonate aquifer remains the same as the base case, at 10 percent, but with the pumping increased in southern valley fill wells.

Figure 4.4-21 shows the simulated 2055 water table drawdown for the north and south shifts in pumping distributions. Shifts in the distribution of pumping create minor differences in the shape and lateral extent of simulated drawdown. In the southern shift scenario, simulated drawdown in the wellfield ranges from approximately 80 to 100 feet in much of the central and northern areas. In the southernmost portion, simulated drawdown is approximately 40 to 80 feet (**Figure 4.4-21**). In the northern shift scenario, drawdown in the northern portion of the wellfield is the greatest at approximately 180 feet with lesser

drawdown of 30 to 70 feet in the southern wellfield area. **Figure 4.4-22** presents a comparison of the projected extent of drawdown under the base case pumping distribution versus the northern and southern distribution shifts. The overall extent of drawdown is similar for all three pumping distributions, with small shifts in the projected drawdown corresponding to shifts in pumping. **Table 4.4-12** gives subsurface inflows, outflows, and ET for all three simulated wellfield distributions. Results are similar for all three simulated pumping distributions.

4.4.4.5 DISCUSSION OF PREDICTED IMPACTS: Potential impacts to water resources due to proposed pumping of groundwater for the Mt. Hope project include:

- Diminished flow from springs
- Diminished flow in perennial streams
- Diminished density and/or occurrence of phreatophytes, including shrub and grass communities
- Increased depth to water in wells

Water resources were considered to be potentially impacted if located within the predicted 10-foot water table drawdown contour. Because the 10-foot drawdown occurs at different times at different places, the "composite" 10-foot drawdown contour was used to show the maximum lateral extent of the 10-foot water table drawdown contour over time. The composite 10-foot drawdown contour represents the maximum extent of the 10-foot drawdown contour over the simulation period.

Potential for impacts to spring resources are assessed using predicted magnitude of water table drawdown, as summarized in **Table 4.4-10**. The occurrence of springs within the predicted area of impact is primarily within the Roberts Mountains (**Figure 4.4-20**). However, there is uncertainty regarding hydraulic connection of springs to the regional aquifer system, and also the ability of the model to simulate drawdown in mountainous areas, where the geology is complex and may include fractured rock flow systems. However, the model offers the best available tool for making predictions, and it suggests a potential for

impacts to spring flows in the Roberts Creek and Henderson Creek watersheds. It should be noted that many of the springs listed in **Table 4.4-10** are located near the outer margin of the predicted composite 10-foot drawdown impact area. These impacts are projected to occur near the end of mining, or decades after mining activities cease.

Springs at Mt. Hope have been included in baseline monitoring by EMLLC. These springs in the vicinity of Mt. Hope have been characterized as seasonal and small. The seasonal springs may reflect either temporary shallow groundwater or perched groundwater, and may not be associated with regional flow systems. Impacts resulting from groundwater pumping and dewatering will probably be minimal at springs that are not directly connected to the regional groundwater system. Spring site 638 (**Figure 4.4-20**) is located within the proposed pit footprint and will be mined out. Spring site 638 was identified from 7.5-minute USGS topographic mapping (**Appendix E**); however, field investigations by EMLLC personnel have not identified a spring at the mapped location.

Springs located in lower altitudes in the Roberts Mountains, such as sites 630 and 640 (**Figure 4.4-20**) are more likely to be impacted due to closer proximity to the KVCWF, resulting in larger predicted drawdown at these locations. Discharge at Mud Spring (Site 721) and Lone Mountain Spring (Site 742), located near the southeast edge of the KVCWF near proposed well 226, are predicted to be impacted and will likely cease to flow based on predicted drawdowns of 40 to 50 feet. Both of these springs discharge less than approximately one gallon per minute.

Roberts Creek and Henderson Creek are the only perennial streams within the predicted Proposed Action composite 10-foot drawdown contour. The base flows in Roberts Creek and Henderson Creek may depend in part on springs that may be connected to the regional groundwater system. If flow from those springs is diminished, base flow in Roberts Creek and Henderson Creek may also be diminished. However, a portion of flow in both streams is supported by spring discharge outside the predicted Proposed Action composite

10-foot drawdown contour, and seasonal runoff due to precipitation and snowmelt would not be affected by regional groundwater pumping.

There are numerous ephemeral drainages and lower reaches of perennial streams that become ephemeral within the predicted composite 10-foot drawdown contour. Flow in these ephemeral reaches is generally not the result of connection to the groundwater system, and occurs primarily in response to high precipitation and/or snowmelt events. These resources would not be affected by groundwater pumping, and therefore are not detailed in this report.

Predicted drawdown of the water table occurs at phreatophyte areas in Kobeh Valley, primarily west and northwest of Bean Flat, and, to a lesser extent, east of Lone Mountain (**Figures 4.4-12, -13 and -16**). The predominant phreatophyte vegetation in these areas is greasewood. The simulated extinction depth for greasewood is 40 feet below ground surface. At the outer extent of these phreatophytes the simulated water levels will exceed the extinction depth, causing some die-off of the greasewood. In the interior of the phreatophyte areas, the depth to groundwater would increase, but not exceed the extinction depth, resulting in a decrease in number and density of the greasewood plants and associated decrease in evapotranspiration of groundwater.

Only a few wells and water rights not directly associated with the EMLLC Mt. Hope project are within the area of predicted 10-foot drawdown contour (**Tables 4.4-8 and 4.4-9**; **Figure 4.4-20**). Notably, significant drawdown is projected for a well at the Roberts Creek Ranch.

The anticipated duration of drawdown and recovery varies over the area of impact (**Tables 4.4-8 through 10**). For purposes of description, the areas have been segregated into the following:

1. Areas close to the open pit lake
2. Areas close to the KVCWF
3. Areas in the Roberts Mountains block north of the KVCWF

For resources close to the open pit lake, such as spring site 639, the predicted drawdown maximum occurs early in time with subsequent drawdown trends toward a new suppressed equilibrium level resulting from the permanent feature of the pit lake. For resources more distant from the open pit lake but within the 10-foot drawdown contour, the drawdown maximum occurs later in time than for resources closer to the pit and corresponds to the equilibrium level of the water table surrounding the pit lake (for example, spring site 580). Predicted drawdown varies depending on proximity to the proposed pit; for details of projected drawdown see **Tables 4.4-8 through 10 and Figure 4.4-20**.

Resources close to the KVCWF are projected to have drawdown maximums within 1 to 15 years post-mining and are projected to recover thereafter. Predicted drawdown varies depending on proximity to the proposed well field; for details of projected drawdown see **Tables 4.4-8 through 10 and Figure 4.4-20**.

For resources in the Roberts Mountains, predicted drawdown reaches a maximum at approximately 30 years post-mining, beyond which there is a gradual recovery trend (**Tables 4.4-8 through 10**; **Figure 4.4-20**). For springs 630 and 641, degree of drawdown is dependent upon proximity both to the KVCWF and to the pit. For other resources within the Roberts Mountains, degree of drawdown is more dependent on proximity to the KVCWF.

4.5 MINE DEWATERING AND PIT LAKE SIMULATIONS

Predictive simulations were conducted first for the 1-year pre-mining period followed by 32 years of mining, which constitute the pit dewatering period, and second for the

subsequent 1,580-year post-project pit lake development period. The 1,580 years represents an arbitrary length of time which exceeds the time required for model pit lake formation to approach equilibrium. A schematic timeline for local model simulations is presented on **Figure 4.4-1**. Both the dewatering and pit lake formation simulations are coupled with the Regional Model. Predictive sensitivity analyses of selected model parameters were conducted to evaluate potential variability in the projected pit lake water balance and pit lake stage.

4.5.1 Simulation of Mine Excavation/Pit Dewatering

Drain cells are used to simulate groundwater discharge into the open pit during the 33-year pre-mining and mining period. The drain cells are specified to match the pit excavation over time as defined by a progression of mine-plan pit shells provided in electronic format (Independent Mining Consultants, Inc., 2007). Groundwater discharge to the drains is representative of groundwater flow into the open pit which will be removed via sump pumping. Passive or active dewatering boreholes or wells are not currently planned for the pit excavation and are not evaluated as part of this study. Pit wall drainage or depressurization may be required depending on geotechnical considerations; however the need for such measures has not been established. Use of such measures would be expected to only minimally increase pit-dewatering rates and result in negligible altering of groundwater impacts at distance from the mine and the lake equilibrium, compared to the pit-sump dewatering simulated in this model.

Drain configurations are constant during a stress period, with specified drain elevations approximately equal to the bottom of the mine pit projected to exist at the end of the stress period, according to the mine-plan pit shell. In concept, the drain cells are specified at locations internal to the pit shell in the void space of the open pit. **Figure 4.5-1** shows the lateral extent of drain cells according to the mine plan. **Figure 4.5-2** shows the

advance of drain cells through time in cross-section for transect B-B'. A conceptual depiction of drain cells specified in the model is shown on **Figure 4.5-3**.

The drain cells are a head-dependent flux boundary condition that simulates discharge from the surrounding formation into the pit void, as long as the simulated groundwater level in the surrounding formation is above the specified drain elevation. As described previously, the drain cells represent the pit void space; therefore, the drain elevations are specified 10 feet below the pit bottoms, resulting in complete dewatering of the simulated pit void. The simulated discharge rate is proportional to the difference between simulated head and the specified drain elevation, multiplied by the conductance term. The conductance of the drains must be set high enough to ensure groundwater discharge inflow into the pit void is controlled by the surrounding formation rather than being artificially constrained by the drain conductance.

Drain cell conductances were varied between 0.01 to 300 feet squared per day (ft^2/d), with the intent to determine the threshold at which drain cell conductances do not constrain pit inflows. Simulated results of total pit inflows for the 33-year excavation period, for each conductance, are presented in the following table:

Drain Conductance (ft^2/d)	**Cumulative Volume (acre-feet)**
0.01	6,099
0.1	12,766
1	14,965
10	15,540
100	15,699
200	15,741
300	15,811

For each increase in simulated drain conductance there is an increase in pit inflow, with the largest simulated inflow occurring at the 300 ft^2/d conductance value. The 300 ft^2/d conductance simulation required longer computer run times. The 200 ft^2/d simulation

computer run time was shorter and resulted in pit inflows negligibly smaller than the 300 ft^2/d simulation; therefore, the 200 ft2/d drain conductance is considered appropriate for the pit-dewatering simulations and does not constrain pit inflows.

4.5.2 Simulation of Pit Lake Development

Following cessation of mining and pit dewatering, groundwater levels will begin to recover and will eventually "daylight" in the pit, forming a pit lake. To simulate hydrogeologic conditions during this period, the MODFLOW lake software package, LAK2 (Council, 1999), was used. As formulated, the LAK2 software accounts for precipitation that falls on the lake catchment area, evaporation from the lake surface, and storage in the lake. The lake package was developed as a head-dependent boundary condition that simulates groundwater flow into the lake when the calculated lake stage is lower in altitude than groundwater levels in the formation surrounding the pit. Conductance for the head-dependent boundary between the lake and the surrounding formation was specified as the lake cell conductance. For the post-project simulation, the model cells that correspond to the final pit shell configuration are specified as no-flow. These inactive cells effectively lie within the area of the simulated pit lake and are not considered in the model calculation.

Use of the LAK2 software requires functional relationships between lake elevation (stage), lake volume, and lake surface area. These relationships were derived from the final pit configuration for the current mine plan (SRK, 2010). A digital terrain model of the open pit was constructed and used to define the bottom of the lake in the numerical model. A feature of the LAK2 software that allows the user to subdivide individual lake cells independent of the model grid was utilized to increase resolution in the vertical direction. This allowed a closer match of the model representation of the proposed mine plan for the stage-area-volume relationship. The relationships among lake surface elevation, surface area, and volume are shown on **Figure 4.5-4**.

4.5.2.1 PRECIPITATION AND EVAPORATION: Precipitation falling on the lake catchment area was assigned a value of 100 percent of estimated precipitation for the pit area, or 14.94 inches per year, or 0.0034 ft/d. This value represents the long-term average precipitation estimated to fall on Mt. Hope, as derived from PRISM and supported by other regional precipitation data (**Section 3.2**).

Evaporation simulated from the lake surface was assigned a value of 37.46 in/yr (0.0086 ft/d). This rate is approximately 73 percent of the average Class A Pan evaporation rate recorded at two meteorological stations: Ruby Lake, located 25 miles northwest of Diamond Valley (elevation 6,010 feet, amsl, 59-year average annual rate 51.46 inches), and the UNR Beowawe Experiment Station farm, located in Grass Valley, directly west of Kobeh Valley (elevation 5,745 feet, amsl, 35-year average annual rate 51.17 inches) (WRCC, 2008). Pan evaporation data are not collected at these stations during the winter months (November through March), during which evaporation at these sites is expected to be small. The average partial-year Class A Pan evaporation rate observed at these sites is 51.315 inches, and this value is used as the Class A Pan evaporation rate at Mt. Hope. The average of the partial-year evaporation rates observed at these sites (51.315 inches) is a conservative assumption with respect to the development of the pit lake because using a partial-year evaporation rate overestimates the elevation of the pit lake surface compared to what would be expected with a full-year evaporation rate. Although a pan coefficient of 0.70 is commonly used to reduce the pan evaporation rate to a lake evaporation rate, 18 empirical studies conducted between 1947 and 1984 demonstrated that physical and climatological conditions influence pan coefficient (Linacre, 1994). The range of pan coefficients calculated by these studies is 0.60 to 0.82, with a mean of 0.73 and a median of 0.75 (Linacre, 1994). Applying these pan coefficients to the pan evaporation data from Ruby Lake and Beowawe, the minimum, mean, and maximum evaporation rates for the pit lake are 30.70, 37.46, and 48.37 in/yr, respectively. Therefore, the base simulation value specified evaporation rate was 37.46 in/yr, or 0.0086 ft/d.

4.5.2.2 RUNOFF: Thirty percent of the precipitation that falls in the catchment area surrounding the lake (i.e. above the lake stage) was simulated as runoff into the lake. Therefore, runoff is approximately 0.00103 ft/d in the base case simulation. The remaining 70 percent of the precipitation is assumed to be lost to evaporation on the pit walls, which will be benched and will tend to catch and hold precipitation. The LAK2 software internally calculates the portion of precipitation that enters the lake as runoff, depending on the simulated lake size and the resulting size of the catchment area not covered by the lake.

A small area of pit catchment located northwest of the pit is not included in the lake package but will contribute runoff to the lake (**Figure 4.2-2**). Runoff from this area is constant during the pit lake formation period because the lake surface will never rise to encroach upon the area. Runoff from this area was specified as 11,708.1 ft^3/d.

4.5.2.3 LAKE CELL CONDUCTANCE: Lake cell conductance terms were computed externally to the LAK2 software. Lake cell conductance terms were adjusted so that initial inflow rate for the approximate first month after the end of dewatering approximately matched the final month of simulated dewatering outflow in the dewatering model (approximately 64,100 ft^3/d). Lake cell bottom conductance was specified as 1.20 ft^2/d; lake cell side conductance was specified as 0.60 ft^2/d.

4.5.3 Local and Regional Model Coupling

Simulation of pit dewatering and pit lake formation in the Local Model, combined with simulation of mine supply pumping and other pumping in the Regional Model, requires an iterative coupling process between the two models in order to achieve projections in each model that correctly incorporate the influence from all stresses in the study area. Specified-heads were simulated for the lateral boundaries of the Local Model (**Figure 4.2-12**). The specified heads for the Local Model boundary change over time due to influence from Local Model stresses including pit dewatering and pit lake formation, and due to Regional Model

mine supply pumping. For each stress period, Local Model specified heads were determined based on iterative Regional Model simulations of pit dewatering, pit lake formation, and regional mine supply pumping, and on iterative Local Model simulations of pit dewatering and pit lake development. Specified heads for each Local Model layer boundary were assigned by vertically interpolating from the corresponding Regional Model layer heads located above and below the Local Model layer.

As part of the coupling process, the Regional Model was temporally divided into three distinct models to correspond with the timing used in the Local Model. The first is referred to as the historical model and simulates the period from 1955 (Regional Model steady-state) to 2009. The second corresponds to the 1-year pre-mining and 32-year mine dewatering period. The third corresponds to the post-project pit lake formation period.

Methodology for linking the Regional and Local Models is described below for both dewatering and pit lake formation simulations.

Mine Dewatering Coupling

Step 1. The Regional Model 33-year mine-dewatering simulation is run (described in **Section 4.4.1.3**) using drain cells to represent the pit excavation. The Regional Model simulation includes estimated KVCWF mine supply pumping.

Step 2. Projected heads from the Regional Model over the 33-year mine-dewatering period are used to update the specified heads for the Local Model boundary. The Local Model simulation is then run.

Step 3. Projected Local Model pit inflows are evaluated to determine available water to satisfy mine processing water requirements, with the remaining substantial majority to be supplied by KVCWF pumping. KVCWF pumping is updated for subsequent Regional Model simulation.

Step 4. Steps 1 through 3 are repeated until consecutive Step 2 Local Model pit inflows change less than 1 percent. Process stops at Step 2.

Pit Lake Formation Coupling

Step 1. A Local Model pit lake formation simulation is run using the LAK2 software package (described in **Section 4.5.2**). Initial estimates are made for the Local Model specified head boundaries.

Step 2. A Regional Model simulation is run using projected Local Model LAK2 pit lake inflow rates for the 1,580-year post-project period (groundwater discharge). Pit inflow rates are simulated with wells. Pumping well locations approximate the pit extent at full build-out.

Step 3. Simulated heads from the Regional Model over the 1,580-year post-project period are used to update the specified heads for the Local Model boundary.

Step 4. Steps 1 through 3 are repeated until consecutive Step 1 Local Model pit inflows change less than 1 percent. Process stops at Step 1.

4.5.4 Predictive Base Case Results

4.5.4.1 MINE DEWATERING: Projected average inflow rate during pit dewatering is shown on **Figure 4.5-5** and summarized in **Table 4.5-1**. Local model MODFLOW-SURFACT and Groundwater Vistas input and output files are found in **Appendix L, Part 2**. Projected average inflow rates increase from approximately 58 gpm within year 1 of proposed mining operations to 460 gpm in year 30, and then decrease to approximately 420 gpm at mine completion in year 32.

Simulated groundwater level elevation at the end of mining operations is projected to be approximately 4,690 feet, amsl and occurs at the pit bottom. Due to the low hydraulic conductivity in the mine area, groundwater levels increase substantially with distance from the pit resulting in a hydraulic sink with steep gradients in the area of the pit. Contours of simulated groundwater level elevation at the end of mining operations in the vicinity of the pit are shown on **Figure 4.5-6**. Simulated groundwater levels shown on **Figure 4.5-6** were used as initial head conditions for the pit lake formation simulation.

4.5.4.2 PIT LAKE FORMATION: Projected water balance for the pit lake after cessation of mining is shown on **Figure 4.5-7**. Development of the pit lake was simulated for 1,580 years after end of mining, which is longer than required for equilibration of the pit lake water balance. The LAK2 software is less stable and requires smaller time steps at the beginning of pit lake formation when groundwater inflows and evaporative losses alternate between time steps as the dominant stress. Groundwater inflows to the open pit decrease gradually from an initial rate of 285 gpm after the first year to approximately 236 gpm at 10 years after mining approximately 159 gpm at 100 years after mining, and approximately 98 gpm at 940 years, after which inflows remain relatively constant at approximately 98 gpm through year 1,580. Projected lake stage and groundwater level elevation contours for 0, 10, 50, 100, 200, and 1,580 years after the end of mining are shown on **Figures 4.5-7 through 4.5-12**, respectively.

10 Years Post-Project

The groundwater model predicts that the lake stage will be at an elevation of about 5,029 feet, amsl, which corresponds to a maximum lake depth of approximately 304 feet. Projected surface area of the pit lake is approximately 37.9 acres. Lowest elevation of the groundwater divide encircling the pit is 6,241 feet, amsl, which is 1,212 feet higher than lake stage, as shown on Figure 4.5-8. Hydraulic gradient is maintained towards the pit from all directions, demonstrating that the pit is a hydraulic sink 10 years after mining (**Figure 4.5-8**).

50 Years Post-Project

The groundwater model predicts that the lake stage will be at an elevation of about 5,349 feet, amsl, which corresponds to a maximum lake depth of approximately 624 feet. Projected surface area of the pit lake is approximately 82.9 acres. Lowest elevation of the groundwater divide encircling the pit is 6,242 feet, amsl, which is 893 feet higher than lake stage, as shown on **Figure 4.5-9**. Hydraulic gradient is maintained towards the pit from all directions, demonstrating that the pit is a hydraulic sink 50 years after mining (**Figure 4.5-9**).

100 Years Post-Project

The groundwater model predicts that the lake stage will be at an elevation of about 5,524 feet, amsl, which corresponds to a maximum lake depth of approximately 799 feet. Projected surface area of the pit lake is approximately 112.0 acres. Lowest elevation of the groundwater divide excircling the pit is 6,238 feet, amsl, which is 714 feet higher than lake stage, as shown on **Figure 4.5-10**. Hydraulic gradient is maintained towards the pit from all directions, demonstrating that the pit is a hydraulic sink 100 years after mining **(Figure 4.5-10)**.

200 Years Post-Project

The groundwater model predicts that the lake stage will be at an elevation of about 5,697 feet, amsl, which corresponds to a maximum lake depth of approximately 972 feet. Projected surface area of the pit lake is approximately 146.2 acres. Lowest elevation of the groundwater divide encircling the pit is 6,256 feet, amsl, which is 559 feet higher than lake stage, as shown on **Figure 4.5-11**. Hydraulic gradient is maintained towards the pit from all directions, demonstrating that the pit is a hydraulic sink 200 years after mining **(Figure 4.5-11).**

1,580 Years Post-Project

The groundwater model predicts that the lake stage will be at an elevation of about 5,912 feet, amsl, which corresponds to a maximum lake depth of approximately 1,187 feet. Projected surface area of the pit lake is approximately 194.2 acres. Lowest elevation of the groundwater divide encircling the pit is 6,302 feet, amsl, shich is 390 feet higher than lake stage, as shown on **Figure 4.5-12**. Hydraulic gradient is maintained towards the pit in all directions, demonstrating that the pit is a hydraulic sink 1,580 years after mining **(Figure 4.5-12)**.

4.5.5 Predictive Sensitivities

A predictive sensitivity analysis was conducted to assess the effect of varying selected model input parameters on pit lake formation and ultimate pit lake stage, as well as whether the pit lake will be a hydrologic sink or a flow-through pit lake. The predictive sensitivity analyses were run for 1,580 years, which is conservatively longer than required for the lake formation to reach equilibrium. The predictive sensitivity analysis was conducted by varying five input parameters: specific yield, percentage of precipitation run-off to lake, precipitation to the lake surface, evaporation from the pit lake surface, and LAK2 lake cell conductance. Specific yield was varied in both the mine dewatering and pit lake formation simulations. Runoff, precipitation, evaporation, and lake cell conductance apply only to the pit lake formation simulations.

Predictive model sensitivity was conducted in two phases. The first predictive sensitivity analysis varied each of the parameters individually (single variable sensitivities). The second predictive sensitivity analysis varied all key input parameters simultaneously (multivariate sensitivities) to evaluate two bounding scenarios. The first bounding scenario is characterized conceptually as the "upper" bounding scenario in terms of predicting a maximum final pit-lake stage. The second bounding scenario represents the "lower" bound in terms of predicting a minimum final pit-lake stage.

4.5.5.1 SINGLE VARIABLE: Single variable sensitivity analyses were run for five input parameters. The parameters are:

- Specific yield
- Percent of precipitation runoff to the pit lake
- Precipitation to the pit lake surface
- Evaporation from the pit lake surface
- LAK2 lake cell conductance

The sensitivity variations for these five parameters are summarized in **Table 4.5-2**. Projected final pit lake stages for base and individual sensitivity simulations are summarized in **Table 4.5-3**. Simulated pit lake water balance for the base and individual sensitivity simulations for post-project years 1, 10, 50, 100, 200, and 1,580 are summarized in **Table 4.5-4**; simulated groundwater balance for the same years are summarized in **Table 4.5-5**. The individual sensitivity analyses are described as follows:

Specific Yield

Specific yield was decreased by a factor of 2 and increased by a factor of 3 compared to the base simulation yield values. Projected pit inflows during dewatering and projected lake stages during pit lake development for the specific yield sensitivity simulations are shown on **Figures 4.5-5 and 4.5-13**, respectively, along with the corresponding base simulation results.

The decreased specific yield simulation resulted in a decrease in pit inflows during dewatering. Projected average inflow rate during pit dewatering is approximately 35 gpm within year 1 of proposed mining operations (base simulation 58 gpm), 360 gpm in year 30 (base simulation 460 gpm), and 351 gpm at mine completion in year 32 (base simulation 420 gpm).

The increased specific yield simulation resulted in a increase in pit inflows during dewatering. Projected average inflow rate during pit dewatering is approximately 144 gpm within year 1 of proposed mining operations (base simulation 58 gpm), 823 gpm in year 30 (base simulation 460 gpm), and 642 gpm at mine completion in year 32 (base simulation 420 gpm).

For steady-state conditions (pit lake equilibrium), groundwater is not removed or added to storage. Therefore, specific yield has no effect on equilibrium lake stage. Both the decreased and increased specific yield sensitivity simulations resulted in lake stages which

are nearly identical to the base simulation projections; final lake stages for both sensitivity simulations are the same as the base simulation. For both simulations the lake remains a complete hydraulic sink.

Percentage of Precipitation Runoff

Percentage of precipitation runoff was decreased to 20 percent and increased to 40 percent compared to the base simulation 30 percent rate. Projected lake stages over time for the percentage of precipitation runoff sensitivity simulations are shown on **Figure 4.5-13**, along with the corresponding base simulation results. The decreased runoff percentage resulted in lower lake stage during pit-lake development, compared with the base simulation, with final lake stage approximately 88 feet below the base simulation. The increased runoff percentage resulted in higher lake stage during pit-lake development compared with the base simulation, with final lake stage approximately 76 feet above the base simulation. The results indicate the lake stage is moderately sensitive to variations in runoff. For both simulations the lake remains a complete hydraulic sink.

Precipitation to Lake Catchment Area

Precipitation rate to the lake surface was decreased to 12.7 and increased to 17.18 in/yr compared to the base simulation precipitation rate of 14.94 in/yr (a 15 percent decrease and increase from base). Projected lake stages over time for the lake precipitation sensitivity simulations are shown on **Figure 4.5-13**, along with the corresponding base simulation results. The decreased precipitation resulted in lower lake stage during pit-lake development, compared with the base simulation, with final lake stage approximately 78 feet below the base simulation. The increased precipitation resulted in higher lake stage during pit-lake development compared with the base simulation, with final lake stage approximately 80 feet above the base simulation. The results indicate the lake stage is moderately sensitive to variations in precipitation to the lake surface. For both simulations the lake remains a complete hydraulic sink.

Lake Evaporation

Lake evaporation was decreased to 30.79 and increased to 42.08 in/yr compared to the base simulation evaporation rate of 37.46 in/yr, which corresponds to 73 percent of the estimated Class A pan rate (a 12 percent increase and 18 percent decrease from base case). This decrease and increase corresponds to the range of pan coefficients used to reduce the pan evaporation rate to a lake evaporation rate (**Section 4.5.2.1**). Projected lake stages over time for the evaporation sensitivity simulations are shown on **Figure 4.5-13**, along with the corresponding base simulation results. The decreased evaporation resulted in higher lake stage during pit lake development, compared with the base simulation, with final lake stage approximately 139 feet above the base simulation. The increased evaporation resulted in lower lake stage during pit lake development, compared with the base simulation, with final lake stage approximately 83 feet below the base simulation. The results indicate the lake stage is moderately sensitive to variations in evaporation. For both simulations the lake remains a complete hydraulic sink.

Lake Cell Conductance

Lake cell conductance controls the ability of groundwater to move from the surrounding formation into the lake. As described in **Section 4.5.2**, lake cell conductance for the base simulation was specified so pit lake groundwater inflows for the first month were equal to the pit dewatering inflows for the last month. For the sensitivity analysis: 1) bottom lake cell conductance was decreased to 0.12 ft^2/d and increased to 12 ft^2/d compared to the base simulation lake cell conductance of 1.2 ft^2/d (a one magnitude decrease and increase from base); and 2) side lake cell conductance was decreased to 0.06 ft^2/d and increased to 6 ft2/d compared to the base simulation lake cell conductance of 0.6 ft^2/d (a one magnitude decrease and increase from base). Projected lake stage over time for the lake cell conductance sensitivity simulations is shown on **Figure 4.5-13**, along with the corresponding base simulation results. The decreased bottom and side lake cell conductance resulted in lower lake stage during pit lake development compared with the base simulation, with final lake stage approximately 44 feet below the base simulation. The increased lake cell

conductance resulted in higher lake stage during pit-lake development compared with the base simulation, with final lake stage approximately 12 feet above the base simulation. Decreasing the lake conductance by one order of magnitude results in a moderate decrease in lake stage, indicating the conductance should not be lowered below what is specified for the base simulation. Increasing the lake conductance by one order of magnitude results in a small increase in lake stage, indicating the conductance specified for the base simulation did have some influence over groundwater inflow. For both simulations the lake remains a complete hydraulic sink.

4.5.5.2 MULTIVARIATE: Based on results of the individual sensitivity analyses for specific yield, percentage of precipitation runoff, precipitation to the lake catchment area, lake surface evaporation, and lake conductance, upper and lower bounding multivariate predictive sensitivity simulations were conducted. Projected final pit lake stages for base and multivariate sensitivity simulations are summarized as follows:

MODEL SENSITIVITY SIMULATION	FINAL PIT LAKE STAGE (feet, amsl)
Base Case	5,912
Multivariate, Lower	5,612
Multivariate, Upper	6,227

Simulated pit lake water balance for the base and multivariate sensitivity simulations for post-project years 1, 10, 50, 100, 200, and 1,580 are summarized in **Table 4.5-4**; simulated groundwater balance for the same years are summarized in **Table 4.5-5**. The multivariate sensitivity analyses are described as follows:

Lower

This simulation comprised specific yield one-half that specified in the base simulation, runoff at 20 percent of precipitation to lake catchment area, which was lowered to 12.7 in/yr, lake evaporation at 42.08 in/yr (82 percent of the estimated Class A pan rate),

and lake conductance one order of magnitude lower than specified in the base simulation. Projected lake stage over time is shown on **Figure 4.5-14**, along with the corresponding base simulation results. Results indicate lower lake stage during pit lake development compared with the base simulation, with final lake stage approximately 300 feet below the base simulation.

Projected lake stage and groundwater level elevation contours for the lower multivariate simulation at 1,580 years after the end of mining are shown on **Figure 4.5-15**. Projected lake stage is about 5,612 feet, amsl. Lowest elevation of the groundwater divide encircling the pit is 6,291 feet, amsl, which is 679 feet higher than lake stage, as shown on **Figure 4.5-15**, demonstrating that the pit is a hydraulic sink. A section view of the lower multivariate projected groundwater level surface at 1,580 years after the end of mining is shown on **Figure 4.5-16**, along with the higher groundwater level surface projected for the base simulation.

Upper

This simulation comprised specific yield three times higher than specified in the base simulation, runoff at 40 percent of precipitation to lake catchment area, which was increased to 17.18 in/yr, lake evaporation at 30.79 in/yr (60 percent of the estimated Class A pan rate), and lake conductance one order of magnitude higher than specified in the base simulation. Projected lake stage over time is shown on **Figure 4.5-14**, along with the corresponding base simulation results. Results indicate higher lake stage during pit lake development compared with the base simulation, with final lake stage approximately 315 feet above the base simulation. The lake remains a complete hydraulic sink.

Projected lake stage and groundwater level elevation contours for the upper multivariate simulation at 1,580 years after the end of mining are shown on **Figure 4.5-17**. Projected lake stage is about 6,227 feet, amsl. Lowest elevation of the groundwater divide encircling the pit is 6,372 feet, amsl, which is 145 feet higher thatn lake stage, as shown on

Figure 4.5-17, demonstrating that the pit is a hydraulic sink. A section view of the upper multivariate projected groundwater level surface at 1,580 years after the end of mining is shown on **Figure 4.5-16**, along with the lower groundwater level surface projected for the base simulation.

4.5.6 Modeling Summary

The Mt. Hope local groundwater flow model was constructed for the purpose of evaluating impacts of mine dewatering operations on the groundwater system and the subsequent development of a pit lake after the end of mining. Assumptions and methodologies affecting Local Model results include:

- Mine pit advancement for each model stress period was applied at the start of the stress period, resulting in large calculated groundwater inflows at the beginning of each stress period. Mining operations and pit advancement will proceed much more gradually than simulated, which would be expected to reduce the maximum rate of groundwater inflows compared with what is projected initially for each stress period.
- The regional and local models are coupled, resulting in more realistic estimates of impacts to the regional groundwater system. By incorporating regional drawdown effects into the local model the effects of regional pumping on the inflows to the pit are represented.
- Simulation of the post-project pit lake formation was developed using the LAK2 software. The simulation was executed for 1,580 years to allow a quasi-steady-state lake elevation to develop, and to predict volumetric rates of inflow and outflow for the pit lake.

4.5.6.1 SUMMARY OF RESULTS FROM LOCAL MODEL SIMULATIONS:

- Results of Local Model simulations indicate that average annual pit inflow rates will be approximately 296 gpm, indicating that groundwater inflow to the mine

during excavation can be managed using a pit sump operation. However, inflow rates will be larger at times, particularly in areas where fracture zones are encountered.

- Based on review of mine survey data provided by EMLLC, existing underground workings will not be intercepted by the pit excavation or provide a discharge conduit for the pit lake. Historical mine workings exist in two distinct locations in the vicinity of the proposed open pit, as shown on **Figures 4.2-2 and 4.5-16**. The western workings, at the approximate elevation of 6,858.1 feet, amsl, are located above the current groundwater table and will be completely mined out. The eastern workings (Zinc adit), ranging in elevation from approximately 6,646 to 6,860 feet amsl, extend partially below the current groundwater table, and are located a minimum of 250 feet outside of the final pit shell (year 32 of mining). The eastern mine workings will be dewatered during early pit excavation and final equilibrium groundwater levels 1,580 years after excavation are projected to be 400-600 feet below the eastern workings. Impacts from the mine workings during dewatering will be negligible and the workings are not simulated in the numerical model.
- A groundwater-fed lake is projected to form in the mine pit after mining operations cease. Water levels in the lake will rise slowly and will not reach an elevation which will result in movement of water from the lake into the aquifer. Sensitivity simulations conducted to evaluate the potential lower and upper bounds of the lake stage support the conclusion that the pit lake will remain a complete hydraulic sink.
- For existing climatic conditions, the pit lake is projected to behave as a hydrologic sink with evaporation consuming all precipitation and groundwater inflow to the lake.
- Groundwater discharge to the pit lake is projected to ultimately decline to 98 gpm, a negligible groundwater sink in the regional flow system.

4.6 EVALUATION OF LAND SUBSIDENCE

This section describes the processes and results of estimating potential land subsidence in Kobeh Valley associated with proposed groundwater withdrawals for mining and milling of molybdenum ore by EMLLC at Mt. Hope. This work complements existing estimates for the potential for land subsidence prepared by John Bell of NBMG (Bell, 2008; **Appendix N**). Estimates of land subsidence in Kobeh Valley have been made using remotely sensed time-series land deformation data from adjacent Diamond Valley and using those results to predict possible future subsidence in Kobeh Valley. The following sections briefly outline the mechanical and physical processes associated with land subsidence, identify current trends in land deformation in Diamond Valley, and describe the methods associated with estimating possible future subsidence in Kobeh Valley.

4.6.1 Physical and Mechanical Processes Associated with Land Subsidence

Subsidence is defined as the settling or compaction of the ground surface when intergranular pore pressures are reduced (Sneed, 2001). Several processes that cause subsidence include soil compaction, dissolution of carbonate rocks, hydro-compaction (wetting of dry and low-density soils), and groundwater withdrawal. Prolonged depressurization of the valley fill aquifer associated with groundwater withdrawals is considered to be the most important factor controlling subsidence in both Diamond and Kobeh Valleys.

Compaction of valley fill materials occurs differentially, depending largely on grain size and the compressibility of sediments. Aquifer systems consist of variable thicknesses for aquifers and aquitards. Aquifers refer to a volume of permeable rock or unconsolidated material where water can be stored, while an aquitard is a relatively impermeable zone adjacent to an aquifer. Aquifers composed of coarse-grained sands and/or gravels can behave differently from aquitards when subjected to changes in pore pressure related to fluid

withdrawal. Aquitards are typically composed of fine-grained material such as silt or clay. The difference in compressibility is largely related to differences in elastic and inelastic storage coefficients of the sediments. An excellent overview and discussion of the mechanical properties of differential compaction due to differing elastic properties of sediments can be found in Terzaghi (1925) and in Sneed (2001). That discussion is summarized briefly below.

Changes in hydraulic head in saturated sediments can cause changes in intergranular effective stress. This effective stress change can be estimated either from well hydrographs or by modeling the transient changes in hydraulic head in an aquifer system. Depressurization of an aquifer system induces stress that results in either elastic or inelastic strain. In a perfectly elastic system, changes in stress caused by the expansion or compaction of sediments, or the expansion and compaction of water, result in a proportional strain to the system. All deformation caused by elastic strain is, by definition, reversible. In inelastic systems, increases in effective stress result in a disproportional amount of strain, and some degree of resulting deformation is not reversible. Although both aquifers and aquitards have elastic and inelastic properties, in coarse-grained aquifer units the inelastic component is generally negligible and may be ignored (Sneed, 2001). In fine-grained aquitard units, the inelastic component may be dominant if applied stress exceeds the maximum pre-consolidation stress of the system; that is, if the applied stress exceeds any other previous maximum hydraulic head decline. Thus aquitards may behave elastically until a threshold strain is achieved and thereafter behave in an inelastic manner. The maximum effective stress is generally thought of as the greatest amount of stress applied to an aquifer/aquitard system which exceeds any previous maximum stress. It can be confidently assumed that a system has exceeded its previous maximum stress if water levels have consistently continued to decline as a result of continued groundwater withdrawals, particularly for a number of years or decades.

Mathematically, these concepts can be applied to an aquifer system as a whole by the following relationship (Sneed, 2001):

$S^* = S'k + Sk + Sw$, where

S^* = aquifer storage coefficient of a compacting aquifer (see storativity, **Section 3.6**)

$S'k$ = skeletal storativity of aquitard units,

Sk = skeletal storativity of aquifer units, and

Sw = storativity of water

As indicated above, an important concept related to aquitards is that $S'k$, the storativity (storage coefficient) of the aquitard unit, is composed of two components, elastic and inelastic. Once the maximum strain threshold is exceeded, $S'k$ will dominate and the sediments will behave inelastically. Therefore, for aquifer systems undergoing compaction due to groundwater withdrawal, the maximum effective stress of the system has been exceeded, and the storage coefficient is then the sum of the inelastic storage coefficient of aquitard units, the storage coefficient of the aquifer units (elastic), and the storativity of water (elastic). Put simply, because the compressibility of water is very small (Freeze and Cherry, 1979), it can be ignored. Thus, the storage coefficient (S) in compacting systems can be reasonably defined by two components: the elastic component of coarse-grained materials and the inelastic component of fine-grained materials.

The elastic storage coefficient, as used here, is defined by the volume of water taken into or released from storage per unit area of aquifer per unit of change in head. Water derived from this type of source is completely derived from the elastic compression of the aquifer. Typical values of elastic storage coefficients are not precisely known in the study area, but other detailed studies of land subsidence, particularly in the San Joaquin Valley of California, have indicated that specific elastic storage (the elastic storage coefficient divided by aquifer thickness) for coarse-grained materials is in the range of 1x10-6, although Morgan and Dettinger (1996) indicate that this value is generally higher than that derived from

pumping tests. Hoffman and Zebker (2001) estimated the elastic storage coefficients to range between 4.2x10-4 and 3.4x10-3 from land deformation and extensometers placed at several well sites in the Las Vegas Valley. Bell et al. (2008) derived values ranging between 2.0 - 3.7x10-3 in the same area, using a variety of remote sensing and empirical techniques.

The inelastic component of the storage coefficient refers to the "water released from storage as a result of compaction of fine-grained interbeds of the aquifer system" (Morgan and Dettinger, 1996). During inelastic compaction, these fine-grained sediments may release large quantities of water from storage, particularly over prolonged periods of head decline (Morgan and Dettinger, 1996). In fact, the overall storage capacity of an aquifer system may be dictated more by the inelastic component than the elastic component (Jacob, 1940). In an evaluation of well logs, specific unit compaction, and volumetric analysis of subsiding sediments in the Las Vegas Valley, estimates of the inelastic storage coefficients for valley fill materials ranged from 9x10-4 to 1.4x10-2 for shallow, near-surface aquitards and 7x10-4 to 3.2x10-4 for deeper aquifer/aquitard units (Morgan and Dettinger, 1996). In Las Vegas Valley, Bell et al. (2008) estimated inelastic storage coefficients ranging between 9.0x10-3 and 2.0x10-2 by analyzing ground displacement and pumping data, while Hoffman and Zebker (2001) provided estimates ranging from 9.5x10-4 to 1.5x10-3.

Although the range of elastic and inelastic storage coefficients from San Joaquin Valley, California, and Las Vegas Valley, Nevada, may not correlate exactly to properties in Diamond and Kobeh Valleys, they provide a general range in expected values. Comparisons of inelastic storage coefficient for two different studies indicate that the estimated values are 4.5 to 30 times greater than that estimated for the elastic component of storage (Helm, 1978; Morgan and Dettinger, 1996). This means that for analogous systems, subsidence is largely irreversible, and where caused by groundwater withdrawals, the area will not rise again once groundwater levels rebound.

4.6.1.1 REMOTE SENSING OF LAND SUBSIDENCE ASSOCIATED WITH GROUNDWATER WITHDRAWALS IN DIAMOND VALLEY: Remote sensing of land subsidence utilizes satellite-derived electromagnetic radiation (radar) to record the intensity and phase of reflected, or echoed, signals to map the Earth's surface. The technique of utilizing radar signatures for determining changes in land surface elevation is called Interferometric Synthetic Aperture Radar (InSAR), which exploits an additional quantity measured by the radar, the phase coherence of the signal echoed by the same portion of the ground surface at differing times. Where land surface is stable, the phase of an electromagnetic wave echoed from the land surface should theoretically be unchanged over time. However, where changes in land elevation have occurred, the travel time of the radar signal will be affected.

Specifically, InSAR measures the radar phase (radian values) for each 4×20 meter pixel on two satellite images obtained from two-closely located passes of the SAR satellite at different times. Differences in the signal phase can be used to identify changes in land surface elevation, provided that the difference in signal phase is not disrupted by widespread land surface activities. This quantity is converted to ground displacement values that occurred along the radar line of sight. The separation between the two satellites is called the perpendicular baseline, one of the factors used to select two scenes to be analyzed. The ability to differentially correlate InSAR data, and therefore determine land deformation, greatly depends on the degree of similarity between different image sets. Failure of correlation between datasets due to changes in land surface reflectivity over time is termed temporal decorrelation and is most often caused by changes in vegetative cover or ground disturbance such as agriculture. Other sources of decorrelation can be classified as instrumental, geometric, or atmospheric. Portions of InSAR-derived images that suffer from temporal decorrelation cannot be used to determine land subsidence because no meaningful calculation in the shift of the reflected radar waves can be made.

4.6.1.2 METHODS UTILIZED IN ESTIMATING LAND DEFORMATION IN DIAMOND VALLEY: A total of ten frames of ERS1 and ERS2 satellite data were analyzed for descending track 170 frame 2799, which covers Diamond Valley, Nevada. These individual scenes were paired to make multiple interferograms covering different time periods. A list of all processed pairs for European Remote Sensing (ERS) satellites is provided in **Table 4.6-1**. The data were processed in the NBMG InSAR Lab using the ROI_PAC radar interferometric software developed by the NASA Jet Propulsion Lab. Typical two-pass processing procedures were followed, using a simulated interferogram to remove the effects of topography. The simulation was created using a 60-meter Digital Elevation Model obtained from the USGS National Elevation Data website.

Interferograms were generated from almost every possible pair for time periods of 5 to 51 months between 1992 and 2000. A region in the Diamond Valley with systematic ground displacement was identified on all InSAR pairs. A single interferogram showing total subsidence between 1992 and 2000 was produced by cumulatively adding (stacking) ERS interferograms for separate but consecutive time periods. These stacked radar datasets were generated by adding the phase change values of the processed pairs for specific time span periods. The stacking process and the conversion of the radar phase data to displacement data were done using the geospatial software ENVI. Individual pairs used in the stacking computation are indicated in red in **Table 4.6-1**.

A more detailed description of the methods used to estimate land deformation in Diamond Valley is provided in **Appendix N** which was prepared by Rei Arai, Graduate Research Assistant, and John Bell, Research Professor, University of Nevada, Reno.

4.6.1.3 SUMMARY DISCUSSION OF INSAR ANALYSIS: In evaluating the results of the InSAR analysis, the best coherence between the interferograms is north of the main zone of pumping in Diamond Valley, which is where the maximum subsidence is found on all interferograms. The southern part of Diamond Valley, which contains the majority of

irrigation wells, is generally incoherent on the interferograms. The cause of the incoherence is most likely temporal decorrelation as a result of alfalfa production. Although southern Diamond Valley, the zone of highest groundwater withdrawals, lacks complete correlation through the period 1992-2000, enough data exist to determine that, although the largest withdrawals occur in this area, the largest amounts of land subsidence occur to the north. The cause of this apparent incongruity is most likely attributed to increases in fine-grained sediments and increased potential for subsidence north of the main zone of pumping.

Areas of maximum subsidence may have shifted between time periods and may not have good coherence on all interferograms for the same area. Thus, land subsidence as calculated for the stacked interferograms likely represents a minimum value. Stacked interferograms for 1992 through 2000 indicate that during that time, land deformation in south-central Diamond Valley as a result of groundwater withdrawal has resulted in approximately 1.2 feet of land surface elevation decline. No subsidence was found in Kobeh Valley.

4.6.2 Application of InSAR-derived Subsidence Data to Estimate Future Subsidence in Diamond Valley

In order to estimate possible future land subsidence in Kobeh Valley associated with groundwater withdrawals, InSAR-derived subsidence data for Diamond Valley were used to estimate the inelastic storage coefficient for valley fill materials.

As described in **Sections 4.6.1.2 and 4.6.1.3**, Rei Arai and John Bell of the University of Nevada, Reno computed the amount of subsidence in Diamond Valley between 1992 and 2000. Elastic and inelastic storage coefficient values were then input into the Regional Model (**Sections 4.1 and 4.4**), and these parameters were calibrated to the subsidence estimates.

The first step was to simulate a subset of the water level calibration period from 1992 to 2000. This involved only simulating stress periods 38 through 46 of the transient Regional Model (**Section 4.4**). Starting heads were obtained from the results of stress period 37 (1991). As with the regional calibration, MODFLOW-SURFACT was used for this simulation. Subsidence was simulated using the IBS Package (Leake and Prudic, 1991).

All model parameters, such as hydraulic conductivity and storage, remained unchanged in the subsidence calibration. Only values of inelastic storage were estimated during the subsidence calibration. Elastic storage could not be calibrated because water levels were declining during the calibration period. Elastic storage can only be calibrated when water levels are recovering. An assumption that elastic storage is about ten times less than inelastic storage was used in the current model, which is in the range of values summarized in **Section 4.6.1**.

Figure 4.6-1 provides a map of the distribution of subsidence interpreted for the main agricultural area in Diamond Valley from 1992 to 2000. A set of subsidence calibration targets was generated from the distribution of subsidence shown on **Figure 4.6-1** using one north-south transect through the highest subsidence area, two east-west transects, and two other key points in the north part of the subsidence area. The locations of these calibration targets and results of calibration are listed in **Table 4.6-2**.

The calibration proceeded by starting with a homogeneous distribution of inelastic storage in the upper three model layers with a value of 1x10-4. Deeper valley fill deposits and bedrock were not sensitive in this calibration and were assigned a uniform inelastic storage of 1x10-6. During calibration, it was necessary to vary the distribution of inelastic storage within the area of the calibration targets to achieve a similar non-uniform distribution of subsidence. It was concluded that because drawdown in this area was similar, the variation in subsidence must be related to the variability of clay lenses and other materials that are prone to subsidence. This variability was handled by making the inelastic storage

property heterogeneous. Four different zones of inelastic storage were used in this area ranging from 1x10-4 to 5x10-3 as shown on **Figures 4.6-2 and 4.6-3**.

The maximum subsidence in the area is approximately 1.2 feet (**Figure 4.6-1**), and the maximum subsidence in the calibration target set is approximately 1 foot (**Table 4.6-2**). The mean error for the 22 subsidence targets is -0.009 feet. The absolute mean error and standard deviation of the error are 0.05 and 0.07 feet, respectively. When normalized to the range in subsidence, the latter values represent 5 to 7 percent error, which is within the goals for calibration established for the water level calibration as described in **Section 4.1**. The R^2 between observed and simulated land subsidence for the calibration period is 0.97 as shown in the plot on **Figure 4.6-4**.

4.6.3 Simulation of Subsidence in Kobeh Valley

The following section outlines prediction of subsidence using calibrated inelastic storage. The distribution of pumping from proposed wellfield pumping wells is outlined in **Section 4.4, Table 4.4-1**.

Inelastic storage coefficients for Kobeh Valley are unknown and cannot be determined at this time because widespread subsidence, and subsequent InSAR analysis and model calibration, has not occurred. Therefore, the area-weighted average of the calibrated inelastic storage coefficient for shallow valley fill aquifers in Diamond Valley of 1.7×10^{-3} (**Figures 4.6-2 and 4.6-3**) was assigned uniformly to model cells representing valley fill material in model layers 1 through 3 throughout Kobeh Valley.

The Regional Model was utilized to determine approximate land subsidence in Diamond Valley under the No Action Alternative from current conditions (2009) through year 2055 (end of mining project), which represents continued pumping at a consumptive use of approximately 55,000 AF/yr. Results of the simulation are presented on **Figure 4.6-5** and

IN THE SUPREME COURT OF THE STATE OF NEVADA

EUREKA COUNTY, A POLITICAL SUBDIVISION OF THE STATE OF NEVADA; KENNETH F. BENSON, INDIVIDUALLY; DIAMOND CATTLE COMPANY, LLC, A NEVADA LIMITED LIABILITY COMPANY; AND MICHEL AND MARGARET ANN ETCHEVERRY FAMILY, LP, A NEVADA REGISTERED FOREIGN LIMITED PARTNERSHIP,

Appellants,

vs.

THE STATE OF NEVADA STATE ENGINEER; THE STATE OF NEVADA DIVISION OF WATER RESOURCES; AND KOBEH VALLEY RANCH, LLC, A NEVADA LIMITED LIABILITY COMPANY,

Respondents.

_____/

Case No. 61324

District Court Case Nos.
CV 1108-15; CV 1108-156;
CV 1108-157; CV 1112-164;
CV 1112-165; CV 1202-170

JOINT APPENDIX
Volume 9

KAREN A. PETERSON, NSB 366
kpeterson@allisonmackenzie.com
JENNIFER MAHE, NSB 9620
jmahe@allisonmackenzie.com
DAWN ELLERBROCK, NSB 7327
dellerbrock@allisonmackenzie.com
ALLISON, MacKENZIE, PAVLAKIS, WRIGHT & FAGAN, LTD.

402 North Division Street
Carson City, NV 89703
(775) 687-0202

and

THEODORE BEUTEL, NSB 5222
tbeutel@eurekanv.org
Eureka County District Attorney
702 South Main Street
P.O. Box 190
Eureka, NV 89316
(775) 237-5315

Attorneys for Appellant,
EUREKA COUNTY

CHRONOLOGICAL APPENDIX TO APPEAL FROM JUDGMENT

DOCUMENT	DATE	VOL	JA NO.
Petition for Judicial Review	08/08/2011	1	01-06
Notice of Verified Petition for Writ of Prohibition, Complaint and Petition for Judicial Review	08/10/2011	1	07- 08
Verified Petition for Writ of Prohibition, Complaint and Petition for Judicial Review	08/10/2011	1	09-59
Summons and Proof of Service, Kobeh Valley Ranch, LLC	08/11/2011	1	60-62
Summons and Proof of Service, Jason King	08/11/2011	1	63-65
Affidavit of Service by Certified Mail	08/11/2011	1	66-68
Notice of Petition for Judicial Review	08/11/2011	1	69-117
Summons and Proof of Service, Kobeh Valley Ranch, LLC	08/15/2011	1	118-120
Summons and Proof of Service, Jason King	08/15/2011	1	121-123
Summons and Proof of Service, The State of Nevada	08/17/2011	1	124-128
First Additional Summons and Proof of Service, State Engineer, Division of Water Resources	08/17/2011	1	129-133
Order Allowing Intervention of Kobeh Valley Ranch, LLC, to Intervene as a Respondent	09/14/2011	1	134-135

DOCUMENT	DATE	VOL	JA NO.
Partial Motion to Dismiss, Notice of Intent to Defend	09/14/2011	1	136-140
Order Allowing Intervention of Kobeh Valley Ranch, LLC, as a Party Respondent	09/26/2011	1	141-142
Answer to Verified Petition for Writ of Prohibition, Complaint and Petition for Judicial Review by Kobeh Valley Ranch, LLC	09/28/2011	1	143-149
Answer to Petition for Judicial Review by Kobeh Valley Ranch, LLC	09/29/2011	1	150-154
Answer to Petition for Judicial Review by Kobeh Valley Ranch, LLC	09/29/2011	1	155-160
Order Directing the Consolidation of Action CV1108-156 and Action No. CV1108-157 with Action CV1108-155	10/26/2011	1	161-162
Summary of Record on Appeal	10/27/2011	2-26	163-5026
Request for and Points and Authorities in Support of Issuance of Writ of Prohibition and in Opposition to Motion to Dismiss	11/10/2011	27	5027-5052
Order Setting Briefing Schedule	12/02/2011	27	5053-5055
Reply in Support of Partial Motion to Dismiss and Opposition to Request for Writ of Prohibition	12/15/2011	27	5056-5061

DOCUMENT	DATE	VOL	JA NO.
Kobeh Valley Ranch's Reply to Conley/Morrison's Request for and Points and Authorities in Support of Issuance of Writ of Prohibition and in Opposition to Motion to Dismiss	12/15/2011	27	5062-5083
Kobeh Valley Ranch's Joinder in the State of Nevada and Jason King's Partial Motion to Dismiss	12/15/2011	27	5084-5086
Petition for Judicial Review	12/29/2011	27	5087-5091
Petition for Judicial Review	12/30/2011	27	5092-5097
Summons and Proof of Service, The State of Nevada	01/11/2012	27	5098-5100
First Additional Summons and Proof of Service, State Engineer, Division of Water Resources	01/11/2012	27	5101-5103
First Amended Petition for Judicial Review	01/12/2012	27	5104-5111
Opening Brief of Conley Land & Livestock, LLC and Lloyd Morrison	01/13/2012	27	5112-5133
Petitioners Kenneth F. Benson, Diamond Cattle Company, LLC, and Michel and Margaret Ann Etcheverry Family LP's Opening Brief	01/13/2012	27	5134-5177
Eureka County's Opening Brief	01/13/2012	27	5178-5243
Eureka County's Summary of Record on Appeal - CV1112-0164	01/13/2012	28	5244-5420
Eureka County's Supplemental Summary of Record on Appeal - CV1108-155	01/13/2012	29-30	5421-5701

DOCUMENT	DATE	VOL	JA NO.
Order Granting Extension	01/26/2012	31	5702-5703
Answer to Petition for Judicial Review	01/30/2012	31	5704-5710
Answer to First Amended Petition for Judicial Review	01/30/2012	31	5711-5717
Supplemental Petition for Judicial Review	01/31/2012	31	5718-5720
Petition for Judicial Review	02/01/2012	31	5721-5727
Summary of Record on Appeal	02/03/2012	31	5728-5733
Record on Appeal, Vol. I, Bates Stamped Pages 1-216	02/03/2012	31	5734-5950
Record on Appeal, Vol. II, Bates Stamped Pages 217-421	02/03/2012	32	5951-6156
Record on Appeal, Vol. III, Bates Stamped Pages 422-661	02/03/2012	33	6157-6397
Answer to Petition to Judicial Review	02/23/2012	34	6398-6403
Answering Brief	02/24/2012	34	6404-6447
Respondent Kobeh Valley Ranch, LLC's Answering Brief	02/24/2012	34	6448-6518
Reply Brief of Conley Land & Livestock, LLC and Lloyd Morrison	03/28/2012	34	6519-6541
Petitioners Kenneth F. Benson, Diamond Cattle Company, LLC, and Michel and Margaret Ann Etcheverry Family LP's Reply Brief	03/28/2012	34	6542-6565
Eureka County's Reply Brief	03/28/2012	34	6566-6638

ALPHABETICAL APPENDIX TO APPEAL FROM JUDGMENT

DOCUMENT	DATE	VOL	JA NO.
Findings of Fact, Conclusions of Law, and Order Denying Petitions for Judicial Review	06/13/2012	36	6823-6881
First Additional Summons and Proof of Service, State Engineer, Division of Water Resources	08/17/2011	1	129-133
First Additional Summons and Proof of Service, State Engineer, Division of Water Resources	01/11/2012	27	5101-5103
First Amended Petition for Judicial Review	01/12/2012	27	5104-5111
Kobeh Valley Ranch's Reply to Conley/Morrison's Request for and Points and Authorities in Support of Issuance of Writ of Prohibition and in Opposition to Motion to Dismiss	12/15/2011	27	5062-5083
Kobeh Valley Ranch's Joinder in the State of Nevada and Jason King's Partial Motion to Dismiss	12/15/2011	27	5084-5086
Notice of Verified Petition for Writ of Prohibition, Complaint and Petition for Judicial Review	08/10/2011	1	07- 08
Notice of Petition for Judicial Review	08/11/2011	1	69-117
Notice of Entry of Findings of Fact, Conclusions of Law, and Order Denying Petitions for Judicial Review	06/18/2012	36	6882-6944
Notice of Appeal	07/10/2012	36	6945-6949
Opening Brief of Conley Land & Livestock, LLC and Lloyd Morrison	01/13/2012	27	5112-5133

DOCUMENT	DATE	VOL	JA NO.
Order Allowing Intervention of Kobeh Valley Ranch, LLC, to Intervene as a Respondent	09/14/2011	1	134-135
Order Allowing Intervention of Kobeh Valley Ranch, LLC, as a Party Respondent	09/26/2011	1	141-142
Order Directing the Consolidation of Action CV1108-156 and Action No. CV1108-157 with Action CV1108-155	10/26/2011	1	161-162
Order Setting Briefing Schedule	12/02/2011	27	5053-5055
Order Granting Extension	01/26/2012	31	5702-5703
Partial Motion to Dismiss, Notice of Intent to Defend	09/14/2011	1	136-140
Petition for Judicial Review	08/08/2011	1	01-06
Petition for Judicial Review	12/29/2011	27	5087-5091
Petition for Judicial Review	12/30/2011	27	5092-5097
Petition for Judicial Review	02/01/2012	31	5721-5727
Petitioners Kenneth F. Benson, Diamond Cattle Company, LLC, and Michel and Margaret Ann Etcheverry Family LP's Opening Brief	01/13/2012	27	5134-5177
Petitioners Kenneth F. Benson, Diamond Cattle Company, LLC, and Michel and Margaret Ann Etcheverry Family LP's Reply Brief	03/28/2012	34	6542-6565
Petitioners Benson, Diamond Cattle Co., and Etcheverry Family LP's Notice of Appeal	07/12/2012	36	6950-6951

DOCUMENT	DATE	VOL	JA NO.
Record on Appeal, Vol. II, Bates Stamped Pages 217-421	02/03/2012	32	5951-6156
Record on Appeal, Vol. I, Bates Stamped Pages 1-216	02/03/2012	31	5734-5950
Record on Appeal, Vol. III, Bates Stamped Pages 422-661	02/03/2012	33	6157-6397
Reply in Support of Partial Motion to Dismiss and Opposition to Request for Writ of Prohibition	12/15/2011	27	5056-5061
Reply Brief of Conley Land & Livestock, LLC and Lloyd Morrison	03/28/2012	34	6519-6541
Request for and Points and Authorities in Support of Issuance of Writ of Prohibition and in Opposition to Motion to Dismiss	11/10/2011	27	5027-5052
Respondent Kobeh Valley Ranch, LLC's Answering Brief	02/24/2012	34	6448-6518
Summary of Record on Appeal	10/27/2011	2-26	163-5026
Summary of Record on Appeal	02/03/2012	31	5728-5733
Summons and Proof of Service, Kobeh Valley Ranch, LLC	08/11/2011	1	60-62
Summons and Proof of Service, Jason King	08/11/2011	1	63-65
Summons and Proof of Service, Jason King	08/15/2011	1	121-123
Summons and Proof of Service, Kobeh Valley Ranch, LLC	08/15/2011	1	118-120

DOCUMENT	DATE	VOL	JA NO.
Summons and Proof of Service, The State of Nevada	08/17/2011	1	124-128
Summons and Proof of Service, The State of Nevada	01/11/2012	27	5098-5100
Supplemental Petition for Judicial Review	01/31/2012	31	5718-5720
Transcript for Petition for Judicial Review	04/03/2012	35	6639-6779
Verified Petition for Writ of Prohibition, Complaint and Petition for Judicial Review	08/10/2011	1	09-59

CERTIFICATE OF APPENDIX (NRAP 30(g)(1)

In compliance with NRAP 30(g)(1) I hereby certify that this Appendix consists of true and correct copies of the papers in the District Court file.

DATED: December 21, 2012.

/s/ KAREN A. PETERSON
KAREN A. PETERSON, NSB #366
ALLISON, MacKENZIE, PAVLAKIS,
WRIGHT & FAGAN, LTD.
P.O. Box 646
Carson City, NV 89702

Attorneys for Appellant,
EUREKA COUNTY

3.6.2 Hydraulic Properties for Consolidated Rocks

Belcher et al. (2001) compiled hydraulic conductivity data for use in the Death Valley region groundwater flow model. The Death Valley region and the Study Area share similarities in rock types present, as both areas contain extensive volcanic units as well as consolidated carbonate and clastic rocks. Given the similar lithology, values were extracted from Belcher's compilation that best matched hydrogeologic units defined in the Study Area. Values of hydraulic conductivity ranged from a maximum of 2,690 ft/d for faulted and/or karsted carbonates, to a minimum of 9.8E-08 ft/d for quartzites (**Table 3.6-5**). It should be noted that Belcher's 2001 compilation was recently used by the USGS when describing the likely hydraulic properties of the Basin and Range Carbonate-Rock Aquifer System in southeastern Nevada and western Utah (Welch et al., 2007). The system described by Welch et al. ranges from Little Smoky Valley to Snake Valley along the Nevada/Utah border.

In addition to the work of Belcher, Maurer et al. (2004) provides a comprehensive dataset of hydraulic conductivity values derived from numerous scientific studies, both from government agencies and from private consultants. The dataset includes hydraulic conductivity values for a range of rock types present throughout Nevada and, in particular, the Study Area. Rock types and their corresponding range in hydraulic conductivity values are provided in **Appendix H**.

Site-specific hydraulic property values for consolidated rocks in the Study Area around Mt. Hope are presented in Montgomery & Associates (2010b). The report summarizes the existing packer, falling head, and aquifer testing performed on core holes, and completed wells, and piezometers around Mt. Hope. The results indicate a range of hydraulic conductivities for various geologic media. Data are limited to the volcanic, metamorphic, and siliciclastic rocks present within and adjacent to the proposed pit area and may not reflect the hydraulic properties associated with most other rock types found within the Diamond Valley Regional Flow System, particularly carbonates or valley fill sediments.

Seven aquifer tests conducted on wells adjacent to the proposed pit were analyzed by Montgomery & Associates (2010b), to provide transmissivity values ranging from 0.5 to 180 ft^2/d. Estimated hydraulic conductivity of fractures ranged from approximately 2.4E-03 to 1E-01 ft/d, and matrix hydraulic conductivity ranged from 1.9E-08 to 9.4E-04 ft/d. Fracture-specific storage ranged from 3.7E-10 to 3.5E-06, while matrix-specific storage ranged from 8.3E-07 to 2.3E-03. The rocks tested include volcanic, metamorphic, and siliciclastic rocks of the Vinini Formation.

A deep core hole program was conducted to test the hydraulic properties of rocks within the planned pit wall and floor area of Mt Hope. Three core holes were advanced to depths ranging from 2,694 to 2,998 feet bgs. The core holes provided important information regarding hydraulic conductivity and its relationship to rock and alteration type, which is briefly summarized by the following excerpt from Montgomery & Associates (2010b).

Hydraulic testing was conducted in potassic altered tuffs, quartz porphyry, and hornfels, where these rocks are cut by prominent fracture zones. Results of packer tests show the hydraulic conductivity to be generally low in the potassic-altered rocks, even within the fracture zones. However, where potassic alteration passes downward into silicic alteration, hydraulic conductivity increases to relatively high values. Partly due to the large test intervals, there is little discernible association of hydraulic conductivity with RQD (rock quality designation). This may also reflect the filling of fractures (especially in the potassic zone) with soft alteration minerals.

Hydraulic conductivity values ranged from approximately 3.8E-04 to 1.2E-01 ft/d for the altered rocks within the pit area. Outside of the proposed pit area, a core hole was advanced through the Vinini Formation and analyses of hydraulic testing indicated a general decrease in hydraulic conductivity with increasing depth from approximately 1.2 ft/d to around 1.0E-07 ft/d.

Three aquifer tests were conducted in the carbonate rocks in the northern portion of Kobeh Valley (Interflow, 2010). The tests were conducted on wells 206T, 220T, and 214T, and the tests were conducted for 32, 7, and 11 days, respectively. The 32-day test conducted at 206T initially indicated very high transmissivity values (~170,000 ft^2/d); however, the rate of drawdown in the well increased over time throughout the test, indicating negative boundary conditions. Because of the boundary conditions, the high computed transmissivity value is unlikely to represent conditions at all scales within the carbonate rock assemblage. The long-term response of the carbonate rocks at the 206T location was consistent with an aquifer having a transmissivity value of 6,000 to 7,000 ft^2/d. Very similar overall transmissivity values were observed at test well 214T, located several miles to the north in the same structural carbonate block; the storage coefficient of the carbonate block was determined to be between 1.0E-03 and 2.0E-03. Well 220T was tested for 11 days, and analysis of the drawdown data indicated a transmissivity value of approximately 3,700 ft^2/d with a storage coefficient of around 1.0E-04. Additional information on the aquifer testing in carbonate rocks can be found in Interflow (2010).

3.7 WATER CHEMISTRY

Groundwater chemistry was compiled using published data from USGS/NDWR basin Reconnaissance Series Reports, as well as data collected by consultants on behalf of EMLLC (SRK, 2008a and 2008b; Interflow, 2010; Montgomery & Associates, 2010b). Because data were compiled from several sources, a numbering system was devised to track and communicate groundwater quality sample information. The numbering system tracks samples from C-1 to C-273, some of which are duplicate samples from the same source for quality assurance. Results are included in **Appendix I**. A separate technical report on pit lake geochemistry will be issued.

In 2006 and 2007 baseline water quality of the Mt. Hope area was delineated by SRK, and regularly scheduled sampling of springs, wells, and streams was initiated (SRK, 2008a). In the summer of 2007, samples were collected for chemical analyses at over 250 springs, seeps, and other surface water bodies where sufficient flow was available (SRK, 2008b).

Information on groundwater chemistry from wells in the Study Area is generally limited to data collected from wells and piezometers drilled by EMLLC, the basin Reconnaissance Series Reports, and data in the USGS NWIS database. The information presented in this section describes hydrogeochemistry in a regional perspective, though site-specific data from the Mt. Hope area are included. A detailed summary of water chemistry from wells and boreholes at the Mt. Hope project site is presented in Montgomery & Associates (2010b).

Hydrochemical Facies

Local and regional trends in common ion chemistry were developed based on the concept of hydrochemical facies. The facies concept was developed in the 1960s to categorize water types, sources, and mixing scenarios, and depends on the relative abundance of certain cations and anions. The primary ions of concern are usually the cations calcium, magnesium, sodium, and potassium and the anions carbonate, bicarbonate, chloride, and sulfate. Data are typically expressed in milliequivalents per liter (meq/L) and plotted on a Piper Diagram, a ternary plot, in order to graphically portray which cations or anions dominate a given water chemistry sample.

Total Dissolved Solids and Electrical Conductivity

In addition to the facies concept, the concentration of total dissolved solids (TDS) and the ratio of stable isotopes of oxygen and hydrogen are also presented for discussion. The TDS is a sum of the inorganic salts and small amounts of organic matter that are dissolved in water and, in general, is similar in magnitude to the sum of the concentration of the major

cations and anions. TDS measurements were not available for all chemical samples reported in the Study Area, particularly data gathered for Kobeh, Antelope, and North Monitor Valleys by Rush and Everett (1964) and Diamond Valley in Harrill (1968), though the authors did provide electrical conductivity (EC) measurements which can be used to estimate TDS in some situations, as described below.

Specific EC is expressed in microSiemens per centimeter (μS/cm) at 25 °C and measures the ease with which electricity flows through water or other media. In water, the EC is largely a function of TDS and thus is closely related. In areas with similar chemistry, TDS can be closely approximated from EC measurements by first establishing the relationship between TDS and EC for that area. EC and TDS concentrations were collected for 62 springs within the Study Area. A regression of the TDS-EC relationship reveals that a good approximation of TDS can be obtained by multiplying the EC measurement by 0.7 (**Figure 3.7-1**). Using this relationship, TDS concentrations were estimated for 23 sites for which only EC data were available.

Stable Isotopes

Many samples from springs, streams, and groundwater in the Study Area were submitted to the University of Nevada-Reno Stable Isotope Laboratory for analysis of the ratios of stable isotopes of both oxygen and hydrogen. The ratio of the heavier and lighter isotopes respectively (18O/16O and 2H/1H) are presented relative to the international standard for ocean water, the Vienna Standard Mean Ocean Water (VSMOW), and are presented as delta (δ) values expressed in per mil (‰) units. Negative numbers indicate isotopically lighter, or depleted, ratios relative to the VSMOW, while more positive values indicate an increased abundance of the heavier isotope. The ratios are useful for comparison, both on a local and regional level, and can help identify areas with similar recharge sources Factors that may affect the fractionation of the isotopes include water temperature, geothermal effects, snowpack sublimation, and evaporation (Mazor, 1991).

Matched pairs of $\delta 18O$ and $\delta 2H$ routinely follow a linear pattern within a specified geographic range, as described first by Craig (1961). The Global Meteoric Water Line is a linear relationship derived from samples collected on a global scale with widely differing elevations, latitudes, and temperatures of recharge. It is relatively constant unless atmospheric waters are subjected to evaporation (Craig, 1961). The equation of the line is $\delta 2H=8\delta 18O +10$ and is a useful benchmark for evaluating stable isotope data. Because much of Nevada is subjected to considerable evaporative losses and "rain-out" effects of storms over high-elevation ranges, Flynn and Buchanan (1990) developed a Great Basin Meteoric Water Line that considers these effects. They developed what may be a more appropriate curve for cold-water springs in Nevada. The equation for the Great Basin Meteoric Water Line is $\delta 2H=7.55\delta 18O -0.5$.

In developing the meteoric water line for the Great Basin, Flynn and Buchanan (1990) recognized the effects of heat and water-rock reactions on the stable isotope ratios and excluded warm and hot springs. The interaction of water with geologic materials can alter the 18O/16O ratio but rarely affects the deuterium/hydrogen ratio (2H/1H) as hydrogen is not common in abundance in most rocks (Mazor, 1991).

Several comprehensive studies of the distribution of $\delta 18O$ and $\delta 2H$ in both spring water and groundwater as well as summer and winter precipitation are available for the Great Basin Region. Friedman et al. (2002) and Flynn and Buchanan (1990) presented isocontour maps of depleted winter precipitation and isotopic ratios for cold springs in the Great Basin. Both studies came to the conclusion that the most isotopically light waters in Nevada occur in the extreme northern portion of the state with 2H/1H ratios of -128 per mil. The heaviest natural waters in Nevada are found in the southern portion of the state with 2H/1H ratios of -96 per mil, reflecting southern, warmer storm tracks, extensive fractionation, and loss of the lighter 1H due to evaporation.

3.7.1 Regional Hydrochemical Facies Interpretation

The distribution of hydrochemical facies, as determined from spring, creek, and groundwater chemistry, is shown on **Plate 4**. It is a function of many factors, including source rock geochemistry, influence from geothermal sources, mixing with other facies, residence time in a geologic environment, and mineral precipitation and/or dissolution reactions associated with evapo-concentration of inorganic salts. Eight facies have been delineated in the Study Area, based on the relative abundance of common ions. Water types (facies) were determined objectively by the geochemistry software package AquaChem, and distribution of facies on **Plate 4** is based on those categories designated by the software package.

3.7.1.1 Ca (+/-Mg)-HCO_3 FACIES: The most common facies present in the Study Area is the Ca (+/-Mg)-HCO_3 waters found throughout the upland spring systems and creeks of the mountain ranges dominated by carbonate rocks. The Ca (+/- Mg)- HCO_3 facies is the product of bicarbonate produced from weakly acidic rain and/or snowmelt mixing with carbon dioxide from atmospheric and/or soil gases. Calcium and magnesium ions from limestone, dolomite, and calcite in soils are dissolved in this weak acid to form the Ca (+/- Mg)- HCO_3 solution. TDS in this group is typically low, with values ranging from near zero to 500 mg/L. The facies as a whole displays relatively little influence from water-rock reactions.

Areas that display a dominantly Ca (+/-Mg)-HCO_3 hydrochemical facies include the Roberts Mountains, the majority of the Diamond Mountains, the Fish Creek Range, and the Mahogany Hills. Two springs positioned west of Devils Gate (C-61 and C-62) are also similar in composition and probably derive their water from the carbonate terrain of the Fish Creek Range/northern Mahogany Hills to the southwest (**Plate 4**). In addition, the springs northwest of Lone Mountain are included in this group, as are two wells southeast of Mt. Hope.

3.7.1.2 (Ca>Na) HCO_3-SO_4 FACIES: A mixed cation (Ca, Na) HCO_3-SO_4 facies is present throughout the Simpson Park Range and extends southward to include portions of North Monitor Valley. This chemistry is probably the result of water-rock reactions with volcanic rocks, which typically result in higher sodium content. The dissolved sulfate is likely present as a result of hydrothermal alteration and/or co-mingling with geothermal waters. Both the Simpson Park Range and the Monitor Range have experienced extensive igneous intrusions, episodic volcanic activity, and localized hydrothermal alteration. In addition, North Monitor Valley contains several hot spring complexes, such as Dianna's Hot Spring (C-1 and C-2).

3.7.1.3 Na-HCO_3 FACIES: A distinct band of Na-HCO_3 waters extends from the Bartine Ranch and Hot Springs Hill in south-central Kobeh Valley to Klobe Hot Springs in northern Antelope Valley, which can likely be attributed to groundwater from the northern Monitor Range (mostly volcanic rocks) circulating along the fault zones present east and north of the range. Both areas display elevated temperatures, up to 150 °F, and similar chemistry.

Another zone of Na-HCO_3-dominant water occurs along the northeastern edge of Diamond Valley and is defined by three springs that discharge waters where the alluvial fan meets the playa surface. TDS concentration is much higher along the playa margin than that observed elsewhere in the Study Area.

3.7.1.4 Na/Ca-HCO_3 FACIES: East of the Na-HCO_3 zone described near Klobe Hot Springs is an intermediate facies that may be the result of mixing of Na-HCO_3 waters from the hot spring complex of north Antelope and Kobeh Valley mixing with Ca-HCO_3 waters recharged to the valley fill aquifer from the Fish Creek Range and Lone Mountain area. Chemistry data reported from a well near Bean Flat in central Kobeh Valley (well 52, C-241) is similar to that reported from a well southwest of the Roberts Mountains (Atlas-1, C-95), indicating that west central Kobeh Valley contains an Na-Ca HCO_3-type groundwater.

3.7.1.5 Ca-HCO_3-SO_4 FACIES: A relatively small, but distinctive and well-defined grouping of samples represents a Ca-HCO_3-SO_4 facies in east-central Pine Valley. This group is slightly anomalous for an upland area and may represent co-mingling with waters or hydrocarbon influences associated with the Blackburn oil field located immediately to the northwest (**Plate 4**).

3.7.1.6 Mg-Ca-Na-HCO_3-(+/- Cl) FACIES: Wells screened in valley fill deposits within Diamond Valley have a mixed cation bicarbonate water type that may or may not contain additionally dominant chloride anions. The facies is interpreted to be a transitional water type between the Ca(+/-Mg)-HCO_3 facies of the Diamond Range and waters near the center of the basin which contain higher TDS, SO_4, and Cl.

3.7.1.7 MIXED ANION HCO_3-SO_4 FACIES: Within central Diamond Valley, a mixed anion bicarbonate-sulfate facies is present and delineated by groundwater samples obtained from wells. The facies is characteristically high in TDS (typically over 500 mg/L).

3.7.1.8 MIXED ANION SO_4 FACIES: This facies is rare and is limited to wells or piezometers at Mt. Hope that tap waters exposed to spatially limited sulfide-enriched zones presumably near ore bodies. Reduction-oxidation reactions, at or near the water table, enrich the zones in sulfates, which are characteristically elevated in sulfate, thallium, zinc, iron, and other common metals (SRK, 2008b; Montgomery & Associates, 2010b). Samples displaying this facies also displayed low pH and little to no carbonate or bicarbonate anion fraction.

3.7.2 Basin-Specific Discussion of Water Chemistry

The following section outlines the general geochemistry of springs and groundwater by hydrographic basin. Where sufficient data exist, discussions of possible origin, mixing, and implications are briefly provided.

3.7.2.1 KOBEH VALLEY: General water chemistry within Kobeh Valley is variable, as shown on **Figure 3.7-2**. Upland springs of the Roberts Mountains and Roberts Creek are nearly uniformly a Ca-HCO_3 type, while the Simpson Park Range and most alluvial wells display an increased abundance of sodium. Outliers include the geothermal springs and wells near the Bartine Ranch, a well completed in basalt (C-100, Test Well 203), and a well at Devils Gate (Well 9211R), which also has a high TDS content. Chemistry from well 9211R is similar to water from Slough Creek during a discharge event (**Section 3.7.2.3**, Diamond Valley), and the high TDS, sodium, and sulfate concentrations are likely due to evapo-concentration. Groundwater chemistry of both 9211R and Slough Creek differ from that observed in groundwater in southern Diamond Valley. Wells completed in alluvium and carbonate rocks in northern Kobeh Valley generally have a Ca- HCO_3 water type, though some have an elevated SO_4 fraction.

Stable isotopes of water obtained in Kobeh Valley presented on **Figure 3.7-3** have ratios similar to other areas within the Great Basin and track closely along the Great Basin Meteoric Water Line of Flynn and Buchanan (1990). Stable isotopes of water from Roberts Creek and low-flow springs indicate the effects of evaporation. As expected, geothermal springs are depleted in $\delta 18O$, relative to cold-water springs and surface water bodies, while Tonkin Spring (Pine Valley) and a test well completed in the carbonate rocks west of Mt. Hope (206T) may indicate high-elevation recharge sources as they have the lightest (most negative) isotope ratios within the Roberts Mountains. For their elevation, water from springs and flowing wells at the Bartine Ranch in central Kobeh Valley are seemingly light and may indicate that the source waters are from distant, higher-elevation areas.

3.7.2.2 ANTELOPE VALLEY: Groundwater and spring water samples from Antelope Valley are relatively sparse, as indicated on **Figure 3.7-4**. Upland springs are typically Ca (+/-Mg)-HCO_3 waters, with Na-HCO_3 waters present along the eastern and northern edge of the Monitor Range (Klobe Hot Springs). Between these sources, samples obtained from wells have an intermediate composition and indicate some degree of mixing

between the Ca (+/-Mg)-HCO_3 and Na-HCO_3 facies (**Figure 3.7-4**). Few stable isotope samples were obtained in Antelope Valley, but Klobe Springs (shown on **Figure 3.7-3** with Kobeh Valley) indicates similarity to samples obtained from springs on the Bartine Ranch. TDS for all samples obtained in Antelope Valley were below 500 mg/L.

3.7.2.3 DIAMOND VALLEY: Compared with most of the basins in the Study Area, spring and groundwater chemistry in Diamond Valley is rather well defined. Existing data and analysis of chemical quality of groundwater was discussed by Harrill (1968), who delineated hydrochemical facies within Diamond Valley water samples from springs, wells, and shallow auger holes. The data presented by Harrill demonstrate a mixing line from the Ca-CO_3-type waters to two end members, Na-Cl-HCO_3 type and Na-Cl-SO_4 type, with increasing TDS concentrations (expressed as electrical conductivity) as groundwater travels along flow paths from the mountain fronts to the playa. Harrill's data, as well as additional water chemistry data assimilated from multiple sources, is presented on **Figure 3.7-5**. As is typical in areas with uplands composed of carbonate terrain, the mid-high elevation springs are almost exclusively a Ca-HCO_3type.

Some springs along the base of the Sulphur Spring Range have a Ca (+/-Mg)-Na-HCO_3 type, such as Shipley Spring (~103-108°F). The increase in sodium is likely the result of water flowing along the fault system bounding the west side of Diamond Valley, although, as a whole, the chemistry is similar to other wells and springs in the basin along the mountain front.

Most samples from springs, wells, and piezometers at and near Mt. Hope display a relatively unique chemistry in that most display elevated sulfate content compared to other samples from mountainous regions in the Study Area. Other samples with similar sulfate content, such as some auger holes near the playa in Diamond Valley, also have higher sodium and chloride. This suggests that the elevated sulfate may not be from evapo-

concentration or residence time in playa deposits as in central Diamond Valley but may be derived from the ore body and igneous complex at Mt. Hope.

Stable isotope samples from Diamond Valley are presented on **Figure 3.7-6** and display wide groupings until the data points are categorized by their geographic locations. Spring samples from the Diamond Range plot closely to the Great Basin Meteoric Water Line of Flynn and Buchanan (1990), while isotopic samples from the Sulphur Spring Range plot slightly off the trend. This condition may be due to factors related to elevation, aspect of spring and recharge areas, and temperature of precipitation/recharge.

Representative spring samples from the Diamond Range display δ18O/16O ratios of -15.3 to-16.3 per mil and δ2H/1H ratios of -117 to -124 per mil and are assumed to represent the compositional range of modern recharge. The isotopic composition of Fish Creek Springs in Little Smoky Valley, south of the Diamond Range (-15.6 δ18O, -120 to -123 δ2H) falls within this range and may be the discharge point for some recharge in the southern Diamond Mountains or Fish Creek Range.

A distinctive group of outliers is consists of three springs along the northeast edge of the playa in Diamond Valley. These samples were significantly lighter in stable isotopes when compared with other spring samples in Diamond Valley, including samples obtained near sources of geothermal heat such as Shipley Spring. The springs issue from the edge of the playa and have a distinctive Na-HCO_3 chemistry. The source of these springs would appear to be from high elevation recharge, perhaps in the Diamond Range to the east, with little exposure to the playa environment prior to discharge, perhaps indicative of a fault structure and/or shallow underlying bedrock.

3.7.2.4 MT. HOPE: Samples from piezometers and wells at Mt. Hope have highly-variable stable isotope ratios compared with isotopic samples from springs, as shown on **Figure 3.7-7**. One observation is the consistent loss of the heavier isotopes with depth for

samples obtained from piezometers 232P and 235P. This consistent decrease of heavy isotopes is best illustrated from 235P where samples were obtained from 620 feet bgs, 1,020 feet bgs, and 1,500 feet bgs. The cause for the decrease is unknown but may be related to flow system paths.

3.7.2.5 PINE VALLEY: The majority of water samples from Pine Valley were obtained from the southeastern portion of the valley and may not be representative of the entire basin. Chemistry of the Pine Valley water samples is presented on **Figure 3.7-8**. Of the samples obtained, the Roberts Mountains and the Sulphur Spring Range generally displayed a Ca-HCO_3 chemistry while a small portion of the northern Sulphur Spring and southern Piñon Ranges display a Ca-CO_3-SO_4- type water (**Figure 3.7-8**). The increased sulfate may be from association with the Piñon Range-frontal fault and sulfur content associated with the Blackburn oil field, located west of these springs. Oil seeps have been reported in the Bruffey Springs area, and several of the warm springs emit methane gas bubbles (Johannesen and Cole, 1990). Water recovered from oil wells in the Blackburn field contained up to 226 mg/L SO_4, which is well above that seen in the upland springs of the Sulphur Spring Range (Johannesen and Cole, 1990). Movement of this water through the Piñon Range-frontal fault zone or exposure to the known oil seeps in the range may be the cause of the elevated sulfate content.

On **Plate 4**, a hydrochemical facies were not assigned to all springs discharging in the basin because of a lack of consistency in chemical composition. Although variablity exists in the samples obtained, the most common water type is Ca-HCO_3-Cl, which is relatively unique in the Study Area.

Stable isotopes of oxygen and hydrogen for springs in Pine Valley are presented on **Figure 3.7-9** and plot off both the Global Meteoric Water Line and the Great Basin Meteoric Water Line and, as a group, are somewhat unique compared with springs in the Diamond Range and Roberts Mountains, as shown on (**Figure 3.7-10**).

CHAPTER 4 – ENVIRONMENTAL CONSEQUENCES

Two groundwater flow models were developed concurrently in support of the Mt. Hope Project: a large regional-scale model, "Regional Model", and a smaller embedded local-scale model, "Local Model", for the vicinity of the mine pit. The Regional Model domain encompasses the Study Area and the Local Model utilizes telescopic mesh refinement (TMR) to separately simulate the smaller area for the proposed mine pit and facilities. The refined Local Model grid allows a more detailed simulation of pit dewatering and subsequent development of a pit lake. The Regional Model and Local Model are "coupled" to allow accurate representation of groundwater stresses between the two model domains. Combined the two models are used to predict:

- Regional groundwater level drawdown effects due to operation of the KVCWF mine supply pumping and due to pit-dewatering; and
- Local mine area groundwater impacts due to mine excavation, pit-dewatering, and pit-lake development.

The Regional Model was compiled by Interflow, Inc. of Truckee, California, and the Local Model was compiled by Montgomery & Associates of Tucson, Arizona. Coupling of the two models was conducted in close coordination between the two firms.

Development and calibration of the Regional Model and Local Model are described in **Sections 4.1 and 4.2**, respectively. A discussion of potential error and model limitations is presented in **Section 4.3**. Predictive results from the Regional Model and Local Model are presented in **Sections 4.4 and 4.5**, respectively.

4.1 REGIONAL MODEL DEVELOPMENT AND CALIBRATION

4.1.1 Introduction

Section 4.1 describes Regional Model development and calibration for simulation of pre-development steady-state conditions and of transient conditions from 1955 to 2006. Location of the Regional Model domain is shown on **Figure 4.1-1**. The model simulates groundwater movement and surface water-groundwater interaction for the interconnected valley fill and fractured rock flow system encompassed by Kobeh, Antelope, Diamond, and Pine Valley basins. The model was constructed with the finite-difference code MODFLOW-SURFACT Version 3.0.

4.1.2 Conceptual Model

The baseline conditions from which the conceptual model was developed are described in **Chapter 3** of this report. Mt. Hope is situated on or near the hydrographic basin divide for Kobeh Valley, Diamond Valley, and Pine Valley (Garden Valley subbasin) and groundwater movement occurs from Mt. Hope into these basins. Antelope Valley is included in the model domain because it is contiguous with, and up-gradient from, Kobeh Valley. Because there are no known physical barriers to outflow from Antelope Valley to Kobeh Valley, such as faults or mountain ranges, basic principles of subsurface flow (e.g., Darcy's Law) suggest that outflow must be occurring.

The model domain includes mountain ranges dividing the hydrographic basins, the mountain slopes forming the tributary watersheds to the basin floors. Inclusion of the interior mountain ranges, such as the Roberts Mountains, Mt. Hope, Whistler Mountain and the Sulphur Spring Range, was necessary due to the geographic location of the mine (**Figure 4.1-1**). The Roberts Mountains were also included in the model domain because the planned wellfield is south of the range and pumping of some wells has the potential to affect

groundwater levels within the mountain block. For consistency in treatment of hydrogeologic parameters, such as recharge distribution, the bounding mountain ranges are incorporated in the model domain up to the crest of the ranges that define the hydrographic basin boundaries. Beyond the crests and outside the hydrographic basin boundaries, there are no-flow model cells, defining the lateral extent of the simulated flow systems. During development of the numeric flow model, these boundary conditions were reviewed and found to be sufficiently distant from wellfield pumping stresses, minimizing concerns regarding drawdown simulations near fixed boundary conditions. The bottom of active flow represented in the Regional Model is sea level, which is approximately 6 to 20 times greater than the existing and proposed pumping depths simulated in the model. Reviews during model development and calibration indicate that this depth appears to be sufficient to represent a deep regional flow component in Paleozoic sedimentary (carbonate) rocks.

As defined in **Section 3.4**, the Diamond Valley Regional Flow System comprises much of the model domain. While Monitor Valley North and South are also part of the regional flow system, they are geographically removed from areas of proposed pumping and are believed to be located well beyond any appreciable effects of pumping. Subsurface inflow from Monitor Valley to the model domain can therefore be adequately represented as a boundary condition.

Diamond Valley was incorporated within the model domain because of proximity to the mine and because of potential sensitivity to additional pumping stresses. Diamond Valley is presently interpreted to be in an overdraft condition (**Section 3.4.3.3**).

Pine Valley is not defined as a part of the Diamond Valley Regional Flow System; however, it is included in the model domain because of its proximity to both the mine and wellfield. The Garden Valley subbasin of Pine Valley also may contribute significant recharge to Diamond Valley (**Sections 3.4.4.4 and 3.5.1**). Only the southern and central

portions of Pine Valley are incorporated in the model domain, as the northern portions are believed to be geographically beyond the potential influence of the mine pumping.

Geologic conditions, aquifer parameters, surface water runoff infiltration, groundwater recharge from the surrounding mountain blocks, subsurface inflow and outflow to neighboring basins, groundwater discharge by ET and playa evaporation, groundwater discharge by flowing artesian wells and springs, and existing agricultural pumping are all significant variables in the hydrogeologic setting of the model domain and are described in **Chapter 3**. These variables are represented to the extent that they are currently defined. However, the magnitude of water balance parameters in the hydrologic system are only estimated on a reconnaissance level and, during model calibration, there were minor adjustments to water balance parameters as a means of modifying the model to better represent known benchmark conditions in the field, such as measured water levels in wells.

The thickness of the geologic units represented in the model is believed to be sufficient to address potential for deep flow systems in the carbonate rocks. Pumping from existing and proposed wells is only envisioned from the upper 1,000 feet and will be derived primarily from the alluvial aquifer that overlies the carbonate-rock aquifers. Conceptually, the deep model structure reflects the north-south trend of the deep basins within the model domain, and intrusive bodies that are apparently influenced by the Northern Nevada Rift (**Section 3.1.1**).

Within the numeric flow model, the layer construction and the hydraulic property distributions conceptually represent the aquifer systems as described for the study area in **Section 3.4**.

4.1.2.1 HYDRAULIC PROPERTIES: **Section 3.6** describes hydraulic properties for the model area, including some statistical data for rock types in the model area but collected at locations elsewhere in the Great Basin and Basin and Range Province. Data

from pumping tests (Interflow et al., 2010) are used to define aquifer properties in upper valley fill materials and sedimentary rocks in north-central Kobeh Valley. Aquifer testing, packer permeability testing, and falling head permeability testing data are also available from numerous boreholes completed in sedimentary and intrusive rocks in the pit area (Montgomery & Associates, 2010b). Hydraulic conductivity and storage coefficients from the calibrated Local Model were also used to develop distributions of hydraulic properties in the Regional Model. Transmissivity values estimated based on well specific capacity data from drillers logs were also used in areas where pumping test data are unavailable (**Section 3.6.1**).

4.1.2.2 WATER BUDGET: **Section 3.5** presents an overview of existing interpretations of water budgets for the model area. A conservative (i.e., near the lower end of possible budgets) yet defensible set of water budget parameters are used in the model. In general, these parameters are based on recharge and discharge estimates from the published literature, with some adjustments, as discussed below. When simulating pumping effects, use of the conservative estimates for water budget parameters will generally result in a larger percentage reduction in natural outflow from the groundwater system than simulations than using higher water budget estimates.

The conceptual water budget for the model area, including sources and sinks of water represented in the numeric flow model, is summarized in **Table 3.5-2**. For the most part, water budgets are derived from published USGS Reconnaissance Reports for the model area (**Section 3.5**), with the following modifications:

1. The total precipitation recharge to Kobeh Valley was increased from 11,000 to 13,300 AF/yr based on an updated Maxey-Eakin computation (**Table 3.2-6**).
2. The estimated recharge to Antelope Valley is based on the 1964 USGS Reconnaissance Report (Rush and Everett) as determined by the Maxey-Eakin method. Some subsurface outflow from Antelope Valley to Kobeh Valley is

expected at a magnitude estimated in the range of 150 to 3,060 AF/yr (**Section 3.4.4.2**). The Reconnaissance Report did not recognize any subsurface outflow to Kobeh Valley, so to maintain a water balance in Antelope Valley the estimated groundwater discharge by ET was reduced by the amount of subsurface outflow.

3. Outflow from Kobeh Valley to Diamond Valley has been estimated in the USGS Reconnaissance Reports to be minor (Harrill, 1968), no greater than 40 AF/yr at Devils Gate. Outflow from Kobeh Valley to Diamond Valley could be greater if deep flow occurs through structures or carbonate rocks at Devils Gate and north of Whistler Mountain. The magnitude used for numerical model simulations was established during model calibration, but was not expected to exceed several thousand AF/yr given that Kobeh Valley is interpreted to function as a closed basin.
4. Subsurface inflow to Kobeh Valley from North Monitor Valley was estimated in 1964 the USGS Reconnaissance Report (Rush and Everett) to be approximately 6,000 AF/yr. Data from which to calculate subsurface inflow are sparse and, in this study, the range was estimated at 200 to 3,450 AF/yr using Darcy's Law (**Section 3.4.4.1**). The inflow was adjusted during calibration to be within this reduced range.
5. Harrill (1968) estimated that 90 percent of Garden Valley subbasin recharge (approximately 9,000 AF/yr) becomes outflow to northern Diamond Valley. Eakin (1962) did not recognize any subsurface inflow to Diamond Valley from Garden Valley. During model calibration, flow between Garden Valley and Diamond Valley, occurring through sedimentary rocks in the Sulphur Spring Range, was simulated by maintaining consistency in hydraulic properties for similar rock types in the model area. To the degree that the inflows may be less than determined by Harrill (1968), a deficit was reflected in the total ET and playa discharge in Diamond Valley.

Recharge is specified for three geographic areas within each basin, consisting of the mountain blocks, piedmonts (alluvial fans), and major ephemeral drainages crossing the piedmonts. Fundamental concepts reflected in the distribution of recharge are discussed in **Section 3.2.3**. The mountain block areas receive the greatest quantities of actual and simulated recharge, ranging from approximately 54 to 72 percent of the basin totals. Additional details on distribution of recharge are presented in **Section 4.1.3.6**.

Distribution of phreatophyte and playa groundwater discharge areas is based on mapping presented in the USGS Reconnaissance Reports, except for Pine Valley where satellite images were used in conjunction with work by Berger (2000a), and with limited field inspections, to make preliminary interpretations of phreatophyte distributions (**Section 3.4.5**).

Except in Diamond Valley, present-day conditions are similar to pre-development conditions. Some ranching and mining have occurred, but pumping stresses are not observed to have created extensive or persistent groundwater level declines. Groundwater levels in Diamond Valley are declining due to substantial agricultural pumping (**Section 3.5.3**) which has increased from pre-development rates of less than 2,000 AF/yr to approximately 55,000 to 65,000 AF/yr. The natural component of groundwater discharge is progressively decreasing as pumping continues and groundwater levels decline. Pre-development rates of groundwater discharge due to ET by phreatophytes and playa evaporation is estimated to be 30,000 AF/yr; model simulations presented in **Section 4.4** indicate this natural discharge has decreased by more than half due to Diamond Valley pumping.

4.1.3 Steady-State Model Development

A steady-state model was developed to reflect pre-development groundwater conditions, when the flow systems were in a state of dynamic equilibrium. This is a first step in testing the numerical model to see if it is an acceptable surrogate for the actual

groundwater system. Model parameters are adjusted to match field conditions within a reasonable margin of error. In much of the model area, dynamic equilibrium conditions are interpreted to currently exist because of the lack of significant historic groundwater pumping in most of the basins, including Antelope Valley, Pine Valley, Garden Valley, most of Kobeh Valley, and the proposed Mt. Hope mine area. Some flowing artesian wells exist in these basins, and they are assumed to have been flowing for a sufficient time to have achieved localized equilibrium. Many of these wells were drilled in the timeframe of the 1940s to 1960s. Southwestern Kobeh Valley is interpreted to be in disequilibrium since pumping for agriculture began at the Bobcat Ranch in the 1960s. Southern Diamond Valley has likewise been in disequilibrium due to pumping. Development of the steady-state model provides an equilibrium condition that serves as a starting point for transient model simulations, i.e., modeling of changing conditions over time. In the transient model, steady-state (starting point) conditions represent year 1955.

4.1.3.1 CODE AND SOFTWARE SELECTION: The groundwater model for this investigation was constructed using MODFLOW-SURFACT Version 3.0. MODFLOW was developed by the USGS, and the SURFACT version of MODFLOW is a modification developed by HydroGeoLogic (1996). MODFLOW is the most commonly used groundwater flow modeling code used in the United States. MODFLOW is an industry standard code that has the requisite capabilities to simulate flow in the Mt. Hope region, and was chosen for this study. MODFLOW is thoroughly documented (McDonald and Harbaugh, 1984; Harbaugh et al., 2000) and has been extensively tested (e.g., Anderson and Woessner, 1992).

MODFLOW-SURFACT is also well documented and validated, and was selected for its capabilities in processing dry cells, which are particularly important for simulations of dewatering and resaturation of the rock formation surrounding the pit during mine excavation and pit lake development. MODFLOW-SURFACT is capable of simulating steady-state or transient groundwater flow in one, two, or three dimensions. A wide variety of boundary

conditions may be simulated, including constant head, constant flux (wells, recharge), and head-dependent flux (ET), drains, rivers, streams, and general head boundaries. The types of boundaries used in this model are described in this chapter **(Sections 4.1 and 4.2)**. MODFLOW-SURFACT can simulate aquifer systems that are unconfined, confined, or a combination of confined and unconfined.

The model was designed using Environmental Simulations, Inc.'s Groundwater Vistas software, Version 5.0 (ESI, 2007), which creates the MODFLOW-SURFACT input files and facilitates analysis of the results.

4.1.3.2 THE MODEL GRID: The movement of groundwater can be described using mathematical equations that form the basis for all computer models used in the field of hydrogeology. Computer models may be subdivided into two broad categories, called numerical and analytical models. Analytical models are exact solutions of the groundwater flow equations, and numerical models are approximate solutions. Analytical models are used for ideal aquifer conditions that are homogeneous with simple boundaries. Numerical models are used to approximate solutions for aquifers that have complex parameter distributions, boundary conditions, and initial conditions, as is the case for the Regional Model.

Numerical models compute hydraulic head (groundwater levels) at fixed points within the aquifer. These points are called nodes or cells and are often arranged in a rectangular pattern called a grid. Many different types of numerical techniques are used to solve the groundwater flow equations. MODFLOW-SURFACT, which is used for the Mt. Hope models, uses a technique called the finite-difference method.

The finite-difference technique requires that the aquifer system be divided into a set of discrete blocks or cells. These blocks are rectangular and form the model grid. The process of creating the grid is called discretization. Water levels computed for a block

represent the average water level over that cubic volume of the aquifer. Thus, adequate discretization is required to resolve features of interest, such as the location of the pumping centers in the Mt. Hope region.

An algebraic equation that describes groundwater flow is written for each block in terms of the surrounding blocks, and the complete set of linear equations is iteratively solved until the change in head between iterations meets set criterion with minimal mass balance error.

The model grid developed for the Mt. Hope region covers approximately 4,950 square miles, with active flow cells covering an area of 2,758 square miles. Model north is true north, and the spatial coordinate datum in the model is UTM Zone 11, NAD83, converted to feet. The model origin lies at an easting of 1,680,103 feet and a northing of 14,181,261 feet. The model domain measures approximately 58 miles from west to east and 86 miles from north to south (**Figure 4.1-1**).

The grid spacing for model cells starts as a uniform 5,000 feet on each side, with incrementally decreasing grid spacing for rows and columns in the vicinity of the KVCWF and Mt. Hope. The minimum grid spacing is 1,000 feet. Grid refinement was utilized in the wellfield and mine area to better represent near-well drawdown geometry and radial flow to the wells and the pit. The model grid contains 151 rows, 118 columns, and 8 layers for a total of 142,544 cells, of which 111,992 are active flow cells. No-flow cells are those outside the active flow cells within the model boundary. The model area, grid, and no-flow cell distribution are shown on **Figure 4.1-2**.

The model grid has eight layers as illustrated on **Figure 4.1-3**. Layer geometries were used to represent some of the aquifers and geologic structures interpreted for the model area. At the valley floors, layer 1 represents the upper 50 feet of alluvium and the upper boundary of layer 1 is land surface. The layer becomes thicker beneath the alluvial fans and

mountains, exceeding 2,000 feet at some locations, with the thickness varying with elevation of land surface. **Figure 4.1-4** shows the top elevation of layer 1, which was interpolated from the USGS digital elevation model (DEM) for the area. The EMLLC wellfield in Kobeh Valley taps layers 2 through 5, but are mostly concentrated in layers 3 and 4.

Layer 2 represents the upper portions of valley floor alluvium below the root zone of phreatophyte vegetation. Over the valley floors, this layer is 50 feet thick. The thickness varies and is increased for the mountain blocks. Layer 3 is approximately 200 feet thick beneath the valley floors and generally represents the primary alluvial aquifers encountered in Diamond Valley and Kobeh Valley, and assumed present in Antelope and Pine Valleys. Over some parts of the valley floors within the model domain, the calibrated hydraulic conductivities for layers 1 and 2 are lower than layer 3, creating confined aquifer conditions in layer 3, facilitating representation of springs and flowing artesian wells in the model domain.

Layer 4 is generally 300 feet thick at the valley floors, but of variable thicknesses beneath mountain ranges. Beneath the valley floors, layer 4 represents the lower aquifer systems that are tapped by some existing irrigation wells in Diamond Valley and the deeper alluvium encountered in Kobeh Valley wellfield exploration drilling (Interflow et al., 2010). The bottom of layer 4 is 600 feet bgs beneath much of the valley floors. The bottom of layer 4 in the Kobeh Valley wellfield area was extended to approximately 1,000 feet bgs to refine the geologic representations in the model in areas where the thickness of alluvium was defined by exploration drilling (Interflow et al., 2010).

Layers 5 through 8 represent the deeper geologic structure, although top and bottom elevations are not tied to any particular geologic unit. Layers 6 and 7 are approximately 2,000 and 1,000 feet thick, respectively. Layer 5 and layer 8 thicknesses vary from several hundred to several thousand feet depending on depth from land surface and the total simulated thickness.

MODFLOW layer Type 3, variable unconfined-confined, is used for all layers. If the water level is below the top of the layer, then specific yield is used for transient computations and transmissivity of the layer varies depending on simulated saturated thickness. When the water level is above the top of the layer, the storage coefficient is used assuming confined conditions, and transmissivity of the layer does not vary. Layers are not constrained to either unconfined or confined conditions. Water table conditions occur on the valley floor in layer 1, where depths to groundwater are typically within 50 feet of land surface. Where depths to groundwater exceed 50 feet, such as at alluvial fans and mountains within the model domain, the water table occurs in layers 2 and 3, and overlying cells are inactive. Layers 4 through 8 are fully saturated under simulated steady-state conditions with an exception in layer 4 at the Sulphur Spring Range where depths to groundwater are simulated to be representative of a deep, regional interbasin flow system from Garden Valley to Diamond Valley.

To aid in accounting for changes in mass balance and flux between hydrographic basins, the Hydrostratigraphic Unit (HSU) package of Groundwater Vistas was utilized, with HSU zones corresponding to defined basin and sub-basin boundaries. As shown on **Figure 4.1-5**, the HSU zones represent hydrologic accounting areas for purposes of calculating mass balance.

4.1.3.3 BOUNDARY CONDITIONS: Once the aquifer system has been discretized, it is implicitly assumed that groundwater outside the model grid can be ignored. The model, however, must account for areas where groundwater enters or leaves the system being modeled. These effects are part of any model using boundary conditions. Ideally, boundary conditions should represent identifiable regional hydrologic features at which some characteristic of groundwater flow is easily described (Franke et al., 1984).

In this model, the regional hydrologic boundaries coincide with the crests of surrounding mountains, or topographic divides, with two exceptions. The southern model

boundary was selected to incorporate Antelope Valley and the hydrographic basin boundary between North Monitor Valley and Kobeh Valley. The north model boundary was selected to be far enough north to incorporate all of Diamond Valley and the Garden Valley subbasin of Pine Valley.

Simulated groundwater flow enters the model area in three ways: 1) recharge from precipitation infiltrating into the mountain blocks and on the alluvial fans, 2) infiltration of stream flow from major ephemeral drainages, and 3) lateral movement of water from adjacent basins (North Monitor Valley). In the steady-state model, groundwater leaves the model area through ET from phreatophyte areas (includes spring discharge) and direct evaporation from the Diamond Valley playa. A lateral outflow from the model area occurs along the Pine Valley portion of the northern model boundary.

Numerical groundwater models, such as MODFLOW-SURFACT, use three types of boundary conditions or ways in which water may enter or leave the model domain: the specified-head, specified-flux, and head-dependent flux boundaries. A description of each type is given below as applied in this model.

4.1.3.3.1 Specified-Head Boundary Conditions: The specified-head boundary condition is called a constant head in MODFLOW-SURFACT. The head, or water level, at a constant head boundary is specified independently of the simulation results and is fixed at the specified elevation throughout the simulation. Constant head boundaries (CHB) are used at the northern Pine Valley boundary as shown on **Figure 4.1-6**.

4.1.3.3.2 Head-Dependent Boundary Conditions: Head-dependent flux boundary conditions are a hybrid between the specified head and specified flux boundary conditions. In a head-dependent flux boundary, the flux (flow rate) of water into or out of the cell is computed by the model based upon the head calculated for the cell, the head specified for the boundary, and a conductance term. MODFLOW-SURFACT offers several

different types of head-dependent flux boundary conditions, including the general-head, ET, drain, and horizontal flow barrier packages; all of which have been used in this model.

General-Head Boundary Conditions. General-head boundary (GHB) conditions are typically used at the lateral margins of a model to allow groundwater to enter or leave the model domain. GHBs compute a flux based on a projected hydraulic gradient at the GHB cell, which is established between a fixed water level elevation at a defined distance beyond the cell and the variable simulated water level elevation in the GHB cell. The model simulates flux across the GHB cell boundary based on the hydraulic gradient and a conductance term calculated from the specified hydraulic conductivity between the two water level locations.

GHB cells were specified to simulate subsurface inflow from North Monitor Valley to Kobeh Valley (**Figure 4.1-6**). During transient calibration, simulated historic pumping at the Bobcat Ranch in southwestern Kobeh Valley creates up to 13 feet of drawdown at this boundary. In predictive simulations during mine pumping, an additional 15 feet of water level drawdown occurs due to future simulated pumping at the ranch (discussed in **Section 4.4**). The GHB accommodates the boundary dynamics better than a CHB, which would maintain water levels at a constant elevation.

Drain Boundary Conditions. The Drain module of MODFLOW-SURFACT was used to represent five springs/artesian wells in the model area: Tonkin Spring in Pine Valley; the Bartine Ranch flowing wells and Hot Spring Hill geothermal spring in Kobeh Valley; and Shipley and Thompson Ranch Springs in Diamond Valley. A sixth drain is used to represent unnamed springs south of the Diamond Valley playa. Use of drains to represent these springs accommodates variable discharge due to water level drawdown by pumping, be it from simulated mine pumping, or in the cases of the unnamed springs near the southern playa edge, Shipley Spring and the Thompson Ranch Spring, occurring as a result of simulated agricultural pumping in Diamond Valley. Drains behave very similarly to GHBs

using a calibrated conductance term and discharge water level elevation for the drain to determine the discharge from the drain (i.e., simulated spring discharge) over time.

Evapotranspiration Boundary Conditions. ET of groundwater by phreatophytic shrub and grass communities was simulated using the MODFLOW ET package. ET areas were divided into zones based on hydrographic basin and delineations between shrub and grass communities presented in USGS Reconnaissance Reports. These ET zones are summarized in **Table 4.1-1** and shown on **Figure 4.1-7**. In each ET zone, the extinction depth was 40 feet for greasewood and rabbitbrush, 10 feet for salt grass and meadow areas (**Section 3.4.5**), and 5 feet for the playa in Diamond Valley. These extinction depths are within a range commonly observed and simulated in Great Basin valleys. Extinction depth is the water level depth bgs where ET ceases to extract water from the aquifer (i.e., deeper than the roots can penetrate).

The maximum ET rate (associated with a zero depth to groundwater) was constrained to a maximum of approximately 4.75 ft/yr (57 inches per year), under the assumption that when groundwater approaches land surface the ET rate would not exceed potential evapotranspiration (PET). The PET in the study area is estimated at approximately 5.4 to 5.6 ft/yr (64 to 67 inches per year) on the valley floors based on the BLM RAWS climate station operated in Diamond Valley and the University of Nevada Gund Ranch station in Grass Valley northwest of Kobeh Valley.

Horizontal Flow Barriers. Three faults in the model with observed hydraulic barrier effects are simulated using the MODFLOW Horizontal Flow Barrier package (HFB) of Hsieh and Freckleton (1993). The faults are: the Diamond Valley fault system, which is a mapped structure on the southeast edge of Diamond Valley and is labeled "West Diamond Range Fault" (**Figure 3.1-1**); a fault at the southern base of the Roberts Mountains as defined in EMLLC wellfield exploration drilling and aquifer testing (Interflow, 2010); and the northern Roberts Mountains bounding fault structure projected to Tonkin Spring in southern Pine

Valley (Childress and Ferdock, 2008). Locations of HFBs in the model domain are shown on **Figure 4.1-6**. Inclusion of these faults in the model improved calibration of water levels in the vicinity of the fault and, in the case of Tonkin Spring, improved the ability to calibrate simulated spring discharge.

The HFB package requires a conductance term that reflects the hydraulic conductivity of the structure. The conductance values were determined through calibration to achieve a reasonable match to water levels in the vicinity of each fault. The calibrated hydraulic conductivity of the Tonkin Spring structure is 1.3×10^{-5} ft/d; the southern Roberts Mountains fault is 6.0×10^{-5} ft/d; and the Diamond Valley fault system is 1.2×10^{-6} ft/d.

The geology in the model area is structurally complex and highly faulted (**Section 3.1**, **Appendix D**, Childress and Ferdock, 2008), and undoubtedly there are many other faults in the model area that have hydrologic significance to the flow system. However, data to both identify and understand the nature and hydraulic significance of other faults in the model area are lacking. The calibrated hydraulic properties for the rock types represented in the model incorporate primary and secondary fracture-fault-related permeability, using the relative equivalent volume concept. The equivalent or effective hydraulic properties are assigned to model cells, thereby representing the fractured porous medium on a regional scale (Anderson and Woessner, 1992).

Sharply contrasting hydraulic conductivities between adjacent model cells are used to represent large-scale structural features. In many instances, the contrast in hydraulic conductivity is due to major faulting, such as mountain front faults or the Roberts Mountains Thrust Fault. Many of the major structural features in the model domain are represented in this manner, without the use of HFBs.

4.1.3.3.3 Specified Flux Boundaries: Specified flux (flow rate) boundary conditions are implemented in MODFLOW-SURFACT using wells, recharge, or no-flow

(i.e., flux equals zero) cells. Specified flux boundary conditions were used extensively in the Mt. Hope model to represent recharge from precipitation falling on the basins and to simulate flows from springs and flowing wells in the model area that were not simulated using drain boundary conditions. In the steady-state model, no significant groundwater pumping by wells is incorporated, as the steady-state model simulates pre-development conditions. However, in the transient model, historic pumping in Diamond Valley and Kobeh Valley is added, along with proposed pumping by EMLLC, using specified flux cells implemented in the Well package.

4.1.3.4 DISCUSSION ON SIMULATION OF SPRINGS AND ARTESIAN (FLOWING) WELLS: A set of 27 site-specific springs and flowing wells was compiled based on magnitude of flow, existence of data to document discharges, and geographic locations. Five sites and one spring discharge region (southern Diamond Valley playa) are simulated using head-dependent flux boundary conditions, implemented using the Drain package. The remaining sites are simulated using specified flux boundary conditions implemented using the Well package.

Some springs and flowing wells in the model area have a water source derived from both shallow and deeper flow systems. To assign spring and artesian well discharges in the model, temperature, geology, topographic setting, and well construction data were reviewed. Temperature classifications used are as follows:

- less than 70°F is "cold"
- 70-120°F is "warm" and
- greater than 120°F is "hot"

Cold discharges are conceptually simulated as deriving flow from shallow model layers (primarily layer 3), but below shallow confining layers. Sources for warm discharges were simulated from intermediate depth layers 3 to 5 depending on geologic setting. Hot discharge sources were simulated from several thousand feet bgs, in model layer 6.

Locations of model boundary conditions used to represent springs and flowing wells in the model area are summarized in **Table 4.1-2** and shown on **Figure 4.1-6**.

Springs and flowing wells in the model are situated on valley floors or peripheries. Many springs exist in the mountain blocks but are not simulated. The model resolution, geologic complexity, topographic relief, and calibration abilities in the mountainous portions of the model limit the ability to represent mountain block springs. In addition, many of the mountain block springs are ephemeral and are not simulated.

The modeled set of springs and flowing wells often coexist with areas of phreatophyte vegetation represented in the model, and are believed to represent the major discharging springs in the model area. There are undoubtedly other springs in the model area; however, data on locations, discharges, and physical characteristics are not sufficiently available to accurately represent these springs in the model.

Springs and flowing wells are simulated by pumping (specified flux boundary condition) or drain discharge (head-dependent boundary condition) from a deeper zone and injecting the same pumped or drained quantity back to layer 1 (specified flux boundary condition). Simulated spring and flowing well discharges are within or adjacent to simulated ET areas with shallow depths to groundwater, whereby the spring flow routes water up to layer 1 and it is available to discharge via ET. Tonkin Spring is an exception, with spring discharge forming the tributary flow to Denay Creek. ET is limited in the area of discharge to a narrow riparian corridor along the stream channel. Spring discharge is not routed back to layer 1 at the location of the spring in this case but is incorporated in stream recharge assigned to layer 1 along down-gradient stream segments (see recharge distribution on **Figure 4.1-8**).

The southern edge of the Diamond Valley playa was historically a wet area, with over 60 mapped springs on USGS 7.5-minute-scale topographic mapping from the mid 1980s.

The distribution and topographic setting suggest that the springs represent discharge of a shallow water table condition. Present-day observations indicate very few discharging springs in this area, and drier conditions than have historically existed. It is presumed that agricultural pumping in southern Diamond Valley has effectively captured this component of spring discharge. **Figure 4.1-7** shows the distribution of simulated evapotranspiration in the model. To represent the historic discharge of groundwater from the springs along the southern edge of the playa, drains were placed in layer 1 (**Figures 4.1-6 and 4.1-7**) with the drain elevations set to the approximate land surface elevation. These drains replace a component of ET and playa evaporation occurring at the southern playa edge. Since the spring sources are simulated as being derived from layer 1, the discharges are not returned to layer 1 but are removed from the model under the assumption that spring discharges were lost to ET and playa evaporation.

In transient simulations, spring discharges were held constant at locations where little to no drawdown by pumping was simulated. Discrete springs simulated near the southern playa in Diamond Valley are observed to be dry in field inspections in 2007 and 2008, including Thompson Ranch Spring and Sulphur Spring. Discharges from the discrete springs simulated in this area were decreased from the time frame of the mid-1980s to zero discharge by the mid-1990s.

As discussed in the Head-Dependent Boundary Conditions section (**Section 4.1.3.3.2**), spring discharges at Tonkin Spring, Thompson Ranch Spring, Shipley Spring, Hot Spring Hill Spring, and the Bartine Ranch flowing wells are simulated using Drain cells rather than Well cells. The quantities of drain discharge are recharged back to layer 1 using a Well cell, thereby keeping the discharge available to support local ET. The quantity of the specified flux assigned to each Well cell was determined using an iterative calibration process, until a balance with Drain output was achieved.

4.1.3.5 DISCUSSION ON PUMPING FOR AGRICULTURE: In Diamond Valley, steady-state conditions are assumed to have existed in the mid 1950s, although a small quantity of pumping for agriculture had commenced prior to this time frame in the late 1940s. The steady-state water level dataset for Diamond Valley utilizes water level measurements reported into the early 1960s. The extent of pumping in Diamond Valley is reported to have been mild in these early years, with estimated crop consumption averaging about 1,000 AF/yr through the 1950s (**Table 3.5-4**). The steady-state model assumes this level of pumping did not significantly influence static water levels in the valley.

In the transient model, historic pumping in Diamond Valley and Kobeh Valley is simulated using the WELL package, with pumping totals per year per model cell being input based on historic records and crop inventory data, assuming 2.5 acre-feet per acre consumptive use (**Section 3.5.3.1**).

4.1.3.6 DISCUSSION ON RECHARGE BY PRECIPITATION: The MODFLOW Recharge package was utilized to simulate recharge resulting from precipitation. The basin-scale recharge rates and regional geographic distributions were determined from the basin water budget presented previously in this report (**Section 3.2**). However, the recharge distribution was refined during model calibration, while maintaining the conceptual water budgets on a basin scale. The process of deriving the simulated recharge rates and distribution is outlined below.

Basin-scale recharge determined by the Maxey-Eakin method and published in USGS Reconnaissance Reports of the study area was distributed to three geographic zones: the mountain blocks, the alluvial fans, and the upper reaches of major ephemeral drainages.

The initial distribution was approximately 60 percent to the mountain block, 20 percent to the alluvial fan, and 20 percent to ephemeral drainages, based on the mid-range recharge distribution concept for Pine Valley presented in Berger (2000a), as discussed in

Section 3.2.3. This served as a starting point from which recharge rates were refined during model calibration.

In Kobeh and Antelope Valleys, the ephemeral drainage recharge component was set approximately equal to estimates of stream losses made using the Hedman-Osterkamp (1982) method (**Table 3.3-11**). In Diamond Valley, the ephemeral channel and alluvial fan components were combined for simplicity and due to lack of data to further differentiate.

The mountain block recharge components were then reapportioned within each basin based on the percentage of PRISM (**Section 3.2.1**; Daly et al., 1994; OSU, 2006) precipitation falling on the mountain range, as compared with the total precipitation falling on all mountainous terrain in the basin. This step was taken to differentiate recharge rates between higher elevation ranges and lower elevation ranges, following the general concept that greater precipitation quantities will produce higher recharge.

In locations where water level data were available for the mountain block and upper alluvial fans, such as the southern Roberts Mountains in the vicinity of the proposed EMLLC wellfield, recharge rates applied to the mountain block and alluvial fan recharge zones were adjusted to achieve satisfactory calibration to water levels in concert with adjusting hydraulic properties in these areas. Also, in the southern Roberts Mountains, differing mountain block recharge rates were applied to the central portion of the mountains, which are dominated by carbonate rocks, versus the western and eastern portions, which are dominated by clastic sedimentary rocks. This adjustment was made during calibration and found to provide a better calibration solution for down-gradient targets in the vicinity of the proposed wellfield. This differentiation by major rock type is consistent with the concept that rock types with higher permeability can accommodate higher recharge rates (**Section 3.2.3**). These finer adjustments to recharge distribution in the Roberts Mountains were conducted within the constraints of the total mountain block apportionment made to the Roberts Mountains, based on precipitation quantities.

During model calibration the total recharge applied to Pine Valley was reduced by about 10 percent (3,000 AF/yr) as an offset to additional simulated subsurface inflow from Garden Valley (**Section 4.1.4.4**). This preserved the conceptual water budget for Pine Valley. In the case where recharge cells in layer 1 are initially dry, or go dry during transient modeling, the recharge was applied to the upper-most active model layer to preserve the total quantity of recharge.

Recharge rates applied to the Regional Model were derived from corresponding areas within the Local Model. For Regional Model cells that overlapped or contained several smaller Local Model cells, the average of the Local Model cell values was assigned as the Regional Model cell value. **Section 4.2** describes the derivation of the recharge rates for the Local Model.

Table 4.1-3 summarizes the recharge rates simulated in the Regional Model, and **Figure 4.1-8** shows the recharge distribution. The final distributions of recharge by geographic zone are summarized in **Table 4.1-4** and compare favorably with distributions estimated in other central Nevada basins by Berger (2000a and 2000b). The mountain blocks are allocated 54 to 72 percent of the total basin recharge, the alluvial fans 12 to 23 percent, and the upper reaches of the ephemeral streams 16 to 28 percent. Two areas near Mt. Hope have relatively high recharge rates along narrow stream courses, specifically Roberts Creek to the southwest of the proposed pit area and Henderson Creek to the north of the proposed pit area. The recharge rates in these areas are high but the areas represented are small, and the recharge rates are considered appropriate for these streams due to the high elevation and associated high rainfall rates.

Total recharge represented in the model by hydrographic basin areas (**Figure 4.1-8**) is summarized in **Table 4.1-5**. Comparison of **Table 3.5-2** with **Tables 4.1-3 and 4.1-5** indicates recharge distributions are in good agreement with conceptual estimates.

4.1.3.7 MODEL PARAMETERS: This section describes the final distribution of hydraulic parameters in the model.

Model input parameters required by MODFLOW for the model include values for horizontal hydraulic conductivity (Kx,y) and vertical hydraulic conductivity (Kz); storage coefficient (S); and specific yield (Sy) for each cell in the model. Hydraulic conductivity determines the ease with which groundwater flows (**Section 3.6**), and is the transmissivity divided by the saturated aquifer thickness. S and Sy are not input parameters in the steady-state model because change in storage is not part of the steady-state flow equation; S and Sy are required input parameters in transient modeling, as they are a computational variable. The usual approach in model construction and calibration is to start with a simple distribution of parameters and add complexity (heterogeneity) during model development and as required during calibration. That approach was followed during model calibration.

4.1.3.7.1 Hydraulic Conductivity: The same K values were used in both the steady-state and transient model simulations. Hydraulic conductivity properties are differentiated by zones, whereby any defined zone has the same set of parameters. Zones have been defined based on hydrogeologic units described in **Section 3.1** and subsurface geologic interpretations. Geologic mapping, petroleum and water well drilling logs, geophysical survey data, hydraulic property ranges defined for the basins, an understanding of the general geomorphologic processes creating the basins and ranges, and the nature of deposition within the basins were all taken into account in constructing and constraining the K distributions. Zones differentiate the major bedrock types including clastic sedimentary rocks (aquitards), carbonate sedimentary rocks (aquifers), and volcanic rocks. The valley fill zones reflect geomorphologic distributions of Quaternary and Tertiary deposits that have been lumped into common groups.

In the portion of the Regional Model coinciding with the Local Model, the calibrated Local Model K, S, and Sy values were used to develop values for hydraulic property zones for the Regional Model.

The final distributions of horizontal hydraulic conductivities (Kx and Ky) for the calibrated steady-state model are shown on **Figures 4.1-9 through 4.1-16** for model layers 1 through 8 and summarized in **Table 4.1-6**. Comparisons of calibrated K values with available aquifer testing data are presented in **Table 4.1-7**.

K zone distributions in bottom layers strive to reflect a north-northwest-trending corridor (**Figures 4.1-14 to 4.1-16**), reflecting north-south-trending intrusive dikes related to the Northern Nevada Rift (**Section 3.1**). Rift-associated dikes are observed throughout the central Roberts Mountains (Zoback et al., 1984), and magnetic surveys suggest that the rift is regional in extent.

Hydraulic conductivity zones have equal Kx and Ky values (K in east-west direction equals north-south direction). Kx and Ky values (horizontal) are generally one order of magnitude greater than Kz values (vertical) but range from approximately equal values to several orders of magnitude lower as determined during model calibration. Horizontal to vertical anisotropy ratios ranging from 1:1 to 1000:1 are common in three-dimensional numeric flow models and generally estimated during model calibration (Anderson and Woessner, 1992). Anisotropy ratios were estimated during calibration in the Regional Model, and are within a similar range to that reported by Anderson and Woessner (1992).

K values in the valley fill deposits and Paleozoic sedimentary rocks represented in the model tend to decrease with increasing depth bgs. Decreasing K values with depth is conceptually consistent with depositional environments and physical processes whereby, in valley fill materials, deeper sediments tend to include those that are lacustrine in origin as well as tuffaceous rock which has been weathered to clay (**Section 3.6.1**); they are also

compacted by overburden weight. Overburden weight in consolidated rocks also generally results in decreasing hydraulic conductivities with depth as documented in many rock types in the Great Basin by Belcher et al. (2001) and observed locally in packer testing of a deep core hole in the clastic sedimentary rocks surrounding Mt. Hope (Montgomery & Associates, 2010b, borehole #248).

4.1.3.7.2 Storage Coefficient and Specific Yield: Transient model runs require that storage coefficient and specific yield values be distributed throughout the active model domain. **Table 4.1-8** contains the values of S and Sy input for the transient model. Storage coefficients have been distributed based on general hydrogeologic units reflected in K distributions. In addition, Harrill (1968) presented an interpretation of Sy distribution in Diamond Valley (**Figure 3.6-2**) from which S and Sy zone distributions in the upper four layers in Diamond Valley were developed. S and Sy coefficients have been determined from aquifer testing in the proposed wellfield area and at Mt. Hope; the developed parameters were used to constrain storage parameter input in these parts of the model domain. Storage parameters in south-central Diamond Valley were determined during transient model calibration (**Section 4.1.4.5**). The S and Sy zone values are consistent with available data and with the range of values to expect in the given hydrogeologic environments.

Figures 4.1-17 through 4.1-24 show the calibrated distributions and values of storage properties input for model layers 1 through 8.

4.1.4 Model Calibration

Calibration of a groundwater model is the process of adjusting model parameters and boundary conditions to obtain a reasonable match between field measurements and model-computed values. The following section outlines the procedures and results of model calibration.

4.1.4.1 CALIBRATION APPROACH: The calibration procedure is generally performed by varying initial estimates of model parameters (hydraulic conductivity, recharge, ET rate, and boundary conditions) until the model can duplicate what has been measured in the field.

The Mt. Hope model calibration was based upon pre-established calibration goals. The primary components of this approach are the following:

- Overall calibration quality is determined through statistical comparison of model results with field measurements at discrete points (wells).
- The primary statistics used in the calibration are the residual mean, residual standard deviation, absolute residual mean, and correlation coefficient (R^2).
- Calibration continues until: 1) the residual mean is at 5 percent or less than the range in observed water levels, 2) the residual standard deviation is 10 percent or less of the same range, and 3) the absolute residual mean is also less than 10 percent of the same range. Calibration continues until the correlation coefficient between observed and computed values is at least 0.85. These statistical goals are considered minimum objectives for the EMLCC Mt Hope modeling efforts, and calibration continued until model statistics were well within these statistical ranges.
- Calibration quality is further evaluated through visual inspection of the spatial bias of residuals, with an objective to see residual highs and lows distributed throughout the model domain, rather than spatially grouped.
- The calibrated model should reasonably duplicate conceptual water budget parameters of recharge, discharge, and flows between defined hydrologic accounting areas (basins and sub-basins).
- Transient simulations should reasonably replicate the observed water level trends as a result of historic pumping (applicable to Diamond Valley), as gauged by the statistical parameters outlined above.

- The calibrated model should be able to reasonably simulate observed short-term responses to aquifer testing conducted in the wellfield area and at Mt Hope.

The calibration approach outlined above is based upon the concept that the model should be calibrated to discrete points rather than contour maps of water levels. Many well-known researchers in the field, including Konikow (1978) and Anderson and Woessner (1992), accept this concept. The comparison between model and field data is achieved through the calculation of an error (called a residual) at each observation point (called a target). The statistical properties of the model errors are then used to judge the quality of the calibration.

4.1.4.2 CALIBRATION TARGETS: A calibration target is a field measurement that the modeler attempts to match with the numerical model. Calibration targets for steady-state groundwater flow models are often water level measurements averaged over a long time period, or they can be water levels measured on a specific date. In the Mt. Hope model, equilibrium conditions are assumed to have prevailed in Pine, Kobeh, and Antelope Valleys, and calibration targets are water level measurements made over the period of 1940 to present. Caution was exercised in selection of steady-state targets in the Bobcat Ranch area of southwestern Kobeh Valley, as moderate pumping has occurred at that location since the 1960s, and some degree of localized drawdown is expected. In Diamond Valley, water levels are declining in the southern and central portion of the basin, and, in these regions, only water level measurements taken from 1940 to 1960 were used as steady-state targets. Steady-state targets are summarized in **Table 4.1-9**. The steady-state water level data set incorporates measurements from 181 wells.

In addition to the hydraulic head value assigned to each target (i.e., the water level measured in the field) each target can be assigned a weight. Weights are used to give higher priority to accurate data and lower priority to data of lower quality. In the current model no weighting is used (i.e., all weights set equal to 1) as the potential errors associated with

location, ground surface elevation, and measurement errors are considered similar for most all of the calibration targets with two noted exceptions. First, the test well and piezometer locations in the vicinity of the mine and proposed wellfield area have been field surveyed for location and elevation using GPS equipment and have slightly greater water level elevation accuracy than other data. Because these targets are located in small geographic areas of the model domain, weighting was not applied to these targets. Second, due to the sparseness of data in Pine Valley, the steady-state target data set was augmented by water level measurements reported from NDWR well logs (**Appendix G**). The water level elevations derived from well logs are subject to larger errors than other data collected by an independent observer whereby well locations and depths of water are confirmed. These targets were not subjected to weighting; therefore, higher residual errors for targets in Pine Valley were not as rigorously refined as in other geographic areas in the model domain.

Discharge at five springs (Tonkin Spring, Shipley Spring, Thompson Ranch Spring, Hot Springs Hill Spring, and the Bartine Ranch flowing wells) was also included among the calibration targets, but the target values were fluxes rather than water levels, and they are not reflected in calibration statistics derived from water level data.

Potentiometric contours, ET discharge, and subsurface flow estimates constitute loosely defined targets. While they are not field measurements, they were reviewed throughout the calibration process. Additionally, these fluxes and qualitative comparisons are not reflected in the calibration statistics.

4.1.4.3 CALIBRATION TECHNIQUE: Model calibration is an iterative process. As model refinements are made, calibration adjustments are made to keep the model running effectively. Refinements were made to the EMLLC Mt. Hope models at many steps, including: after model domain expansion, grid structure adjustments, hydraulic conductivity distribution refinements, recharge distribution refinements, and ET rate adjustments; as additional data were collected as part of several phases of wellfield and mine-area

hydrogeologic exploration and aquifer testing; as part of EMLLC hydrologic monitoring efforts; and as the models went through peer review. In this manner, increasing complexity was integrated into the model while maintaining numeric stability.

Some calibration was achieved by manual trial and error methods whereby a parameter was changed and the model was run to observe the effects. This process was repeated until an acceptable value for the parameter was achieved, as gauged by the improvement in matching target water level elevations and/or conceptual model water fluxes (i.e., ET, interbasin flows, spring flow, etc.) and the conceptual range of suitable parameter values based on the hydrogeologic setting and available data.

Automatic inverse calibration was also used. The computer ran multiple iterations of parameter variations selected by the modeler and constrained with a defined range of parameter values. PEST is a non-linear parameter estimator which is well documented and in common use for calibrating MODFLOW models. PEST (Watermark Numerical Computing, 2002) was utilized for automated calibration efforts. PEST was also used to identify the highest sensitivity parameters, which aided in targeting parameters used to refine calibration. When using automated calibration techniques the modeler carefully considers the outputs from PEST and uses discretion as to when to accept the new parameter values or reject them as being outside the hydrogeologic conceptual model range for the parameter in question. By using a combination of manual (trial and error) and automated PEST calibration techniques, the objectives of final calibration were successfully achieved for the EMLLC Mt. Hope Regional Model. The local model calibration approach was very similar, but included the use of pilot points, as discussed in **Section 4.2.8.1** of this report.

4.1.4.4 STEADY-STATE CALIBRATION RESULTS: Calibration of the EMLLC regional flow model achieved the goals established for an acceptable match for both heads and fluxes. A summary of target residuals is included in **Table 4.1-9**, and calibration results for heads are presented in **Table 4.1-10**. For the entire model domain, residuals

ranged from -89.99 feet to 118.18 feet. The residual mean of the calibrated steady-state model is 4.38 feet, which is 0.2 percent of the range in target heads (1,962.38 feet) and indicates very little bias toward high or low water levels. The residual standard deviation is 40.33 feet, or 2.1 percent of the range in target heads, in other words, most errors are within about 40.33 feet of the observed values. The absolute residual mean is 30.20 feet, or 1.5 percent of the total range in water level targets. All calibration statistics are within the minimum goals of 10 percent of the range for residual standard deviation and absolute residual mean and 5 percent of the range for residual mean.

Table 4.1-10 further differentiates model calibration statistics by hydrographic basin within the model domain. Calibration statistics vary by basin, and show the best fits between observed and simulated values for the Diamond Valley and Kobeh Valley data groups, the basins of most interest for simulation of EMLLC pumping impacts.

Figure 4.1-25 presents a plot of observed versus calculated water levels. For a perfectly calibrated model, all points would lie on a straight line with a 45-degree slope (observed = calculated values), with an R^2 value of 1.00. The degree of scatter indicates the amount of error in matching water levels at targets. Grouping of residual data points above or below the 45-degree line represents a spatial bias in the calibration, i.e., simulated water levels being either too low or too high. In this case, there is very little bias in the calibration, and the linear regressed R^2 value between observed and model computed water levels is 0.988 (**Figure 4.1-25**).

The calibrated water table is shown on **Figure 4.1-26**, and the potentiometric surfaces for layers 3, 5, and 7 are presented as **Figures 4.1-27 through 4.1-29**. The groundwater contours are in general agreement with steady-state gradients and conceptual flow paths understood for the region (**Figure 3.4-2**). Calibrated spring discharges are close to observed, or historic (steady-state), measurements. It should be noted that historic spring discharge measurements show considerable natural variability (**Table 3.3-1**), and calibrated values of

model discharge are near mid-range values within this variability (**Table 4.1-11**). Pre-development discharges from Shipley and Thompson Ranch Springs were based on reported measurements from the mid 1980s and earlier. Tonkin Spring is simulated as discharging approximately 1.6 cfs, Shipley Spring discharges approximately 6.5 cfs, Thompson Ranch Spring discharges 2.2 cfs, Hot Springs Hill spring discharges 0.01 cfs, and the Bartine Ranch artesian wells discharge 0.36 cfs.

Final calibrated K values, assigned on a zone basis, are in reasonable agreement with measured and estimated values as reviewed in **Section 3.6** and summarized in **Table 4.1-7**.

Another objective of the steady-state model calibration was to achieve a reasonable match between the model water budget and the conceptual water budget as presented in the previous sections of this report (**Section 3.5**). Calibrated ET rates are shown in **Table 4.1-1**, and calibrated recharge rates and total quantities are presented in **Tables 4.1-3 through 4.1-5**. Simulated ET volumes by hydrographic basin are summarized in **Table 4.1-12**. A comparison of conceptual interbasin flows and calibrated model flows is presented in **Table 4.1-13**.

Simulated recharge and discharge volumes are near conceptual water budget values and, where differences occur, they appear reasonable. For example, subsurface flow from Kobeh Valley to south Diamond Valley is approximately 500 AF/yr greater in the numeric flow model than in the conceptual model (**Table 4.1-13**). The subsurface flow is predominantly in deep portions of the model and represents a previously unaccounted deep flow system of uncertain magnitude. The differential between the numeric model and conceptual model is acceptable, given the uncertainty.

Likewise, the postulated subsurface flow from Garden Valley to Diamond Valley was envisioned to be less than that estimated by Harrill (1968) of 9,000 AF/yr. The calibrated steady-state model does bring a significant quantity of groundwater flow from Garden Valley

to Diamond Valley, at 5,724 AF/yr (**Table 4.1-13**), representing about 54 percent of the total simulated groundwater recharge in Garden Valley (**Table 4.1-5**). This subsurface flow occurs in deeper model layers 5 through 8. While this is less than the conceptual model by about 2,000 AF/yr, there is uncertainty regarding the existence and magnitude of this subsurface flow. ET quantities in south Diamond Valley are approximately 1,600 AF/yr greater than the conceptual model (**Table 4.1-12**) based on Harrill (1968), which is reasonable since the model is simulating approximately this much additional inflow from Kobeh Valley to south Diamond Valley. Conversely, the simulated ET quantity in north Diamond Valley is approximately 4,300 AF/yr less than the conceptual discharge based on Harrill (1968) because the simulated subsurface inflow from Garden Valley is about this much less. Although the simulated subsurface outflow from Garden Valley to Diamond Valley is lower, the majority of the difference becomes groundwater outflow to Pine Valley.

4.1.4.5 TRANSIENT CALIBRATION:

Transient Calibration to Pumping in Diamond Valley

As a second step in the model calibration process, transient calibration was conducted. The goal of transient calibration is to adjust model storage and specific yield parameters, and other parameters if needed, to achieve a projected pumping response that reasonably reflects an observed pumping response. In the Mt. Hope Regional Model study area, significant pumping stresses have occurred historically in Diamond Valley and the drawdown responses have been documented (**Section 3.5.3**).

The model was calibrated for the transient period from 1956 (assuming 1955 represented the period of the steady-state calibration) to 2006. The main purpose of the transient calibration was to determine the storage properties of the aquifers, although some adjustments to hydraulic conductivity, recharge rates and distributions, and ET rates occurred during transient calibration.

The transient model uses annual stress periods. MODFLOW-SURFACT, like MODFLOW-2000 (Harbaugh et al., 2000), allows each stress period to be defined as steady-state or transient. The first stress period represented 1955 steady-state conditions, followed by 51 transient yearly stress periods.

The pumping well histories for all simulated wells in the model were estimated based on irrigated acreage, crop type, and consumptive water uses as presented in **Section 3.5.3**. Average annual pumping rates were assigned to each well from 1956 to 2006, based on NDWR pumping inventory data for the basin (**Appendix J**). There are perhaps several hundred irrigation wells in Diamond Valley that could be used. To represent pumping distributions in the model, irrigated lands were simulated by pumping one well per each 5,000-foot by 5,000-foot model grid cell (approximately equal in size to one section), with the total crop water use per cell extracted each year, as shown on **Figure 4.1-30**. The pumped volume simulated is the consumptive use, which is the pumped volume minus the return flow portion, as explained in **Section 3.5.3**. During transient calibration the crop consumptive use rate was varied to identify an acceptable rate. The consumptive use rate of 2.5 acre-feet per acre worked well in the model, whereas previous NDWR usage estimates of 3.0 acre-feet per acre (**Section 3.5.3.1**) resulted in a poorer calibration fit. Recent computations of net crop water demand for alfalfa grown in Diamond Valley is reported as 2.5 ft/yr (Huntington and Allen, 2010), which is consistent with the simulated consumptive use.

Pumping wells in Diamond Valley extract water from model layers 1 to 3, representing the upper 300 feet of valley fill materials. Pumping was also simulated in Kobeh Valley at the Bobcat Ranch in a similar manner. A summary table of pumping distributions for stress periods 1 through 51 (1956-2006) appears in **Appendix J**.

Recharge was applied to each stress period based on the steady-state rate. Additional simulations were run where recharge rates were varied based on the total annual

precipitation; however, the latter did not significantly improve the calibration results. Therefore, a simpler approach of using long-term average recharge rates was adopted. ET of groundwater varies over time in Diamond Valley as a function of depth to the water table.

Diamond Valley Transient Calibration Targets

The transient model was calibrated to a select dataset of transient groundwater level records from Diamond Valley. A total of 14 wells in Diamond Valley (**Figure 4.1-30**) were used as target hydrograph wells, consisting of 430 time-series water level measurements. These wells have detailed hydrographs for long-term changes in water level in Diamond Valley. A total of 414 additional water level measurements were added in the model for 1968, 1977, 1984, 1997, and 2005, derived from the water level dataset (**Appendix F**). These data points are spatially distributed in southern and central Diamond Valley where the effects of drawdown have been observed (**Figure 4.1-30**). These years were chosen because they are at reasonably distributed time intervals and the number of water level measurements made in each year was relatively high, as shown by the data frequency plot on **Figure 4.1-31**. Lastly, 40 data points representative of 1956 conditions (steady-state conditions) in Diamond Valley were included in the transient calibration dataset. Data for these calibration targets are summarized in **Appendix K**.

The usual method for calibrating a transient model, at least from a statistical viewpoint, is to match changes in water levels rather than actual water levels. This is done because the model starts out with a calibration bias at each target, either too high or too low, derived from the preceding steady-state calibration. Rather than match changes in water levels using drawdown targets, each observed hydrograph was offset either up or down a fixed amount so that it started without any bias. Note that this offset to remove steady-state calibration bias applies only to the 14 well hydrograph targets in Diamond Valley. The data from 1968, 1977, 1984, 1997, and 2005 were actual water level elevations. Thus, the calibration was compared with both changes in water levels using the hydrographs and actual water level elevations documented over time.

Diamond Valley Transient Calibration Results

Results of the transient calibration are presented using some of the same techniques as described for the steady-state calibration, and statistics represent changes between observed and simulated transient water levels. A statistical analysis of residuals is presented in **Table 4.1-14**, and an overall plot of all water levels versus simulated values is shown on **Figure 4.1-32**. The calibration statistics reported are for match to actual water level elevations and do not incorporate the hydrograph target adjustments discussed above to remove steady-state calibration bias.

In a statistical sense the transient calibration exhibits a degree of error similar to that of the steady-state calibration. The residual standard deviation and absolute residual mean are 21.48 and 16.0 feet, respectively, which is 2.5 and 1.8 percent of the range in head (873.63 feet). The mean residual is -2.35 feet, which is 0.3 percent of the range in head. All of these statistics are well within the goals established for the calibration, as described in **Section 4.1.4.1**. Residuals for calibration targets are presented in **Appendix K**.

Hydrographs for all transient target wells are shown on **Figures 4.1-33 through 4.1-46** and show the drawdown effects from pumping in Diamond Valley. The hydrographs match the overall decline in water levels in Diamond Valley reasonably well, and most of the hydrographs match the decline observed from 1956 through 1980 very well. There is a period of time from the mid 1980s through early 1990s when the water level trends at some observation wells in Diamond Valley leveled out and even recovered a few feet before continuing a declining trend. The rate of water level decline before and after this period appears similar. The model tends to match the rate of decline reasonably well before and after this period.

The mid-1980s water level anomaly in Diamond Valley is not explained by historic pumping records, which suggest that pumping continued at relatively steady rates (**Section 3.5.3.1**). The water level response could be due to wet conditions in the mid-1980s.

A notable year was 1983, which recorded 89 percent above average precipitation at the Eureka Station. Recharge in the transient model was held constant and represents long-term average conditions. Historical climatic variability is not reproduced in the transient calibration. Additionally, it should be noted that all available water level data from the mid-1990s to present are spring measurements made before seasonal irrigation pumping. Earlier measurements are a mixture of pre-irrigation season and post-irrigation season measurements. Seasonal variations in static water levels appear to range from several feet up to approximately 15 feet, and may account for a portion of the apparent absence of drawdown from the mid 1980s to early 1990s, a time period when few water level measurements were made.

Drawdown simulated through 2006 suggests that pumping in Diamond Valley has produced drawdown at the southern edge of the playa and northerly along the east and west edges of the basin. Over the past five decades, agricultural pumping has resulted in drawdown that appears to have affected springs such as Sulphur Spring, which is no longer discharging based on recent field observations (2007-2008). Model results indicate that 20 feet of water table drawdown has occurred in the Sulphur Spring area since 1956. The transient model indicates that Thompson Ranch Spring has ceased to discharge, which is consistent with present observed conditions. Simulated discharge at Shipley Spring shows a reduction over historic discharge rates, which is corroborated by recent discharge measurements (**Table 3.3-2**).

Water level measurements are available for several of the transient target wells for the time period of 2007 to 2010, and have been included on the hydrographs (**Figures 4.1-33 through 4.1-46**). Available data from this time-frame document a continuing trend of drawdown in the agricultural area of Diamond Valley, at rates comparable to those simulated by the model.

Kobeh Valley Transient Calibration to Short-term Aquifer Testing

During the course of exploration drilling to define conditions in the proposed EMLLC Kobeh Valley wellfield area, six aquifer tests were performed, ranging in duration from 5 to 32 days. Data from the aquifer testing are presented in Interflow et al. (2010) and the locations of test wells and observation wells are shown on **Figure 4.1-47**.

Some of the key findings of this exploration program include:

- The central portion of the proposed Kobeh Valley wellfield is located along a north-south-oriented graben structure (down-dropped by faulting) in which over 1,000 feet of alluvium and valley fill materials have been deposited. The alluvial materials have measured hydraulic conductivity values ranging from 5 to 19 ft/d.

- Underlying the valley fill deposits in the graben are clastic sedimentary rocks (Vinini shale formation) which are hydraulically tight in comparison with the valley fill.

- Bounding the graben on the west side are clastic sedimentary rocks which are exposed at land surface. However, carbonate sedimentary rocks were encountered at depth beneath the clastic sedimentary rocks (approximately 960 feet bgs on the western side of the proposed wellfield at test well 220T (**Figure 4.1-47**).

- Carbonate rocks, clastic rocks, and volcanic rocks form the eastern boundary to the graben. The carbonate rocks are highly permeable where fractures or solution features occur with hydraulic conductivity values measured up to 250 ft/d (test well 206T, **Figure 4.1-47**). However, as defined by aquifer

testing, the highly permeable carbonate rocks are bounded by low conductivity rock types and/or faults with barrier properties.

- There is a fault-related low permeability barrier at the base of the Roberts Mountains, immediately to the north of the proposed wellfield, which results in approximately 300 feet of static water level differential on either side of the fault.

- Data from the exploration drilling program provided constraint to aquifer properties input into the numeric flow model, and geologic representations were accomplished by assignment of differing hydraulic property zones. The exploration program also yielded approximately 40 additional water level targets for steady-state calibration in the wellfield area.

- Data from the six aquifer tests were used as transient drawdown targets for the Regional Model. Pumping rates from the aquifer test were input into the model at the test well locations, and projected drawdown at observation wells was simulated and compared with measured values. This was performed for both the pumping and recovery periods of each aquifer test.

- During the transient calibration, recharge assigned to the southern Roberts Mountains and alluvial fans at the base of the Roberts Mountains was refined, along with storage coefficients, specific yields, hydraulic conductivities, fault conductance, and model layer thicknesses in the vicinity of the wellfield. Changes to these properties in the steady-state model were implemented in an iterative process, until acceptable steady-state and transient pumping solutions were achieved. The calibration statistics presented previously for the steady-state model reflect these changes made in the transient calibration.

Kobeh Valley Wellfield Transient Aquifer Test Results

Figures 4.1-48 through 4.1-53 show the simulated versus measured drawdown responses for aquifer testing in the calibrated model. Several criteria were used to gauge success of the effort: the magnitude of the drawdown, the shape of the drawdown and recovery trends, and consideration of the proximity of the observation well to the pumping well.

The model grid spacing is 1000 feet by 1000 feet in the wellfield area, and some observation wells are located within the same model cell as the pumping well or in adjacent cells. These nearby observation wells are subject to grid size resolution error whereby average drawdown in the model cell does not accurately capture the true conical drawdown shape near the pumping well. For observation wells near the simulated pumping wells, the model under-predicts drawdown because a steepening of radial flow gradients near the well is not reflected in the average drawdown simulated over the model cell.

Drawdown data are available from observation wells located within 100 feet of the six pumping wells; therefore, water level data from these observation wells were used in lieu of water level data from the pumping wells, in order to avoid additional error due to head losses in the pumping wells.

The calibrated model captures the magnitude of observed drawdown, including the lack of response noted at some locations due to geologic structures and fault barriers. This achieved the goal of calibrating the model to observed results from the transient aquifer testing.

4.1.5 Calibration Sensitivity Analysis

A sensitivity analysis is typically part of the documentation of model calibration (ASTM, 1993). The purpose of a sensitivity analysis is to document relative sensitivity

among the various parameters and boundary conditions in the model. This provides information about which parameters are most important to the calibration.

Due to the large number of parameters in the Mt. Hope model, hydraulic conductivity and storage parameters were grouped together based on general lithologic units. These units included the valley fill, carbonate rocks, clastic sedimentary rocks, volcanic rocks, and intrusive rocks. These five lithologies were used to vary horizontal hydraulic conductivity, vertical hydraulic conductivity, storage coefficient, and specific yield. Recharge zones were grouped together based on recharge location. Three different locations were simulated including mountain block, alluvial fan, and streambed. ET rates were tested in the 11 individual zones which were separated into different basins for greasewood and salt grass. The sensitivity of ET was also tested as a whole with all zones adjusted together.

Six model simulations were run for each parameter. During each simulation the parameter was multiplied by a factor ranging between 0.5 and 1.5. The calibration statistics were compiled for each of these simulations. **Figures 4.1-54 through 4.1-58** present the percentage of change in the residual standard deviation (also called RMS error). The sensitivity runs were performed in the steady-state model with the statistical change in calibration reported for the steady-state target data set. The exceptions to this were the storage properties which were derived from the transient model using the transient calibration data set (**Section 4.1.4.5**).

The parameter with the largest percentage of change in residual standard deviation is recharge rates (i.e., the quantity of recharge being input to the model) (**Figure 4.1-56**). Recharge quantity was based on conceptual water balances derived from published estimates for the basins with minor changes as described in **Section 3.2**. The total (basin scale) recharge quantities were not a calibration parameter, although distributions within the basins were adjusted during calibration.

The next most sensitive parameter was the specific yield of valley fill deposits (**Figure 4.1-55**). This is mainly due to the large drop in water levels in Diamond Valley from 1955 to present. The rate of decline in the valley is highly dependent on specific yield. The hydrologic flow barrier conductance parameter also exhibits sensitivity, particularly to decreases in the values (**Figure 4.1-58**).

Other parameters that caused more than a 5 percent change in residual standard deviation were the horizontal hydraulic conductivity of the valley fill, carbonate rocks, and clastic sedimentary rocks. Vertical hydraulic conductivity of clastic sedimentary and volcanic rocks also caused more than a 5 percent change.

The model is relatively insensitive to changes in storage coefficient. This was due to the fact that in all basins except Diamond Valley, relatively little change has occurred in water levels through time. Changes in water levels in Diamond Valley are related more strongly to the specific yield since pumping is shallow in the valley and the response related to aquifer drainage under unconfined conditions.

In conclusion, the model was found to be most sensitive to changes in the recharge and specific yield parameters.

4.2 PIT AREA NUMERICAL MODEL

4.2.1 Introduction

EMLLC developed a local-scale groundwater flow model (Local Model) for the Mt. Hope Project to simulate mine dewatering and post-project pit-lake development. Projections of groundwater inflow to the pit during dewatering and pit-lake development post-project for the Proposed Action Alternative are incorporated into the Regional Model

for determination of mine impacts on the regional groundwater system. The Local Model was developed using TMR to allow a more accurate characterization of the mine pit structure and more detailed simulations of localized hydraulic responses to dewatering activities. TMR is a technique used to develop high-resolution groundwater models within larger-scale models. The larger encompassing model is used to define the boundary conditions for a smaller, finer mesh embedded model. Location of the Local Model domain within the Regional Model is shown on **Figure 4.2-1**.

Mine pit excavation is planned to commence in late 2011, with 1 year of pre-production and 32 years of mining. Upon completion the open pit will extend downward from an elevation at the center of the proposed pit of 7,250 feet amsl approximately 2,550 feet bgs to 4,700 feet elevation amsl. The ultimate pit footprint would cover approximately 730 acres. Pre-mining groundwater level in the center of the proposed pit is approximately 300 feet bgs; therefore, groundwater drawdown of approximately 2,250 feet will be required during mining operations to draw the groundwater level to below the ultimate pit bottom. Inflowing groundwater will be pumped from sumps in the pit and removed. During mining water pumped from the pit will be used as part of the mine water supply. After cessation of mining operations a pit lake is expected to form due to groundwater inflows, direct precipitation, and surface drainage into the pit.

The Local Model is used to evaluate:

- Pit dewatering rates during the mining period
- Post-project pit lake formation, including pit lake filling times, equilibrium pit lake water level and quantity of groundwater that contributes to the pit lake water balance, as well as whether the pit lake will be a hydrologic sink or a flow-through pit lake
- Groundwater stresses from pit dewatering and lake-development which will impact water levels regionally

4.2.2 General Setting

The Mt. Hope Project is located as shown on **Figure 4.2-1**. Mt. Hope forms a topographic divide separating Kobeh Valley on the south from Diamond Valley on the east, and Garden Valley (a sub-basin of Pine Valley) on the north. The Mt. Hope Project area is located primarily within the Kobeh and Diamond Valley watersheds and includes about 20,000 acres of mining claims. The project site is accessible via Nevada State Highway 278. The Local Model domain encompasses Mt. Hope and an area extending 2 miles to the north, south and west, and 5 miles to the east from the proposed pit. Land surface elevations range from 8,380 feet, amsl at Mt. Hope peak to 5,900 feet, amsl on the eastern edge of the model domain. The eastern edge of the Local Model domain extends to the east side of the Sulphur Spring Range.

4.2.3 Hydrogeologic Setting

Mt. Hope is located in the central Great Basin within the Basin and Range physiographic province. Block faulting and structural deformation in the area have resulted in a regionally north-south trending topography, expressed as a series of valleys separated by mountain ranges. A detailed discussion of the regional geology is presented in **Section 3.1**. The proposed mine pit lies along the southeastern slope of Mt. Hope, as shown on **Figure 4.2-2**. The rock units and hydrogeology of the proposed mine area are described in "Hydrogeologic Characterization of Pit Area" (Montgomery & Associates, 2010b). A geologic map for the proposed pit area, with groundwater elevation contours, is shown on **Figure 4.2-3**. The geology depicted on the map is based on drill core and surface mapping provided by EMLLC.

Hydrogeology in the proposed mine area is characterized as a low-permeability fractured and faulted bedrock complex. For model simulation purposes the geologic units within the Local Model domain were grouped into the eight hydrogeologic units shown on

Figures 4.2-4 through 4.2-8. Simplifying assumptions were made to assemble similar geologic units into distinct groups that have similar lithologic properties, age, areal extent, and hydraulic properties. The hydrogeologic units in the local groundwater model area, and their equivalent hydrostratigraphic units in the Regional Model, were defined as follows:

- Rhyolite ash-flow tuff (Tv): Oldest volcanic rock in the proposed pit area; appears to represent multiple extrusive events associated with the Mt. Hope volcanic-intrusive complex; Tertiary age. Rhyolite tuff is assigned to hydrostratigraphic unit "VOL1" of the Regional Model (**Table 3.1-2**).
- Potassic Quartz Porphyry (Tqpp): Potassic altered zone of the quartz porphyry which is the dominant intrusive rock of the Mt. Hope igneous complex exposed at the surface; porphyritic intrusive rock of rhyolite composition; brecciated in the east-southeast portions; Tertiary age. Potassic alteration Potassic altered quartz porphyry forms a shell which surrounds and overlies the silicic altered porphyry. Potassic zone is assigned to hydrostratigraphic unit "VOL1" of the Regional Model.
- Silicic Quartz Porphyry (Tqps): Silicic altered zone of the quartz porphyry which is the dominant intrusive rock of the Mt. Hope igneous complex exposed at the surface; porphyritic intrusive rock of rhyolite composition; brecciated in the east-southeast portions; Tertiary age. Silicic alteration has resulted in brittle, fractured rock with little alteration within fractures. The silicic altered quartz porphyry underlies and is surrounded by the potassic altered porphyry. Silicic zone is assigned to hydrostratigraphic unit "VOL1" of the Regional Model.
- Vinini Formation (Ov): Includes sequence of black shale, siltstone, silty limestone, quartzite, calcareous sandstone, and chert; widespread alteration in vicinity of Mt. Hope by contact metamorphism manifested as hornfels; Ordovician age. Vinini Formation is assigned to hydrostratigraphic unit "AQT1" of the Regional model.

- Hornfels (Hf): Thermally metamorphosed black shale-siltstone-silty limestone units of the Vinini Formation; characterized by dense, very fine-grained brown biotite with well-preserved, relict lamination and bedding. Hornfels occurs locally around intrusive rocks and is not described as a separate hydrostratigraphic unit distinct from Vinini Formation in the Regional Model (AQT1).
- Garden Valley Formation (Pgl): Medium-bedded limestone and dolomite, minor interbedding of sandstone and shale; portions metamorphosed to skarn; Permian age. Garden Valley Formation is assigned to hydrostratigraphic unit "AQT1" in the Regional Model.
- Paleozoic Carbonates (Pzca): Unit inferred from Regional Model geology; described in **Section 3.4.6**. Paleozoic Carbonates are assigned to hydrostratigraphic units "CA1", "CA2", or "CA3" of the Regional Model.
- Paleozoic Clastics (Pzcl): Unit inferred from Regional Model geology; described in **Section 3.4.6**. Paleozoic Clastics are assigned to hydrostratigraphic units "CA2", "CA3", or "CA4" of the Regional Model.

An intensive round of hydrogeologic investigations conducted from March through July, 2009 confirmed that groundwater flow is influenced by rock fractures; however, the influence of individual mapped fracture systems was not identified during this fieldwork (Montgomery & Associates, 2010b). Water level elevations in pit area wells and piezometers, together with water level contours, are shown on **Figure 4.2-9**. A geologic map for the proposed pit area, with groundwater elevation contours, is shown on **Figure 4.2-3**. Although some anomalous water levels are present, the water levels in pit area wells are largely consistent with the water level contours, with no obvious influence from mapped fractures or faults.

4.2.4 Groundwater Conditions

The oldest monitor wells in the vicinity of Mt. Hope were constructed in late 2005, and water level records for these wells are from January 2006 through December 2009. Evaluation of groundwater level data for these wells indicate minor water level changes, except for wells with declining water levels in the vicinity of Diamond Valley (Montgomery & Associates, 2010b). This report also includes groundwater hydrographs for individual wells and piezometers in the vicinity of the Mt. Hope pit, including multi-level grouted piezometers, for the period March through September 2009. These hydrographs indicate generally stable conditions, except at wells or piezometers affected by long-term pumping tests conducted during the period of record and at wells or piezometers where groundwater levels have still not achieved equilibrium conditions following well construction.

4.2.4.1 GROUNDWATER ELEVATIONS: Groundwater level measurements were compiled from wells and piezometers in the Local Model domain to characterize occurrence and movement of groundwater. A contour map of groundwater level elevations for the vicinity of Mt. Hope is shown on **Figure 4.2-9**. Observed groundwater level elevations used for the contour map are summarized in **Table 4.2-1**; selection of water levels for contour construction has been presented previously (Montgomery & Associates, 2010a, 2010b). The majority of groundwater level measurements were obtained from wells and piezometers located in the proposed pit area on the southeast side of Mt. Hope. Based on groundwater level measurements obtained from approximately 40 wells and piezometers during the period 2007 through 2009, groundwater levels in the Local Model domain range from lower than 5,800 feet, amsl on the east side of the Sulphur Spring Range to higher than 7,200 feet, amsl at Mt. Hope (**Figure 4.2-9**). In the Mt. Hope pit area, the groundwater level relative to land surface ranges from about 198 feet above land surface (als) at piezometer IGM-152(W-03) to about 530 ft bgs at piezometer GMI-MH-178P and well GMI-PDT-2 (**Figure 4.2-9**). Groundwater level hydrographs for individual wells and piezometers, including multi-level grouted piezometers, for the period March through July 2009, are given